

TSUNAMI HYDRODYNAMICS



Utku Kanođlu, PhD

Middle East Technical University
Department of Engineering Sciences
Ankara, Turkey

kanoglu@metu.edu.tr

**ONCE FOR ALL
MY SINCERE THANKS GOES TO**

Prof. Dr. Costas Synolakis
University of Southern California, Los Angeles, California

and

Prof. Dr. Emile Okal
Northwestern University, Evanston, Illinois

**GENEROUSLY PROVIDING THEIR
PRESENTATION MATERIALS.**



Summary - 1

- To understand tsunami currents, forces, runup on coastal structures and inundation of coastlines, the evolution of tsunamis from their source region to their target must be calculated numerically.
- In the last 50 years of tsunami science, tens of models have been developed and proposed, but less than three are now in wide use.
- Real time forecasts are now possible using the state of the art numerical tools.
- During the 17 November 2003, numerical modeling as the tsunami progressed towards Hawaii led to cancellation of warning was enabled. The same real time forecast took place during the 15 November 2006 and 13 January 2007 Aleutian tsunamis and the 01 April 2007 Solomon Islands tsunamis for far-field impact.
- In all cases, the tsunami inundation was within 10% of the forecast.

Summary - 2

- This success was only possible because the model used (MOST) for the predictions had been extensively tested.
- The validation included comparisons of numerical model results with analytical solutions, experimental data, and field measurements.
- Here, the validation methodology of numerical tools which can be used towards inundation mapping and forecasting is discussed in the context of developments in tsunami hydrodynamic modeling in the past 50 years.
- Useful benchmark problems are identified and emphasized.
- Although the state-of-knowledge was able to successfully forecast the last Pacific events, model development is a continuing process with every physical tsunami constituting a new benchmark.

Summary - 3

Synolakis and Bernard (2006) discuss tsunami hydrodynamics with historical perspective.

PHILOSOPHICAL
TRANSACTIONS
— OF —
THE ROYAL SOCIETY 

Phil. Trans. R. Soc. A (2006) **364**, 2231–2265

doi:10.1098/rsta.2006.1824

Published online 30 June 2006

Tsunami science before and beyond Boxing Day 2004

BY COSTAS E. SYNOLAKIS^{1,2,*} AND EDDIE N. BERNARD³

¹*Coastal Engineering and Natural Hazards Laboratory,
Technical University of Crete, Chanea 73100, Greece*

²*Viterbi School of Engineering, University of Southern California,
Los Angeles, CA 90089-2531, USA*

³*Pacific Marine Environmental Laboratory, NOAA,
Seattle, WA 98115-6349, USA*

Tsunami

The term tsunami now in worldwide use is also known as tidal wave and from the Japanese word which translates as harbor wave.

Even a relatively small tsunami entering harbor can trigger substantial harbor oscillations.

Not only it is not uncommon for these harbor waves to reach substantial heights, with amplification factors of six in the shoreline (with respect to the wave height near the center of the basin), but also water motions can persist for many hours.

Since ancient times, harbors have always been centers of commercial activity, hence most early eyewitnesses observed these giant waves in harbors or small ports, hence the name tsunami.

Tsunami

Improperly called

- Tidal wave
- Raz-de-marée [French]
- Flutwellen [German]

Properly called

- Maremoto [Spanish, Italian]
- Taitoko [Marquesan]
- Tsu Nami (Harbor wave) [Japanese]

After 2004 Indian Ocean (Boxing Day) Tsunami word "tsunami" enter into the most of the world contemporary languages.

Tsunami

In Japan, fairly systematic historical documentation of tsunamis dates back about 1300 years. However, it appears that first historical reference to coastal inundation by tsunami was around 1620BC resulted from eruption of the Thera volcano in the eastern Mediterranean.

Until recently, the tsunami resulting from this eruption of Thera had been considered as the main cause for destruction of Minoan civilization on the island of Crete, Greece. It is now well established from different sources, that the Minoan palaces were not abandoned until about 100 years after eruption. Tsunamis destroyed the fleets of the Minoans and flooded their crops, and thus initiated the end of the Minoans, but did not extinguish them immediately, very much as the 1755 tsunami precipitated the demise of Portugal as a world imperial power. The 1755 earthquake and tsunami killed almost one in ten thousand of the estimated world population of its time.

It had a profound effect in the philosophical thinking of the time. Voltaire wrote *Candide*, a short novel which examines how people react to natural and manmade disasters of such scale, with theological implications.

Death Toll in perspective (Earthquakes)

Year	Region	Death Toll	
		Absolute	Scaled to Global Population
1556	Shansi	800,000	1/625
1976	Tangshan	250,000	
1780	Iran	280,000	1/3000
1920	Kansu	200,000	
1923	Tokyo	200,000	
1927	Tsinghai	200,000	
2004	Sumatra	150,000	1/40,000
1755	Lisbon	70,000	1/10,000
1908	Messina	70,000	
1970	Peru	66,000	
1999	Turkey	40,000	
2003	Iran	40,000	
1896	Sanriku	30,000	
1989	Armenia	30,000	
1939	Chile	25,000	
1906	Valparaiso	20,000	
2001	India	20,000	
.....			
1906	San Francisco	3,000	
1989	Loma Prieta	68	

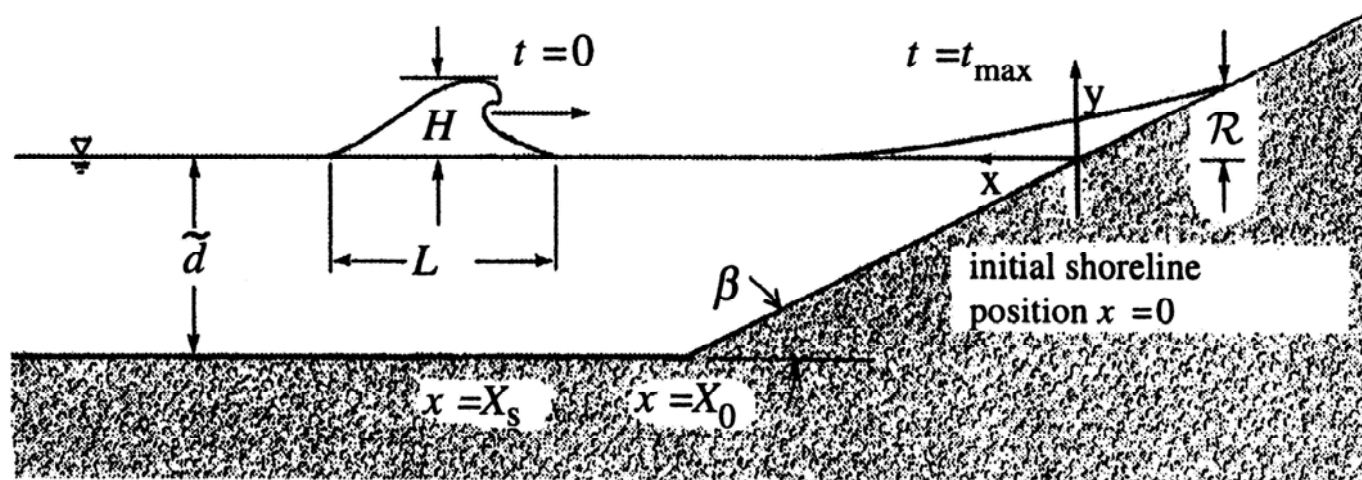
For reference: Hiroshima: 200,000

Death Toll in perspective (Tsunamis only)

Year	Region	Death Toll	
		Absolute	Scaled to Global Population
2004	Sumatra	150,000	1/40,000
1755	Lisbon	70,000	1/10,000
1896	Sanriku	30,000	1/53,000
1952	Kamchatka	5,000	
1960	Chile	5,000	
1933	Sanriku	3,000	
1998	Papua New Guinea	2,200	
1994	Flores	2,000	
...			
1946	Aleutian	170	
1992	Nicaragua	170	
1964	Alaska	122	
1929	Newfoundland	18	
1883	Krakatau (Volcanic)	30,000	1/50,000
<i>For Reference</i>			
Middle Ages	Great Plague		1/30 ?
20th century	WWI +Influenza	30,000,000	1/60

Nomenclature

The canonical problem; *1+1 propagation problem for long wave propagation over a constant depth first then over a sloping beach*



H is the leading wave height

L is the leading wave wavelength

\mathcal{R} is the maximum runup

\tilde{d} is the characteristic length scale for normalization

General - 1

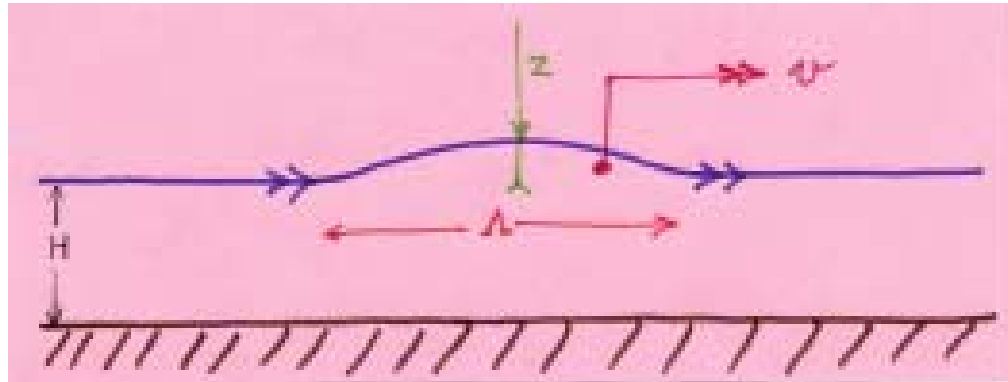
- Tsunamis are generated by impulsive geophysical events of the seafloor and/or of the coastline terrain, i.e., earthquakes, submarine and subaerial mass failures.
- More extreme, but less common generation mechanisms are volcanic eruptions and bolide impacts.
- Tsunamis are long waves of small steepness and undergo substantial deformations as they propagate over shallow bathymetry or when evolving over the continental shelf.

General - 2

- While the basic governing equations have been known for over 150 years, the grand synthesis had to await the development of sophisticated modeling tools, high-resolution laboratory experiments in the 1980s-1990s and the field survey results of the 1990s, which served as crude proxies to free-field recordings and allowed for validation of the numerical models.
- This synthesis is still in progress. State-of-the-art inundation and forecasting codes have evolved through a painstaking process of careful validation.
- The determination of the inundation and runup of tsunamis and forces on coastal structures is one of the quintessential problems in tsunami hazard mitigation.
- Operational tsunami forecasting was only made possible through the availability of instrumental tsunameter recordings, which also allowed for closure, e.g. Titov et al. (2005a,b). Since 2003, every new event in the Pacific Ocean has posed a diminishing challenge.

General - 3

Propagation on the high seas



VELOCITY depends on DEPTH of water H ; $V=(gH)^{1/2}$

In practice for $H=5\text{km}$, $V=220\text{m/s}=800\text{km/h}$
(i.e., the speed of modern airliner)

Maximum AMPLITUDE is a few to a few tens of centimeters

WAVELENGTH is typically 300km

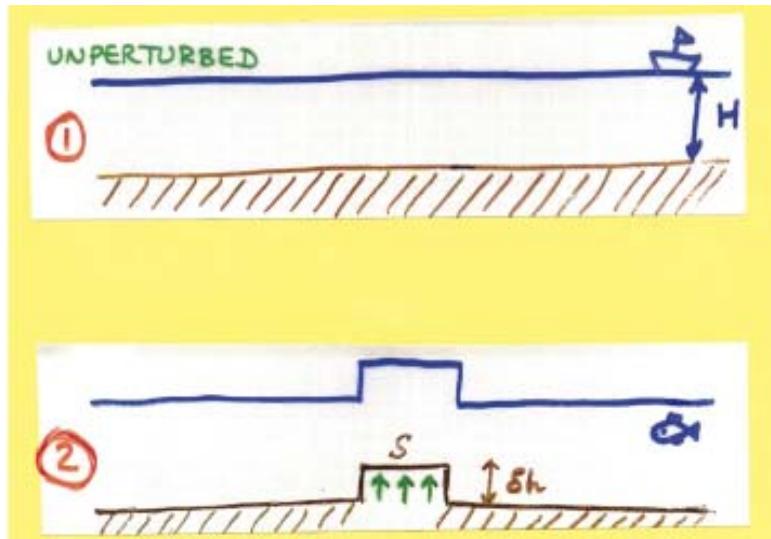
General - 4

Upon shoaling, the wave slows down considerably ($V=(gH)^{1/2}$), and its, energy, which was spread over the deep ocean column, must be squeezed into a now shallow water layer.

Hence, **the wave amplitude increases considerably**, often to several meters, or tens of meters.

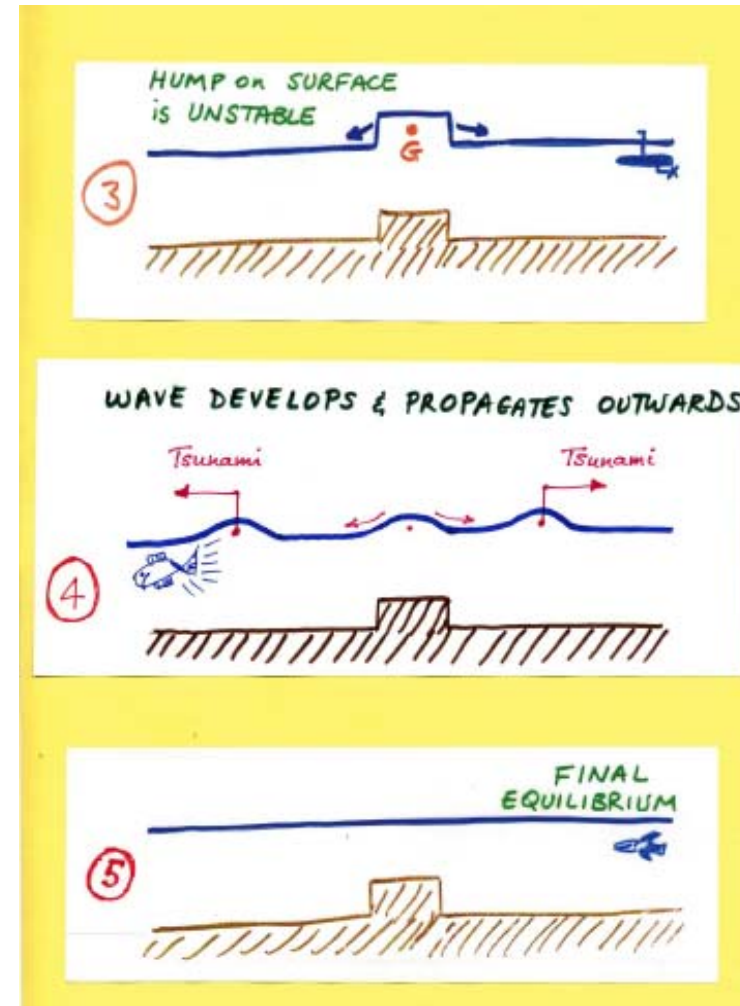
It can penetrate as much as several km inland.

TSUNAMI GENERATION - The earthquake



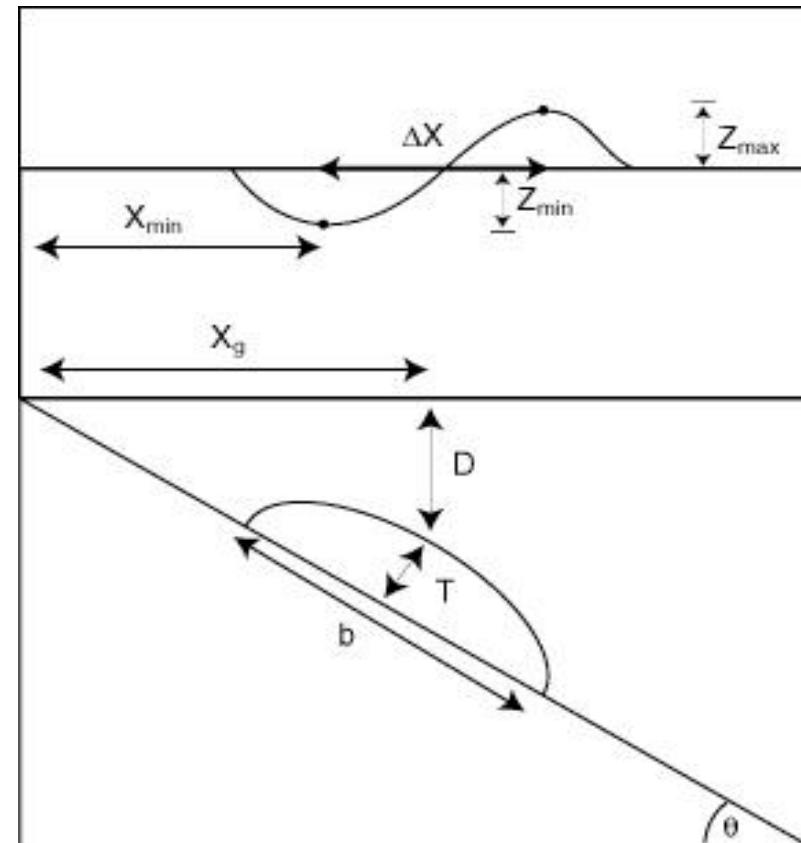
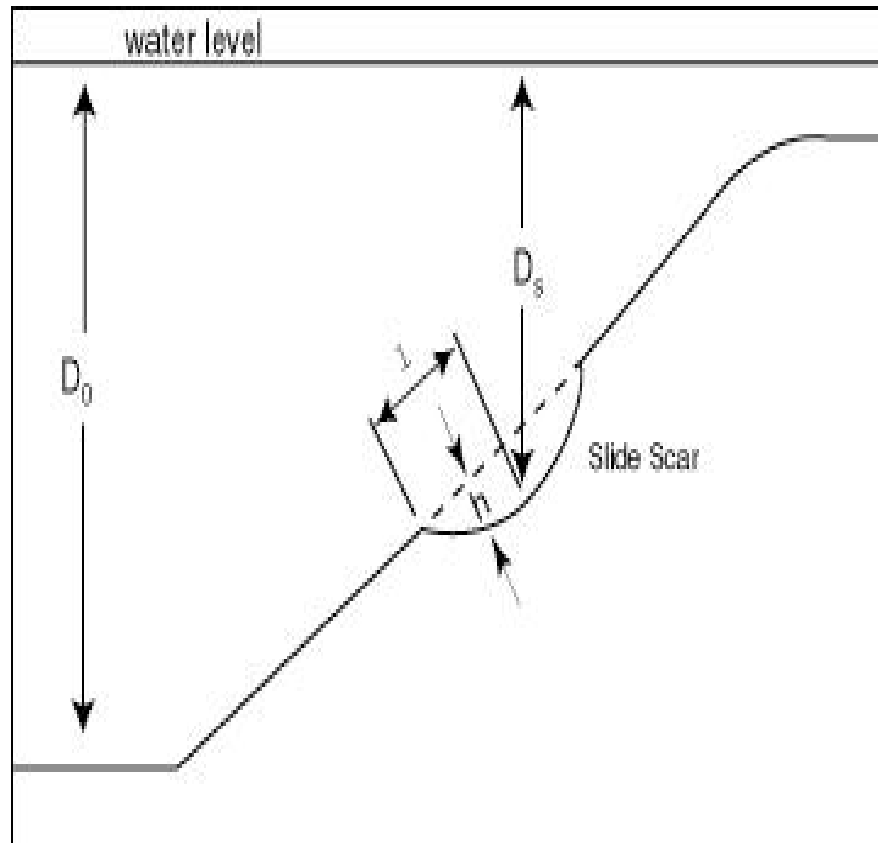
Earthquake deforms ocean floor and displaces it vertically into water mass.

Hump should appear on surface mirroring bottom deformation.



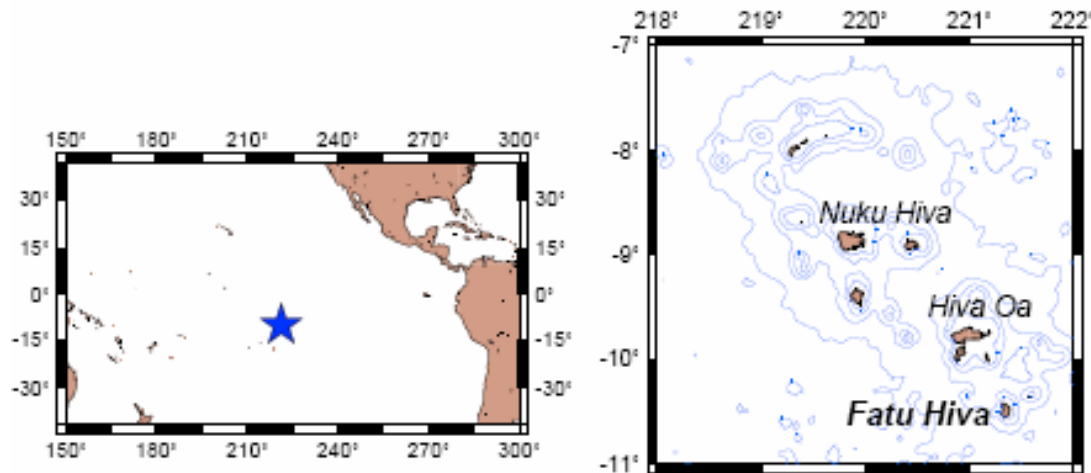
TSUNAMI GENERATION - Landslide

The canonical model for landslide generated waves in the laboratory, proposed by Wiegel (1955), rediscovered with vengeance following the 1998 Papua New Guinea tsunami.



TSUNAMI GENERATION - Landslide

13 September 1999 Fatu-Hiva, Marquesas Islands Tsunami



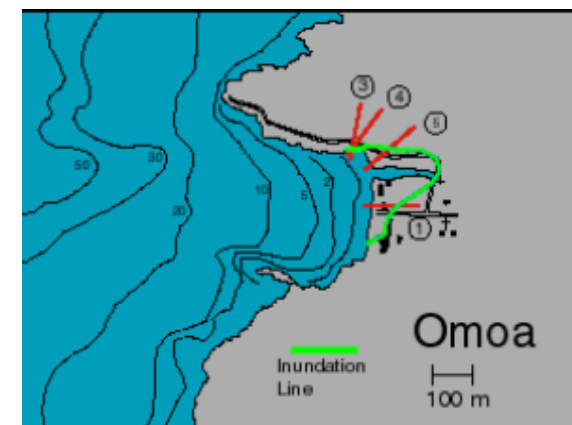
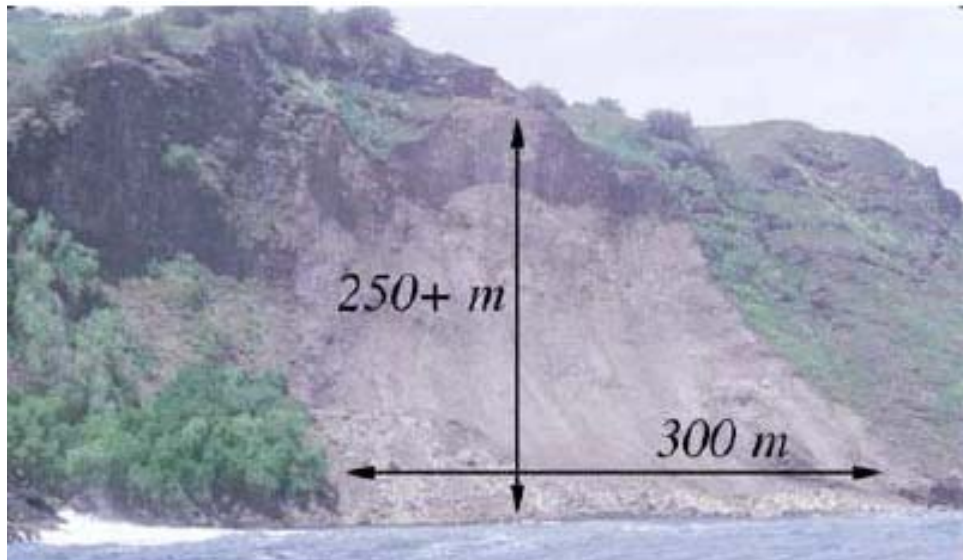
The beachfront school house at Omoa was severely flooded by two waves which also destroyed the ice-making plant and couple of structures.

Miraculously, there were no victims, even though 85 children were attending school.



TSUNAMI GENERATION - Landslide

Estimated volume of rock slide: 4 million m³



TSUNAMI CAN CAUSE FLOODING



26 December 2004 tsunami Port-Mathurin, Rodrigues [Mauritius]

TSUNAMI CAN DESTROY STRUCTURES



Camana, Peru, 2001



Mosque
Banda Aceh 2004

TSUNAMI CAN MOVE ANYTHING



Locomotive, Sri Lanka, 2004



Locomotive moved 1km
Seward, Alaska, 1964



Boats, Sri Lanka, 2004

TSUNAMI CAN FLOOD MATERIALS

More destructive than water



A boat "BETTER FORTUNE"
brought misfortune



Lumbers, once floated,
changed to missiles.
DOMINO EFFECT

Reference: Prof. Shuto

TSUNAMI CAN CREATE SUBSTANTIAL CURRENTS

Even though inundation is an important aspect, currents can not be neglected in tsunami hazard assessment.

Tsunamis can generate large currents that can cause

dramatic damage to structures and move large objects far inland.



It does not required a megatsunami like December 26, 2004 to move large objects.

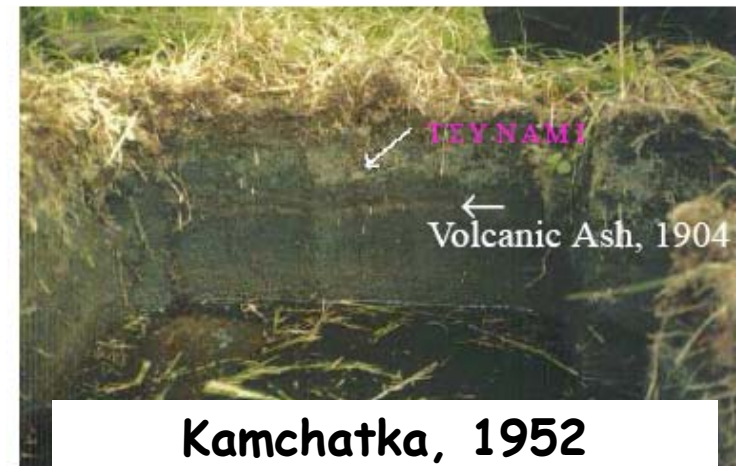
3m tsunami carried 6000ton generating barge

one mile inland down the Baruyan River.
(1994 Mindoro Philippines tsunami)

TSUNAMI CAN LEAVE SEDIMENT



Tofino, B.C., Canada, 1700



Trenches can reveal historical or paleo-tsunamis

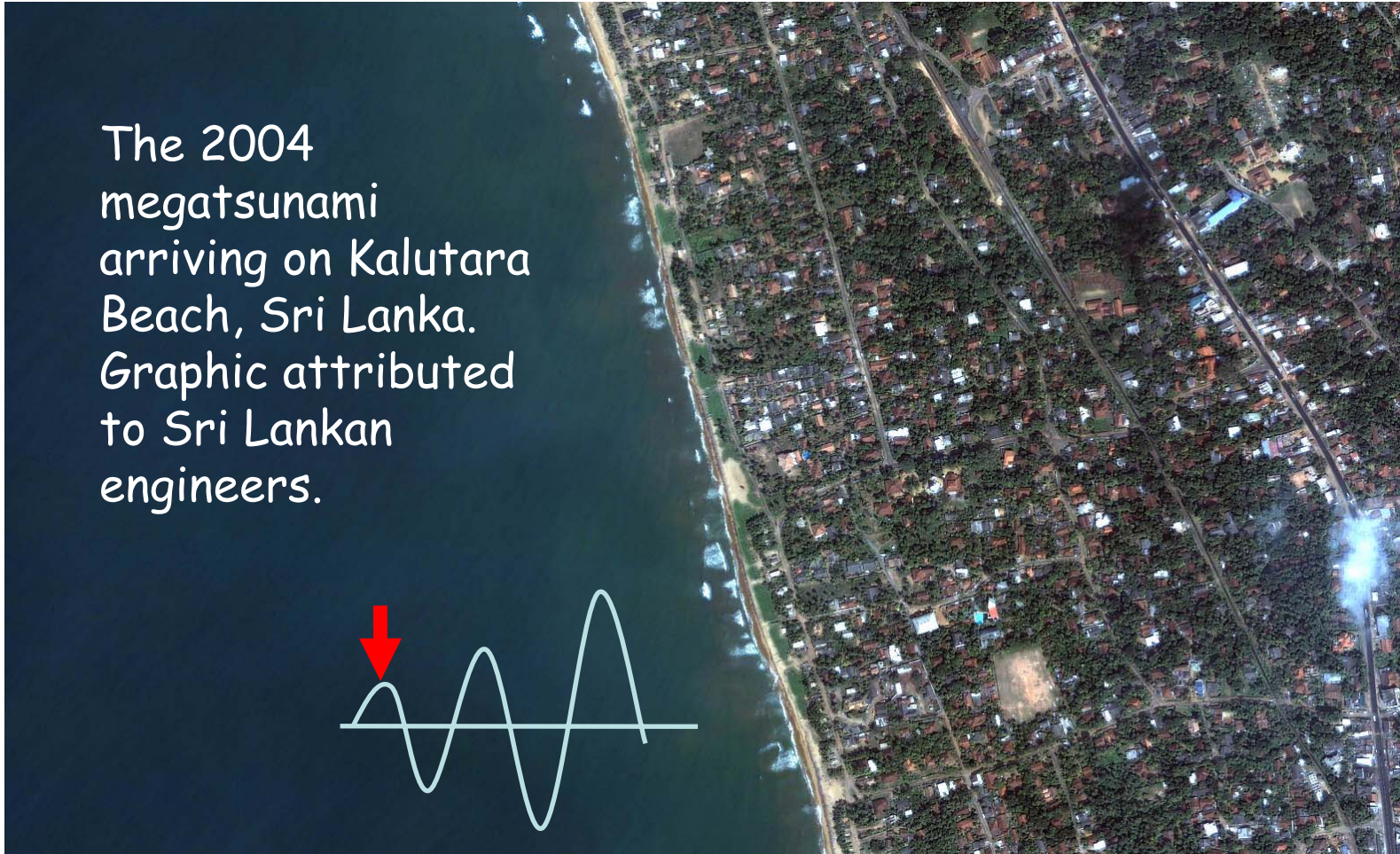
TSUNAMI CAN CAUSE FIRE



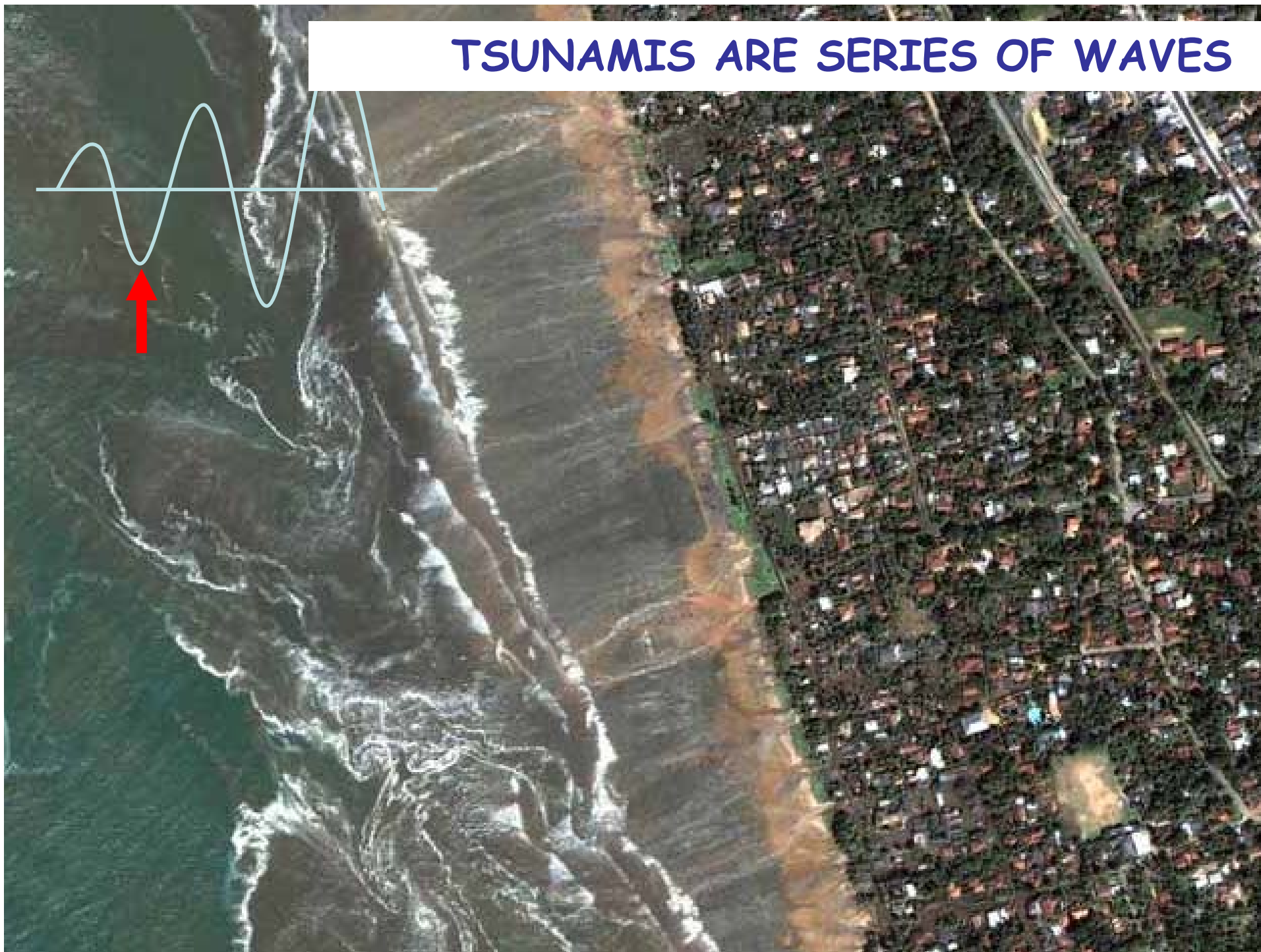
1993 Okushiri Island, Japan tsunami

TSUNAMIS ARE SERIES OF WAVES

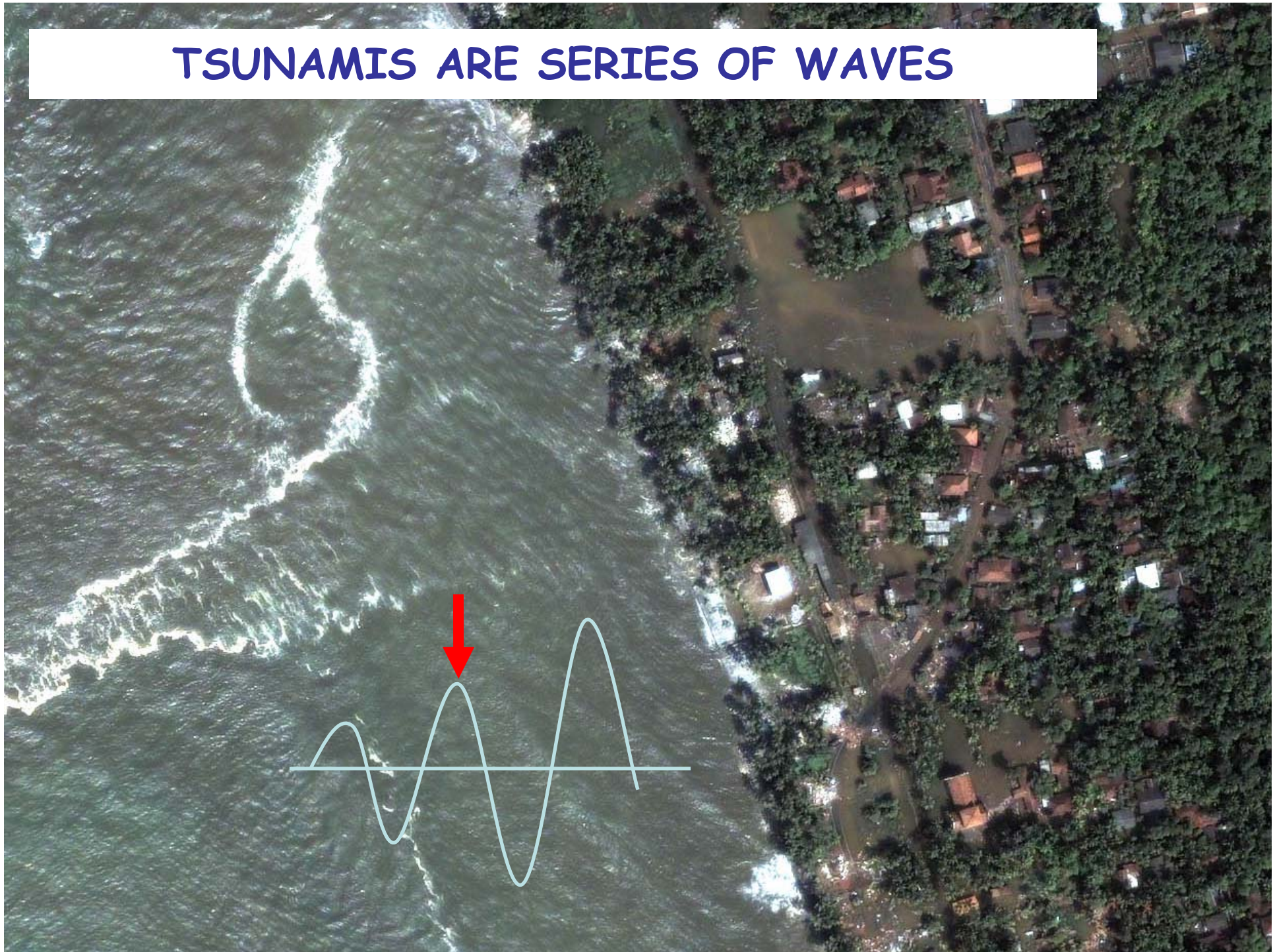
The 2004
megatsunami
arriving on Kalutara
Beach, Sri Lanka.
Graphic attributed
to Sri Lankan
engineers.



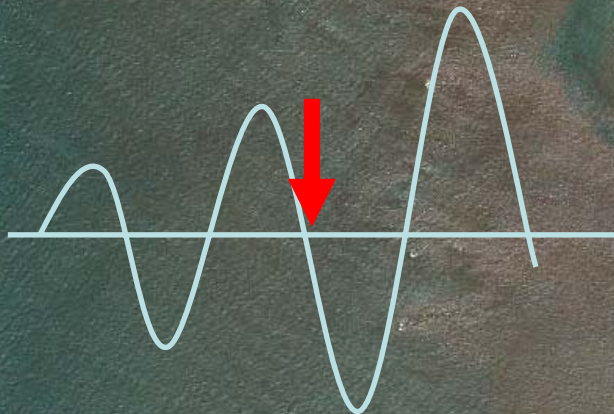
TSUNAMIS ARE SERIES OF WAVES



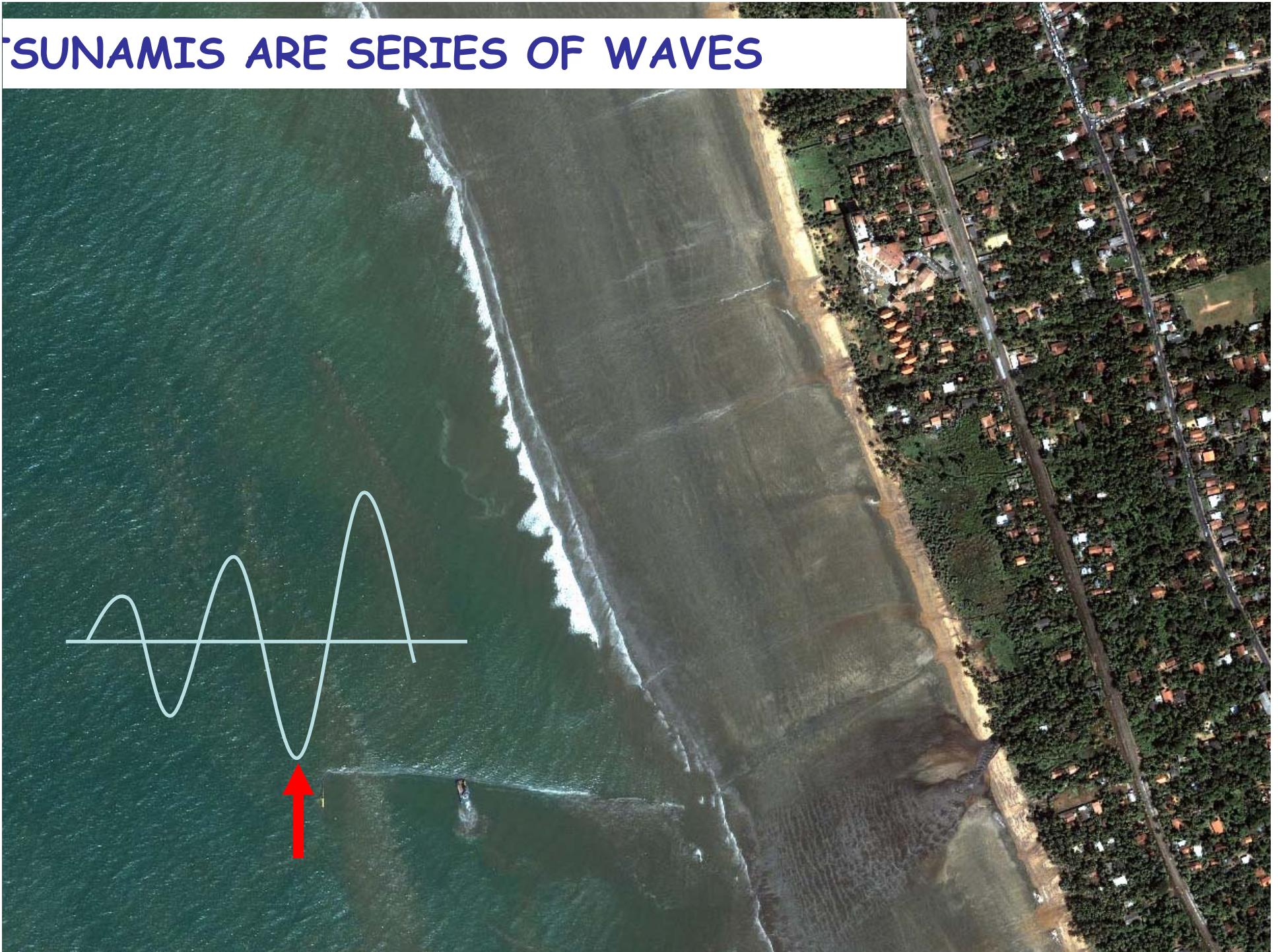
TSUNAMIS ARE SERIES OF WAVES



TSUNAMIS ARE SERIES OF WAVES



SUNAMIS ARE SERIES OF WAVES

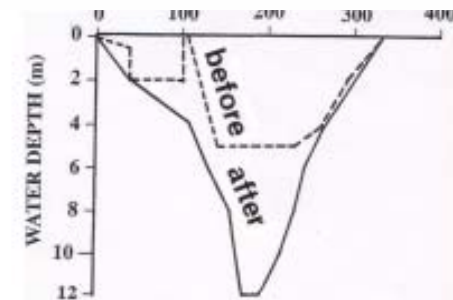
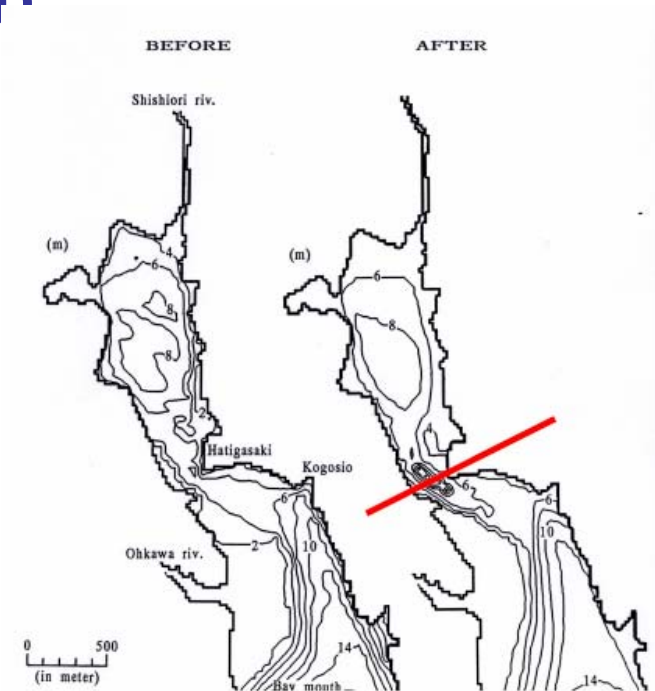


TSUNAMI CAN ERODE (SCOUR) (during run-down)



Road bed
destroyed
Panadura, Sri Lanka
26 December 2004

Tsunami scouring away river bed
Port Mathurin, Rodrigues
26 December 2004



Kesen-Numa Bay; Japan
1960 tsunami (Prof. Shuto)

TSUNAMI CAN CAUSE RESONANCE

Crescent City harbor oscillated approximately 5 hours after the November 15, 2006 event.

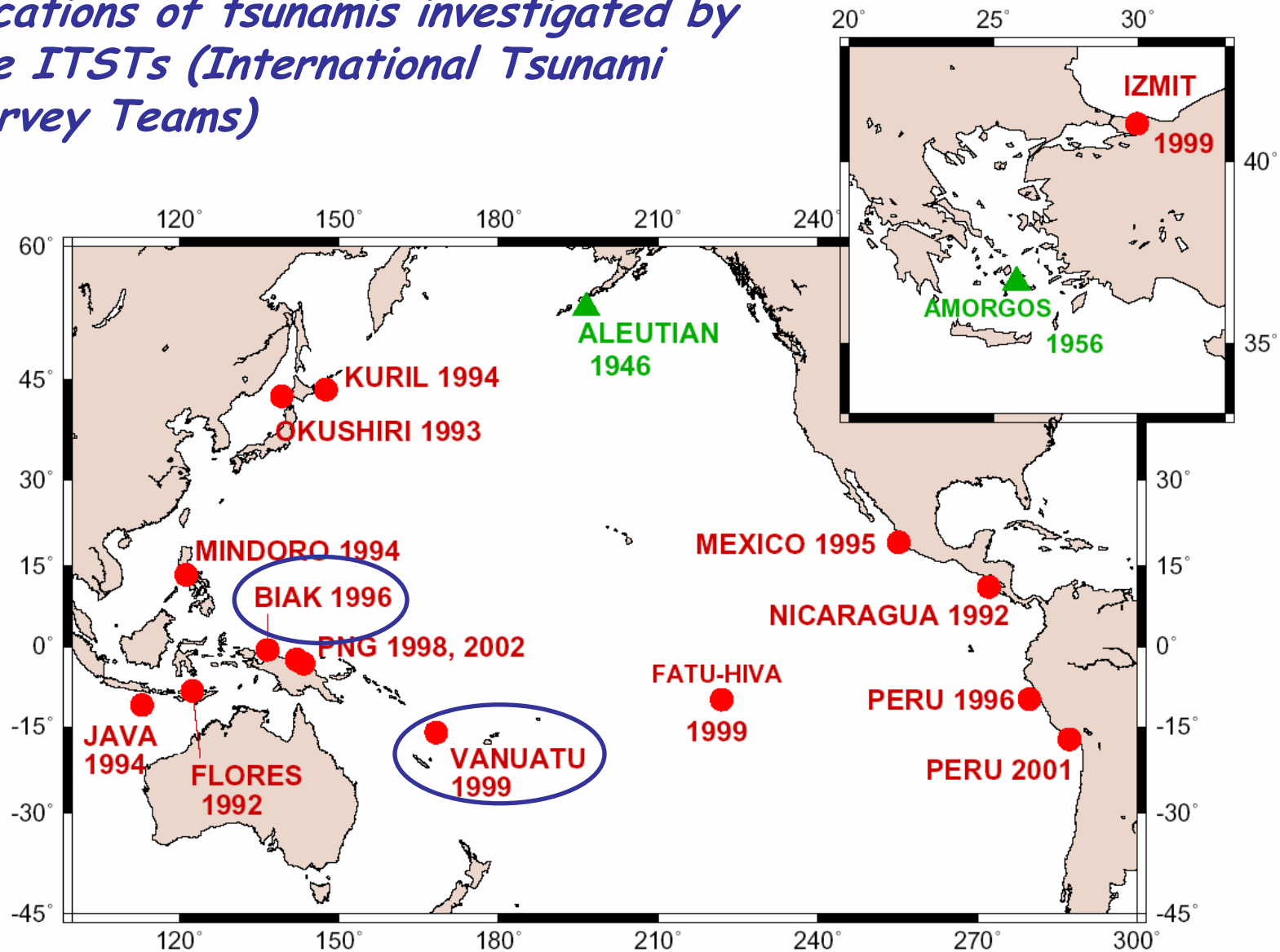
The far field impact has been evaluated qualitatively correctly for the 15 November 2006 event, with the exception of the harbor oscillations observed in Crescent City following the 2006 event - inside ports, computations at much higher resolution are required.

WHAT CAN THE SCIENTIST DO?

- Theoretical studies
- Laboratory experiments
- Post-tsunami surveys
- Numerical simulations
- Research and development for real-time warning
- Education and outreach

Tsunami hydrodynamic modeling had several facets, by necessity, and was driven may be the post tsunami surveys performed during the last decade which kept identifying novel problem geometries.

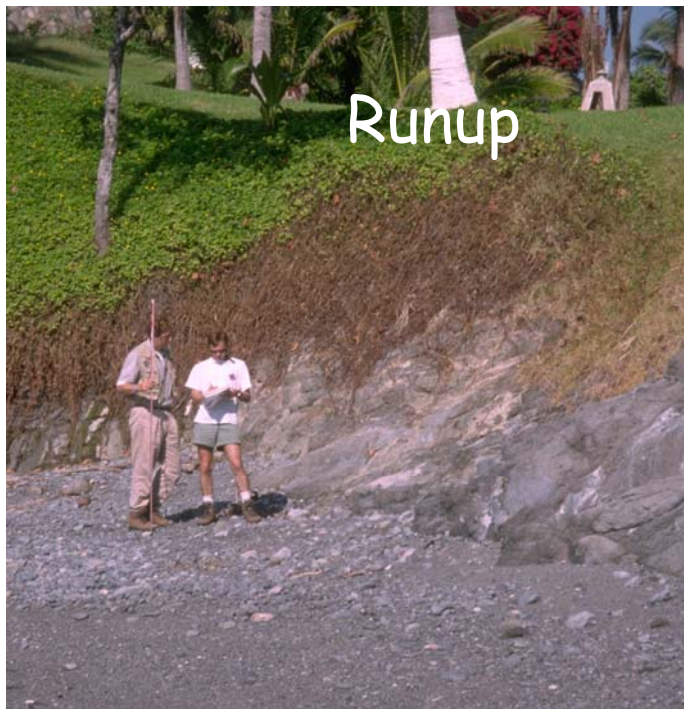
Locations of tsunamis investigated by the ITSTs (International Tsunami Survey Teams)



<http://www.usc.edu/dept/tsunamis/>

Goals of Tsunami Field Surveys - I

Collect Runup and Inundation Data



Mexico 1995



Peru 2001

Note ephemeral nature of watermark data.

Goals of Tsunami Field Surveys - I

Collect Runup and Inundation Data



Flow Depth Measurements in Sri Lanka.

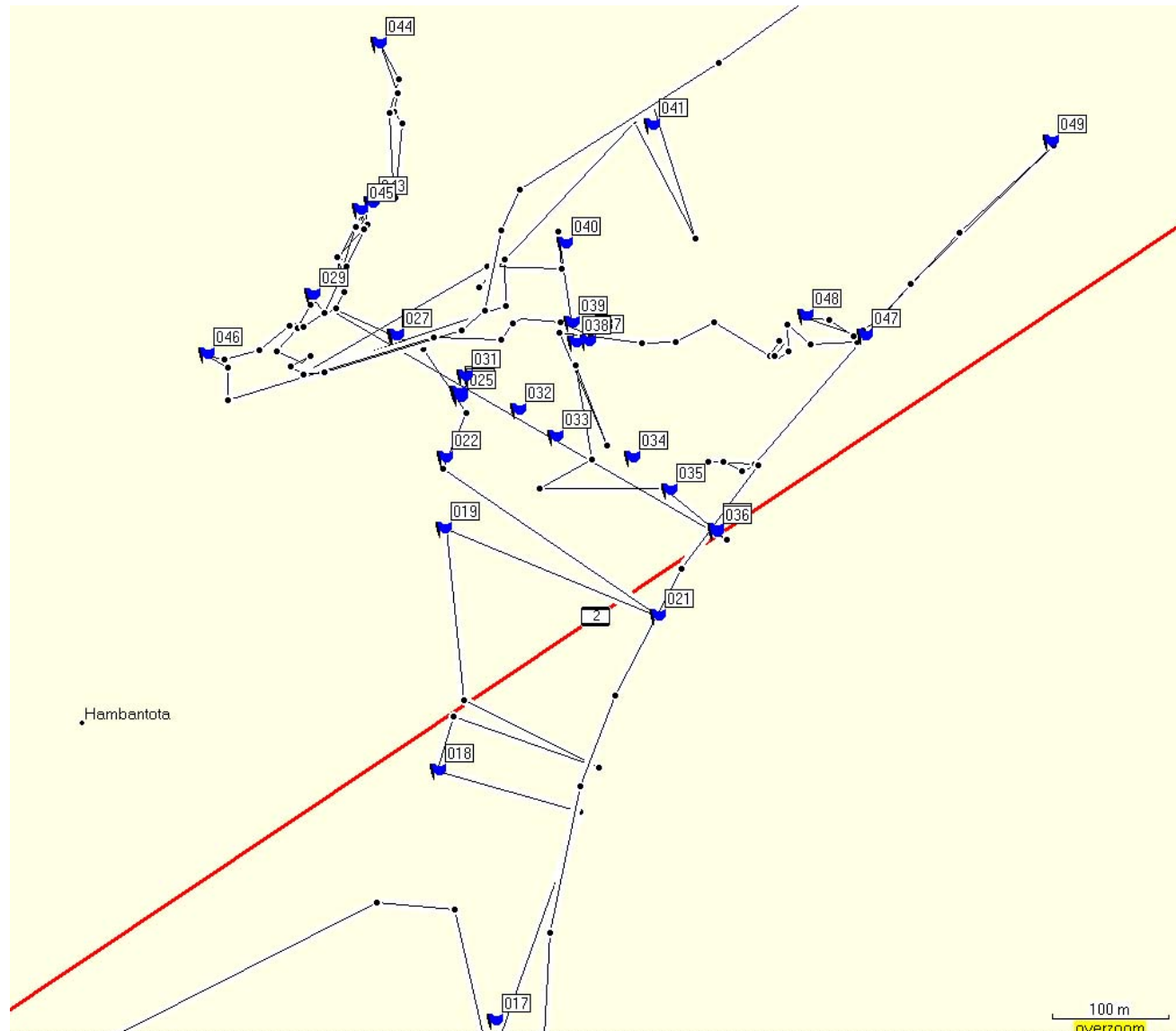
Flow depth measurements in the Maldives

Debris in Trees



Goals of Tsunami Field Surveys - I

Detailed GPS-Location and Elevation



Goals of Tsunami Field Surveys - II

Record eyewitness accounts



Turkey 1999



Vanuatu 1999

Human memory
fades fast

Timing

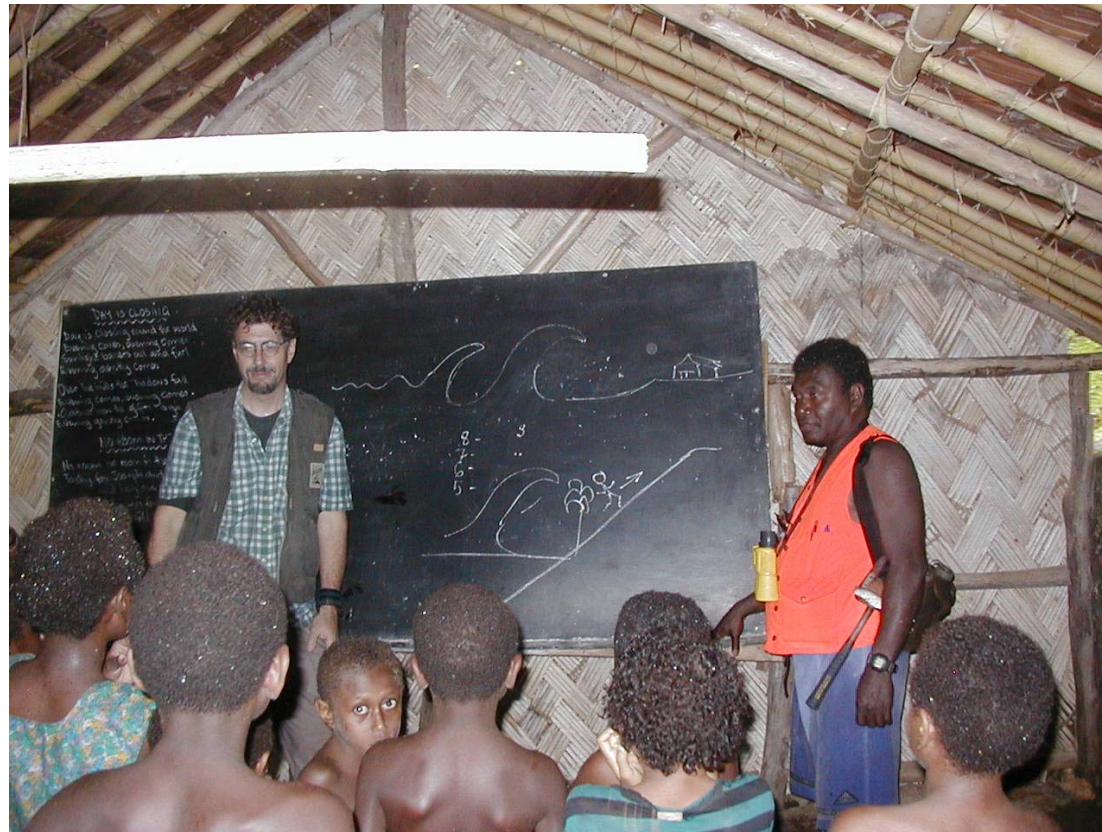
Number of waves

Sequence of events

Direction

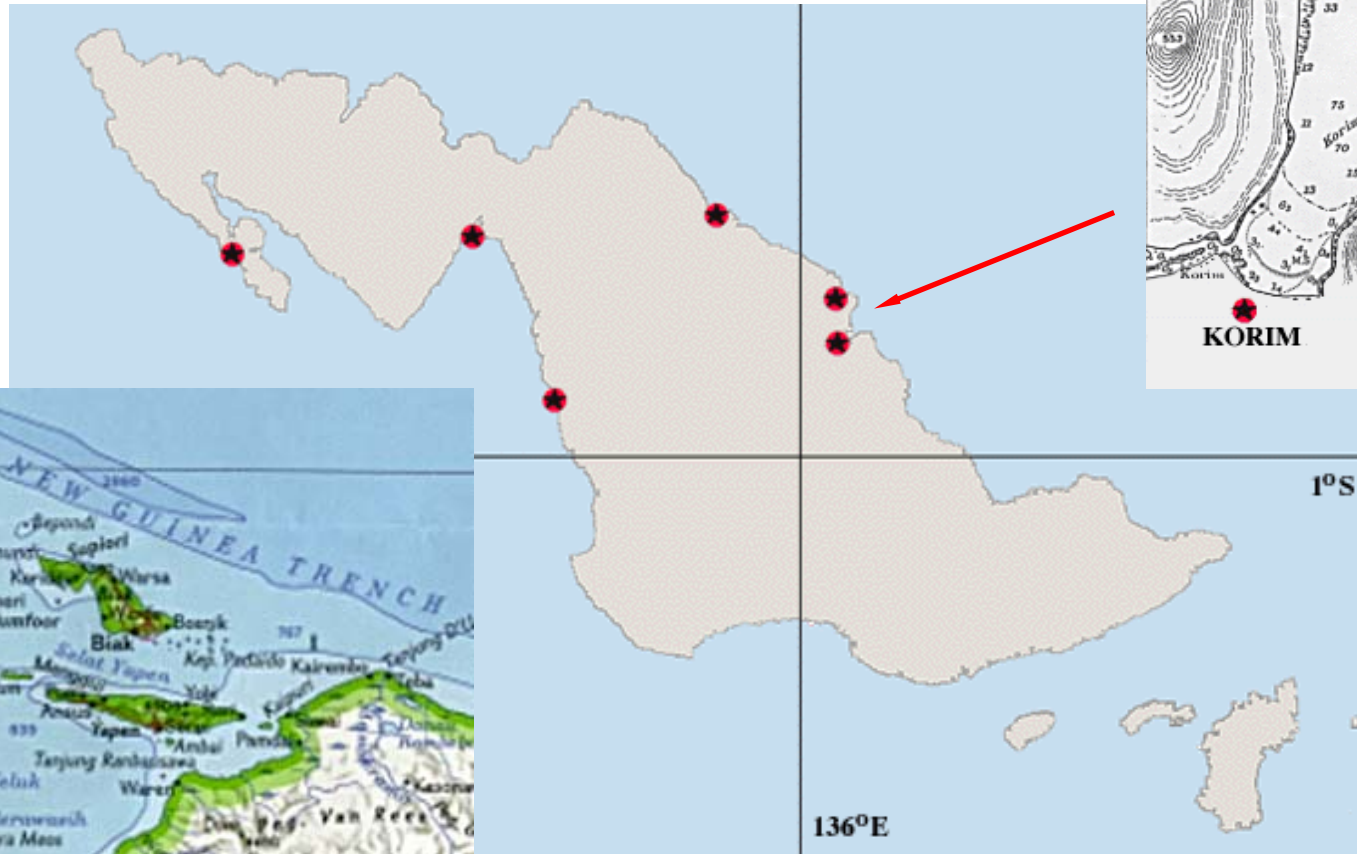
Goals of Field Surveys - III

Education and Public Outreach



Vanuatu 1999

February 17, 1996: Biak Island, Indonesia





Once there was a town here!...



Approximately 600m inland.

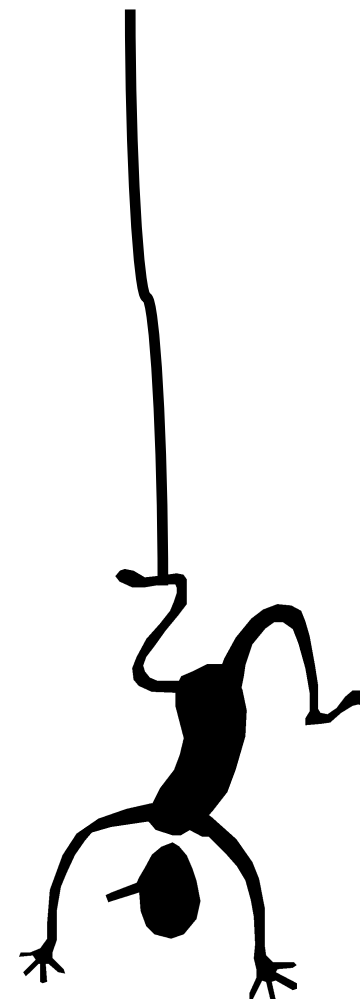
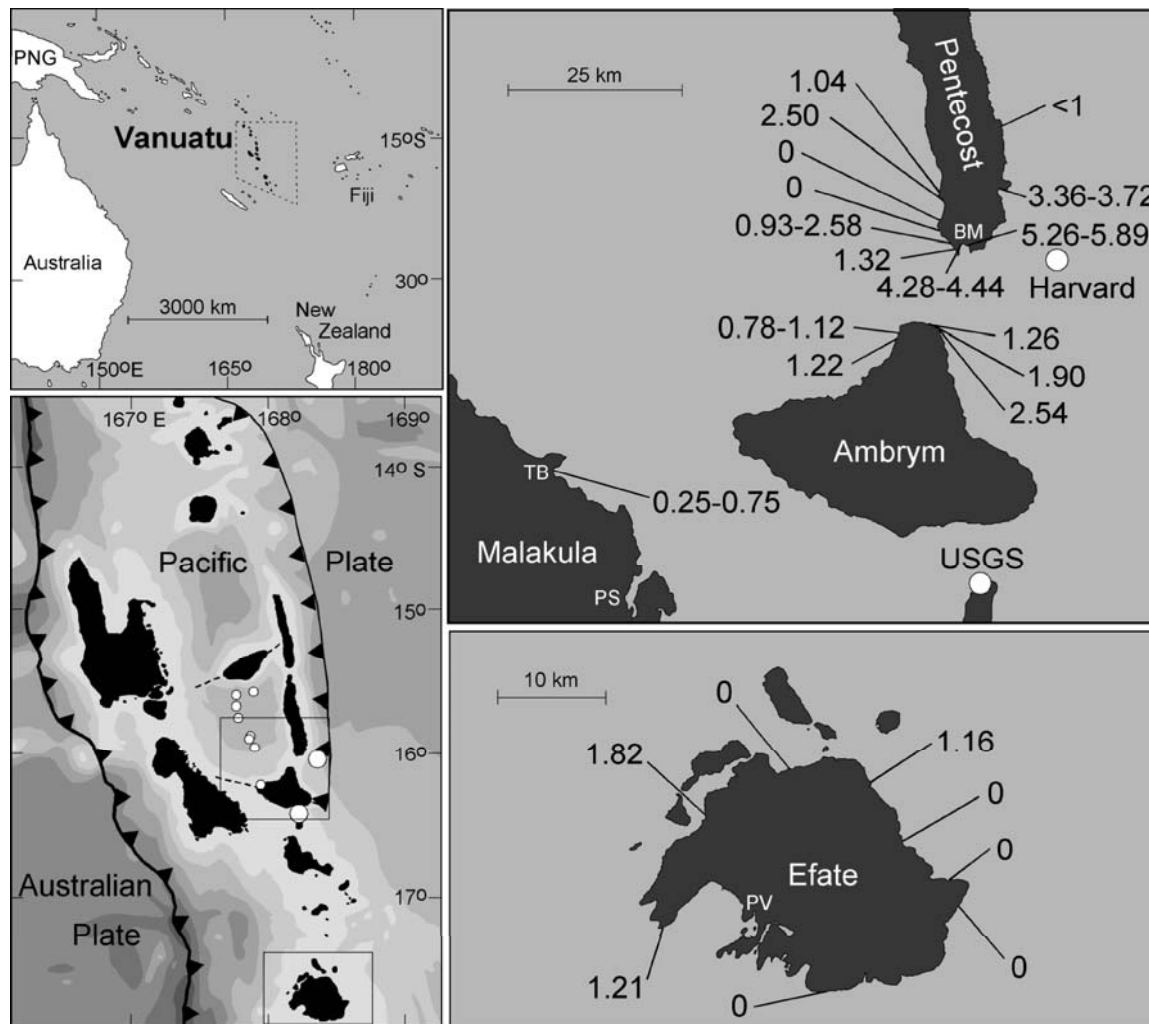
Wave height was about 4m.



This concrete block was moved 200m.



November 26, 1999: Penthacost Island, Vanuatu







The **Shallow Water** Wave (SW) equations are derived directly by depth-averaging the **Navier-Stokes** equations (Newton's law applied on moving fluid element), by assuming hydrostatic pressure, and neglecting viscous forces,

$$\begin{aligned} h_t + (uh)_x + (vh)_y &= 0, \\ u_t + uu_x + vu_y + gh_x &= gd_x, \\ v_t + uv_x + vv_y + gh_y &= gd_y, \end{aligned}$$

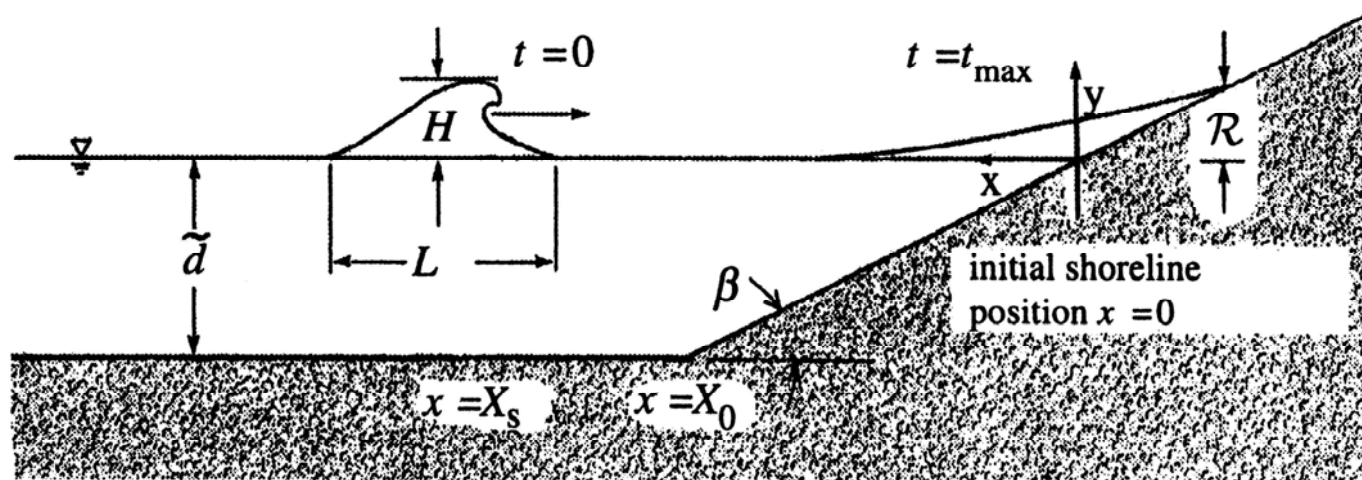
The total depth is $h(x,y,t)$, while $d(x,y,t)$ is the **deforming** seafloor. The undisturbed water surface is a $z=0$, and the **wave amplitude is $\eta(x,y,t)$** where $h(x,y,t) = d(x,y,t) + \eta(x,y,t)$. $d(x,y,t)$ is generally presumed known, so that there are three unknown variables $u(x,y,t)$, $v(x,y,t)$ and $\eta(x,y,t)$, where u,v are the **depth averaged** velocities.

These three equations are referred to as the **Nonlinear Shallow Water** wave equations (NSW). They can also be written in spherical coordinates with the Coriolis accelerations included. When linearized, they can be combined into a single equation,

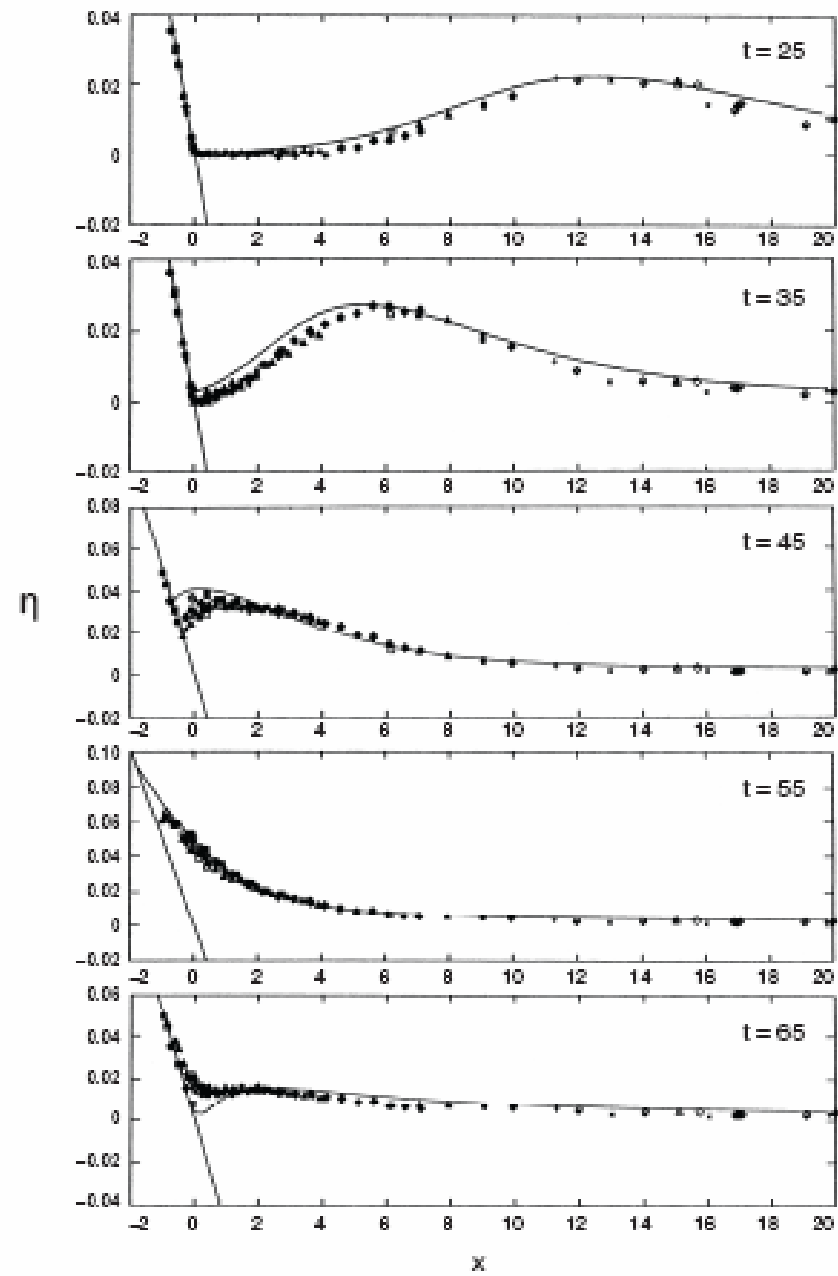
$$g \frac{\partial}{\partial x} \frac{\partial(h\eta)}{\partial x} + g \frac{\partial}{\partial y} \frac{\partial(h\eta)}{\partial y} = \frac{1}{c} \frac{\partial^2 \eta}{\partial t^2}$$

also referred to as the **Linear Shallow Water Wave equation** (LSW).

The solitary wave was the standard model for the leading wave of a tsunami up until the 1990s. It is well described mathematically, and has the unusual property that when it propagates over constant depth, it doesn't change its shape too much. - If in fact one uses nonlinear-dispersive theory, it doesn't change its shape at all. Since tsunamis are such long waves, they generally don't change their shape appreciably as they move over the deep ocean solitary waves were believed to be a good model for tsunamis.



Offshore Height/Depth=0.02. The initial shoreline is at $x=0$, the continental shelf with constant depth starts at $x=20$.



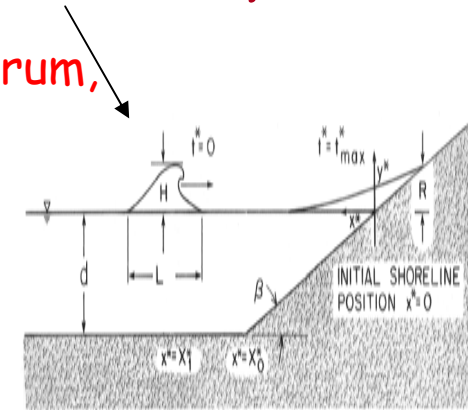
Solving the Linear Shallow Water Wave Equation for this problem

Following Synolakis (1987), for an incoming wave spectrum,

$$\eta(x_1, t) = \int_{-\infty}^{\infty} \Phi(\omega) e^{-i\omega t} d\omega,$$

Then the transmitted wave to the beach is given

$$\eta(x, t) = 2 \int_{-\infty}^{\infty} \Phi(\omega) \frac{J_0(2\omega \sqrt{x \cot \beta}) e^{-i\omega(x_0+t)}}{J_0(2\omega \cot \beta) - iJ_1(2\omega \cot \beta)} d\omega,$$



For an offshore solitary wave, $\Phi(\omega) = \omega \operatorname{cosech}(\alpha\omega)$, then

$$\eta(x, t) = \frac{4}{3} \int_{-\infty}^{\infty} \omega \operatorname{cosech}(\alpha\omega) \frac{J_0(2\omega \sqrt{x x_0}) e^{-i\omega(x_0-x_1+t)}}{J_0(2x_0\omega) - iJ_1(2\tilde{x}_0\omega)} d\omega,$$

For large x_0 the Laurent series is

$$\eta(x, t) = \frac{4\pi^2}{3\alpha^2} \left(\frac{x_0}{x}\right)^{1/4} \sum_{n=1}^{\infty} (-1)^{n+1} n e^{-(\pi/a)\theta' n};$$

The max of the power series is easy to find, hence

$$\frac{\eta_{\max}}{H} = \left(\frac{x_0}{x}\right)^{1/4} = \left(\frac{1}{h_0}\right)^{1/4};$$

This is Green's law rediscovered, but valid with reflection included. All variables are normalized.

Finding the maximum runup of solitary waves using LSW

The shoreline motion is $R(t)=\eta(0,t)$ and one expands for $x \rightarrow 0$

$$R(t) = 8H \sum_{n=1}^{\infty} \frac{(-1)^{n+1} n e^{-2\gamma(x_1 - x_0 - t)n}}{I_0(4\gamma x_0 n) + I_1(4\gamma x_0 n)}.$$

For large $4\gamma x_0$ the series becomes a power series $\sum_{n=1}^{\infty} (-1)^{n+1} n^{3/2} \chi^n$

The maximum runup $\mathbf{R} = R(t)_{max}$ is given simply by the equation

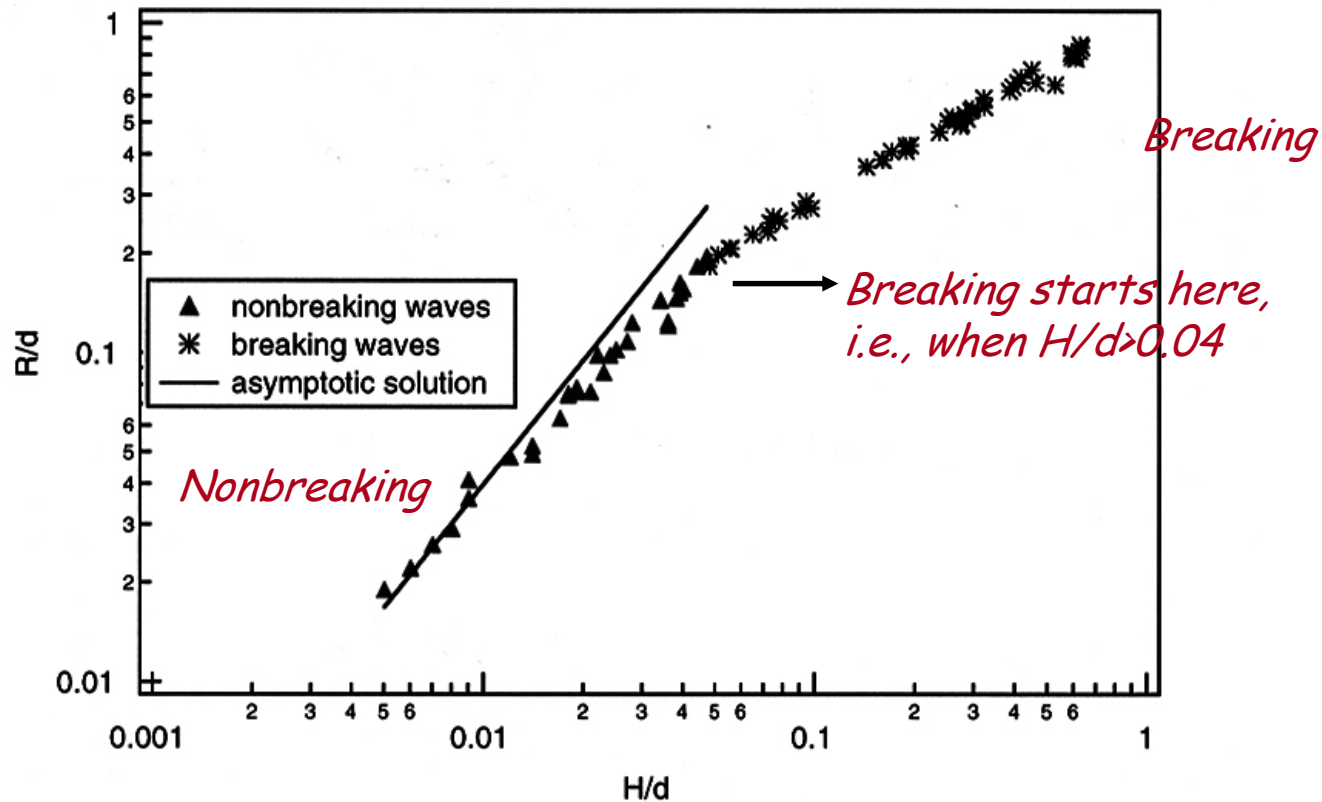
$$\mathbf{R} = 2.831 \sqrt{\cot \beta} H^{\frac{5}{4}}.$$

Recall that H is the "soliton" height from $\eta(x, 0) = H \operatorname{sech}^2 \gamma(x - x_1)$,

Synolakis, JFM, 1987

Comparison of analytic solution of the NSW and LSW with laboratory measurements for solitary wave runup.

Standard for 1+1 in the 1st NSF Workshop on Long Wave Runup.



Symbols are laboratory measurements.

Synolakis, 1987

Note the different regimes for breaking and nonbreaking solitary waves.

Milestones: Nicaragua 1992

Runup = 5 m



Playa Popoyo

Slow, "tsunami" earthquake, locally not felt on the beaches. Reports of spurious shoreline recession.

More than 160 dead.

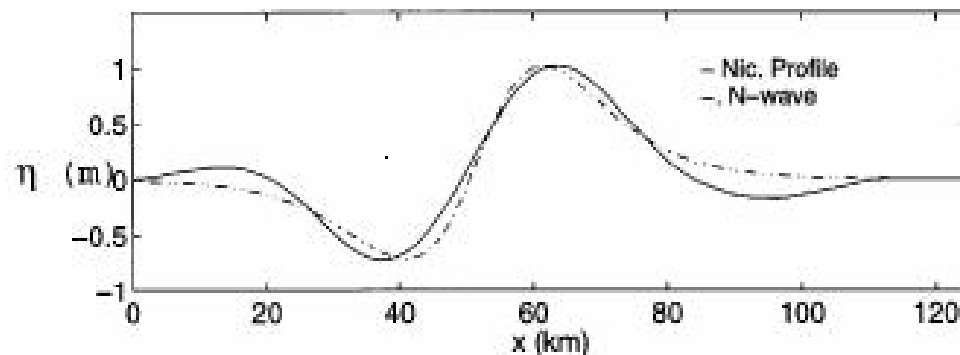
Numerical simulations of event revealed factor of 10 differences with threshold-type SW models of early 90s.

Milestones: Nicaragua 1992 -1-

There were two major observations regarding 1992 Nicaraguan tsunami.

One, for coastal residents, the only evidence of incoming tsunami attack was the shoreline recession, who regrettably (and very much as tens of thousands during the 2004 Boxing Day tsunami) did not identify it as such.

Tsunamis sometimes arrive to the target coastlines as a leading depression N-wave (LDN), i.e., elevation wave with a trough in front.



Milestones: Nicaragua 1992

Before 1992, LDN waves were believed to be hydrodynamically unstable, the crest was supposed to quickly overtake the trough.

This 1992 manifestation of the initial shoreline withdrawal led Tadepalli and Synolakis (1994) to propose a model for the leading depression N-wave.

Yet, even the additional reports of the LDN waves striking the south coast of Java, Mindoro Island and Shitokan Island, three more tsunamigenic earthquakes in 1994, the reports did little to settle the controversy.

Milestones: Mexico 1995

On 9 October 1995, an $M_0=1.15 \times 10^{28} \text{ dyn cm}$ earthquake struck Manzanillo, Mexico and generated a moderate tsunami.

The parent earthquake was the largest to strike the Mexican coastline since the 1932, yet the runup ranged mostly up to 4m with extreme values of 11m on steep coastal cliffs.

The ITST survey was able to acquire two series of photographs from eyewitnesses (Borrero et al. 1997).

Milestones: Manzanillo Mexico, 1995 -1-

In the first, a family was sitting in a veranda of their hotel in the steep coastal cliffs on the south end of Manzanillo. As soon as they felt the ground shake, they noted the Manzanillo Bay emptying. They took a photograph, believed to be the first documented observation of a leading-depression N-wave causing shoreline recession.



First physical evidence of leading depression N-wave, analytical results.

On a usual day.

October 9, 1995

How does one model a moving seafloor rupture ?

Consider the forced linear wave equation,

$$\eta_{tt} - \eta_{xx} = h_{0tt}.$$

With a step function type seafloor forcing (zipping)

$$h_0(x, t) = -(2\mathcal{E}\mathcal{H}/\gamma)\tanh[\gamma(x - t)].$$

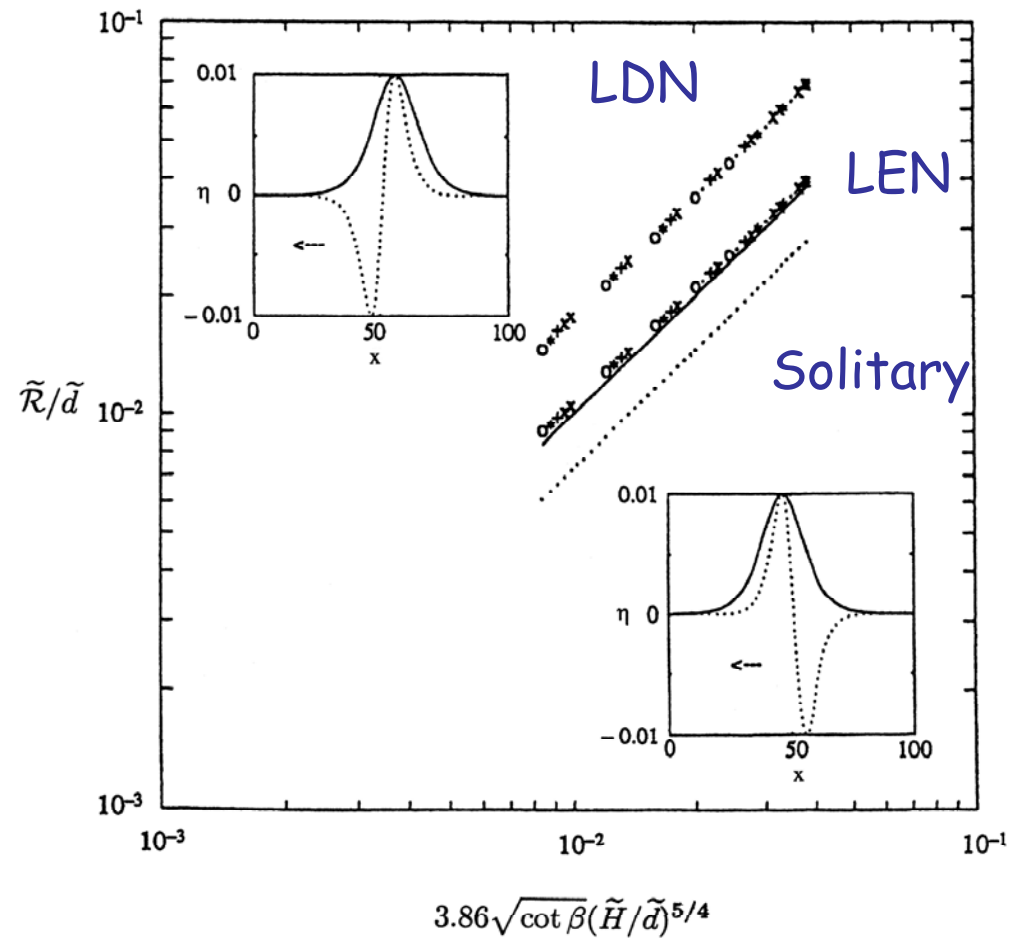
By sheer luck, the exact solution is

$$\eta(x, 0) = \frac{3\sqrt{3}\mathcal{H}}{2}\operatorname{sech}^2[\gamma(x - x_1)]\tanh[\gamma(x - x_1)],$$

Using the earlier asymptotic formalism, the maximum runup is

$$\mathbf{R}_{\text{Nwave}} = 3.86(\cot\beta)^{\frac{1}{2}}\mathcal{H}^{5/4}.$$

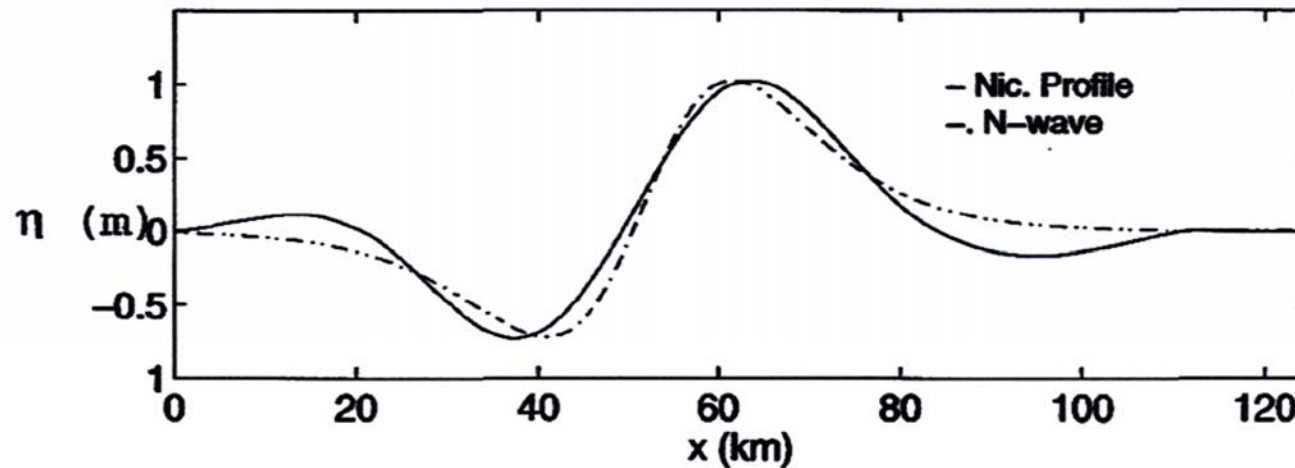
Comparison of the asymptotic expansions for the maximum runup of N-waves and solitary waves.



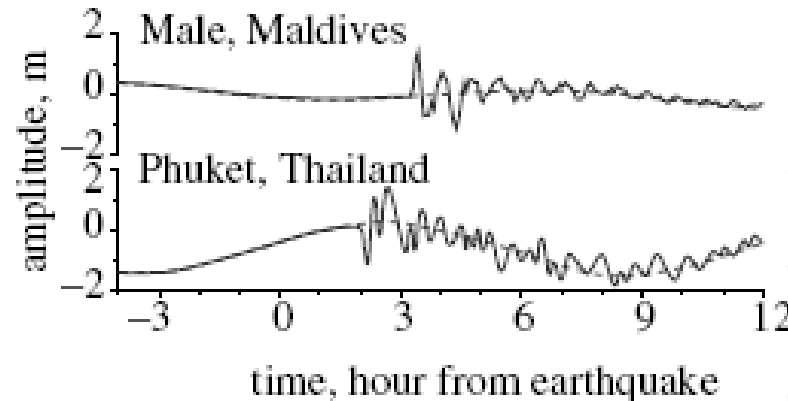
Tadepalli and Synolakis, ProSoc, 1994

Comparison of the initial wave of the 1992 Nicaraguan profile as calculated using MOST and fitted with a leading depression N-wave (LDN).

Runup prediction was 6m using LDN asymptotic solutions, 7m using MOST, 8m measured on the field.



Titov and Synolakis, GRL, 1998

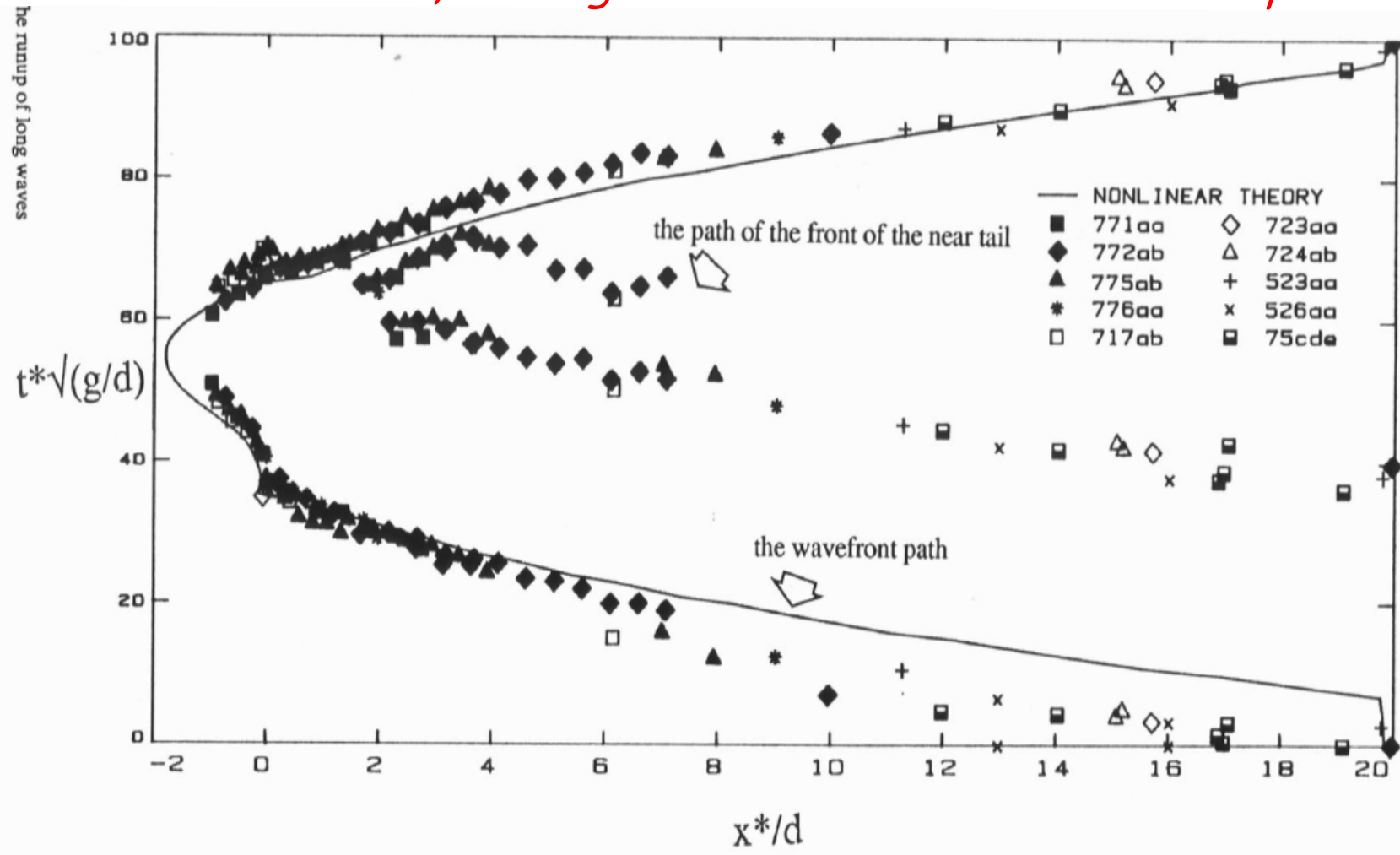


Milestones: Manzanillo Mexico, 1995 -2-



In the other series of photographs, taken by the local tortilla maker in a cart at the square in la Manzanilla, one can see three men running away from the tsunami, which reached a maximum runup of 2m on the mild beach fronting the town. What is remarkable is that despite the thin advancing tsunami front, and its small overall size, the eyewitnesses could not outrun it. The observation was not quantitatively analyzed at the time. Fritz et al. (2006) study tsunami flow velocity for the 2004 Boxing Day Tsunami at Banda Aceh. They applied a cross-correlation based particle image velocimetry rectifying video images to determine instantaneous tsunami flow velocity on dry land in the range of 2 to 5m/s.

The shoreline path (wavefront path) for a $H/d=0.02$ solitary wave up a 1:20 beach. The shoreline is at $x=0$. Notice how the wave speed dx/dt decreases, then increases suddenly when the wavefront hits the shoreline, then again decreases to maximum runup.



Could this be a possible explanation why victims during tsunami attacks appear mesmerized and do not self-evacuate until too late? (Synolakis and Bernard, Phil. Trans. Roy. Soc. A, 2006)

Milestones: Nicaragua 1992 -2-

The second observation is that the runup values along the Nicaraguan coastline ranged up to 11m in El Transito, the most devastated locale. Yet, in the adjoining Playa Hermosa, even the beach umbrellas had been left standing, as widely noted then in local newspapers.

The reef fronting the devastated El Transito during the Nicaraguan 1992 event had an opening to allow for easier navigation, hence its rapid development as a fishing village. The adjacent Playa Hermosa that was largely spared did not.

During the 1993 tsunami at Aonae, a manmade dune and about 50 concrete wave protectors channeled the tsunami into the populated portions of the town, while protecting the unpopulated areas.

In Sri Lanka, the Sumudra Devi, a passenger train out of Colombo, was derailed and overturned by the tsunami killing more than 1000. In the immediate fronting area, significant coral mining had occurred, related to tourism development.

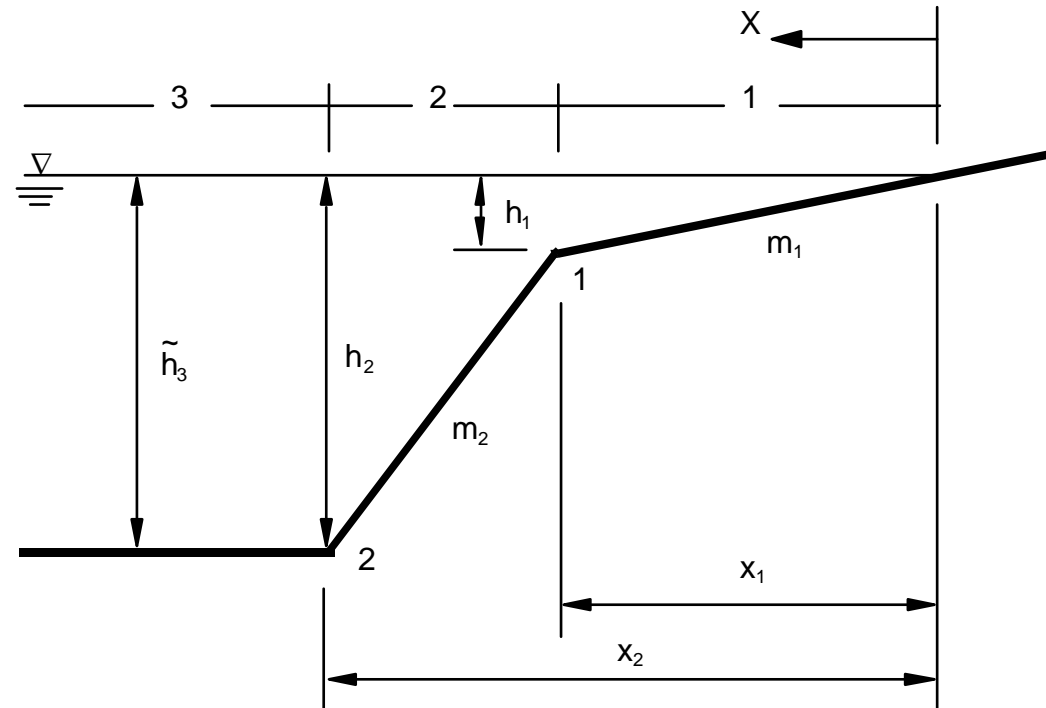
In Patong Beach, Thailand, a less than 60 cm high seawall separating the beach from the road reduced impact velocity.

Mangroves were observed to have protected coastal communities in southeastern India.

Milestones: Nicaragua 1992 -2-

These observations underscored the difficulty with using tsunami intensity scales which had been proposed by analogy to seismic intensity scales. Tsunami damage can vary substantially between adjacent locations, hence characterizing a historic tsunami by a single number from a single historical report may not be meaningful.

Continental Shelf and Slope



Choosing the undisturbed water depth as characteristic length scale; the linear shallow water wave equation that describes a propagation problem in water of variable depth $h_0(x)$ is,

$$\eta_{tt} - (\eta_{xx} h_0)_{xx} = 0.$$

Formulation of the Solution

Assuming a time harmonic dependence of the form

$$\eta(x, t) = \mathcal{A}(x) e^{-i\omega t}, \quad h_0(x) \frac{d^2 \mathcal{A}}{dx^2} + \frac{dh_0}{dx} \frac{d\mathcal{A}}{dx} + \omega^2 \mathcal{A} = 0.$$

In regions of constant depth, $h_0(x) = h_c$,

$$h_c \frac{d^2 \mathcal{A}}{dx^2} + \omega^2 \mathcal{A} = 0,$$

$$\eta(x, t) = \left\{ A^1 e^{-\frac{i\omega x}{\sqrt{h_c}}} + B^1 e^{\frac{i\omega x}{\sqrt{h_c}}} \right\} e^{-i\omega t}.$$

In regions of linearly varying depth, $h_0(x) = mx + n$, ($m \neq 0$),

$$(mx + n) \frac{d^2 \mathcal{A}}{dx^2} + m \frac{d\mathcal{A}}{dx} + \omega^2 \mathcal{A} = 0,$$

$$\eta(x, t) = \left\{ A^2 J_0(2\omega \sqrt{(x + n/m)/m}) + B^2 Y_0(2\omega \sqrt{(x + n/m)/m}) \right\} e^{-i\omega t}.$$

REGION 1 $0 < x < x_1$, $h_1(x) = \frac{h_1}{x_1}x = m_1x$;

$$\eta_1(x, t) = B J_0\left(\frac{2\omega\sqrt{h_1(x)}}{m_1}\right) e^{-i\omega t},$$

REGION 2 $x_1 < x < x_2$, $h_2(x) = \frac{1-h_1}{x_2-x_1}(x-x_1) + h_1 = m_2(x-x_1) + h_1$;

$$\eta_2(x, t) = \left\{ A^2 J_0\left(\frac{2\omega\sqrt{h_2(x)}}{m_2}\right) + B^2 Y_0\left(\frac{2\omega\sqrt{h_2(x)}}{m_2}\right) \right\} e^{-i\omega t}.$$

REGION 3 $x_2 < x < +\infty$, $h_3(x) = 1$;

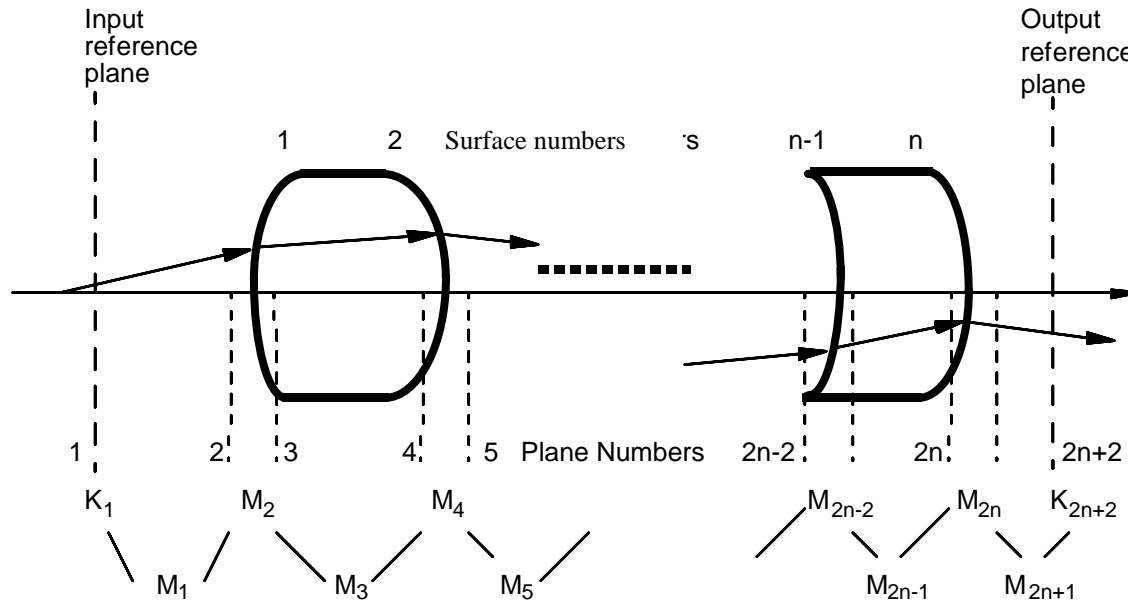
$$\eta_3(x, t) = \left\{ A^i e^{-\frac{i\omega x}{\sqrt{h_3}}} + A^r e^{\frac{i\omega x}{\sqrt{h_3}}} \right\} e^{-i\omega t}.$$

Boundary conditions:
 Continuity of surface elevation and surface slope

$$\mathfrak{x} = \mathfrak{x}_1 \begin{cases} B J_0\left(\frac{2\omega\sqrt{h_1}}{m_1}\right) = A^2 J_0\left(\frac{2\omega\sqrt{h_1}}{m_2}\right) + B^2 Y_0\left(\frac{2\omega\sqrt{h_1}}{m_2}\right), \\ B J_1\left(\frac{2\omega\sqrt{h_1}}{m_1}\right) = A^2 J_1\left(\frac{2\omega\sqrt{h_1}}{m_2}\right) + B^2 Y_1\left(\frac{2\omega\sqrt{h_1}}{m_2}\right). \end{cases}$$

$$\mathfrak{x} = \mathfrak{x}_2 \begin{cases} A^2 J_0\left(\frac{2\omega\sqrt{h_2}}{m_2}\right) + B^2 Y_0\left(\frac{2\omega\sqrt{h_2}}{m_2}\right) = A^i e^{-\frac{i\omega x_2}{\sqrt{h_3}}} + A^r e^{\frac{i\omega x_2}{\sqrt{h_3}}}, \\ A^2 J_1\left(\frac{2\omega\sqrt{h_2}}{m_2}\right) + B^2 Y_1\left(\frac{2\omega\sqrt{h_2}}{m_2}\right) = A^i i e^{-\frac{i\omega x_2}{\sqrt{h_3}}} - A^r i e^{\frac{i\omega x_2}{\sqrt{h_3}}}. \end{cases}$$

Analogy



$$K_{2n+2} = (M_{2n+1} M_{2n} M_{2n-1} \dots M_3 M_2 M_1) K_1$$

The propagation of a paraxial ray through an optical system containing n refracting surfaces separated by $(n-1)$ gaps.

$$\begin{pmatrix} J_0\left(\frac{2\omega\sqrt{k_1}}{m_1}\right) \\ J_1\left(\frac{2\omega\sqrt{k_1}}{m_1}\right) \end{pmatrix} B = \begin{pmatrix} J_0\left(\frac{2\omega\sqrt{k_1}}{m_2}\right) & Y_0\left(\frac{2\omega\sqrt{k_1}}{m_2}\right) \\ J_1\left(\frac{2\omega\sqrt{k_1}}{m_2}\right) & Y_1\left(\frac{2\omega\sqrt{k_1}}{m_2}\right) \end{pmatrix} \begin{pmatrix} A^2 \\ B^2 \end{pmatrix},$$

$$\begin{pmatrix} J_0\left(\frac{2\omega\sqrt{k_2}}{m_2}\right) & Y_0\left(\frac{2\omega\sqrt{k_2}}{m_2}\right) \\ J_1\left(\frac{2\omega\sqrt{k_2}}{m_2}\right) & Y_1\left(\frac{2\omega\sqrt{k_2}}{m_2}\right) \end{pmatrix} \begin{pmatrix} A^2 \\ B^2 \end{pmatrix} = \begin{pmatrix} e^{-\frac{i\omega x_2}{\sqrt{k_3}}} & e^{\frac{i\omega x_2}{\sqrt{k_3}}} \\ ie^{-\frac{i\omega x_2}{\sqrt{k_3}}} & -ie^{\frac{i\omega x_2}{\sqrt{k_3}}} \end{pmatrix} \begin{pmatrix} A^i \\ A^r \end{pmatrix}.$$

$$S_{11}V_1 = S_{12}V_2,$$

$$S_{22}V_2 = D_{23}V_3,$$

$$S_{11}B = S_{12}S_{22}^{-1}D_{23}V_3.$$

- Formally equivalent to the system of equations,
- A direct evaluation of an analytical expression for amplification factor **B** in terms of initial wave amplitude **Aⁱ**,
- Requires simply multiplication of rank two matrices.

General Method

A new formalism to obtain a single matrix equation

Associate each constant-depth segment of depth

$$D_{pr} = \begin{pmatrix} e^{-i\omega x_p / \sqrt{h_r}} & e^{i\omega x_p / \sqrt{h_r}} \\ i\varepsilon e^{i\omega x_p / \sqrt{h_r}} & -i\varepsilon e^{-i\omega x_p / \sqrt{h_r}} \end{pmatrix}.$$

Associate each linearly-varying depth segment of positive slope

$$S_{pr} = \begin{pmatrix} J_0(2\omega \sqrt{h_p/m_r}) & Y_0(2\omega \sqrt{h_p/m_r}) \\ J_1(2\omega \sqrt{h_p/m_r}) & Y_1(2\omega \sqrt{h_p/m_r}) \end{pmatrix}.$$

Associate each linearly-varying depth segment of negative slope

$$S_{pr} = \begin{pmatrix} J_0(2\omega \sqrt{h_p/|m_r|}) & Y_0(2\omega \sqrt{h_p/|m_r|}) \\ -J_1(2\omega \sqrt{h_p/|m_r|}) & -Y_1(2\omega \sqrt{h_p/|m_r|}) \end{pmatrix}.$$

$$P_{11}K_1 = \left\{ \prod_{j=1}^{m-2} Q_{j(j+1)} Q_{(j+1)(j+1)}^{-1} \right\} R_{(m-1)m} K_m.$$

Maximum Runup of Solitary Wave

For the incident wave is of the form

$$\eta(x, t) = \int_{-\infty}^{+\infty} \Phi(\omega) e^{-i\omega t} d\omega,$$

then the transmitted wave to the beach is given by

$$\eta_1(x, t) = \int_{-\infty}^{+\infty} \Phi(\omega) B(\omega) J_0\left(\frac{2\omega\sqrt{h(x)}}{m_1}\right) e^{-i\omega t} d\omega.$$

A solitary wave located at $x = X_s$ at $t = 0$ has

$$\eta(x, 0) = H \operatorname{sech}^2 \gamma(x - x_s), \quad \gamma = \sqrt{(3H/4)}.$$

$\Phi(\omega)$ associated with this profile is given by

$$\Phi(\omega) = (2/3) \omega \operatorname{cosech}(\alpha\omega) e^{i\omega x_s}, \quad \alpha = \pi/2\gamma.$$

$$B = -\frac{m_2}{\pi\omega\sqrt{h_1}} \frac{1}{\varphi + i\chi} e^{-\frac{i\omega x_2}{\sqrt{h_2}}}.$$

$$\mathcal{R}(t) = \eta(0, t) = -\frac{4}{3} \frac{m_2}{\pi\sqrt{h_1}} \int_{-\infty}^{+\infty} \operatorname{cosech}(\alpha\omega) \frac{1}{\varphi + i\chi} e^{i\omega(x_s - x_2 - t)} d\omega,$$

by Cauchy integral formula,

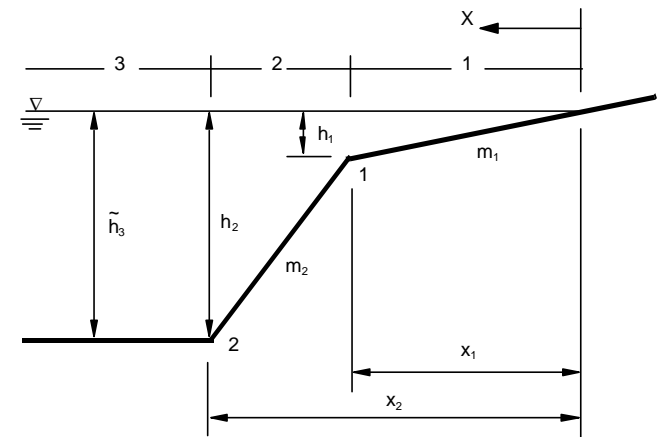
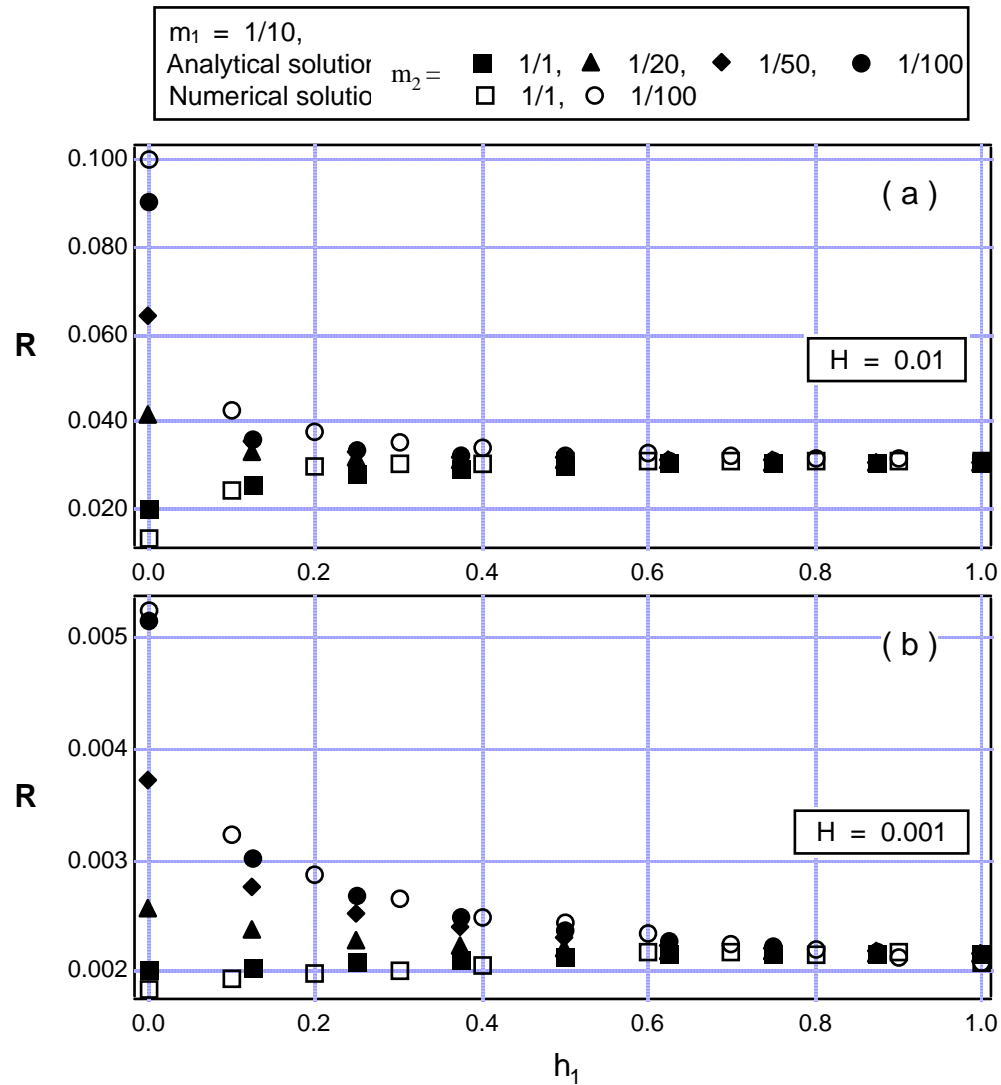
$$\mathcal{R}(t) = -(8/3) \frac{\pi^{3/2}}{\sqrt{m_1}} i \sum_{n=1}^{+\infty} (-1)^n \frac{1}{\alpha} \left(\frac{n\pi i}{\alpha}\right)^{3/2} \frac{e^{-\frac{n\pi}{\alpha}(x_s - x_2 - t)}}{\varphi(n\pi i/\alpha) + i\chi(n\pi i/\alpha)}.$$

Using asymptotic expansions of Bessel functions for large arguments,

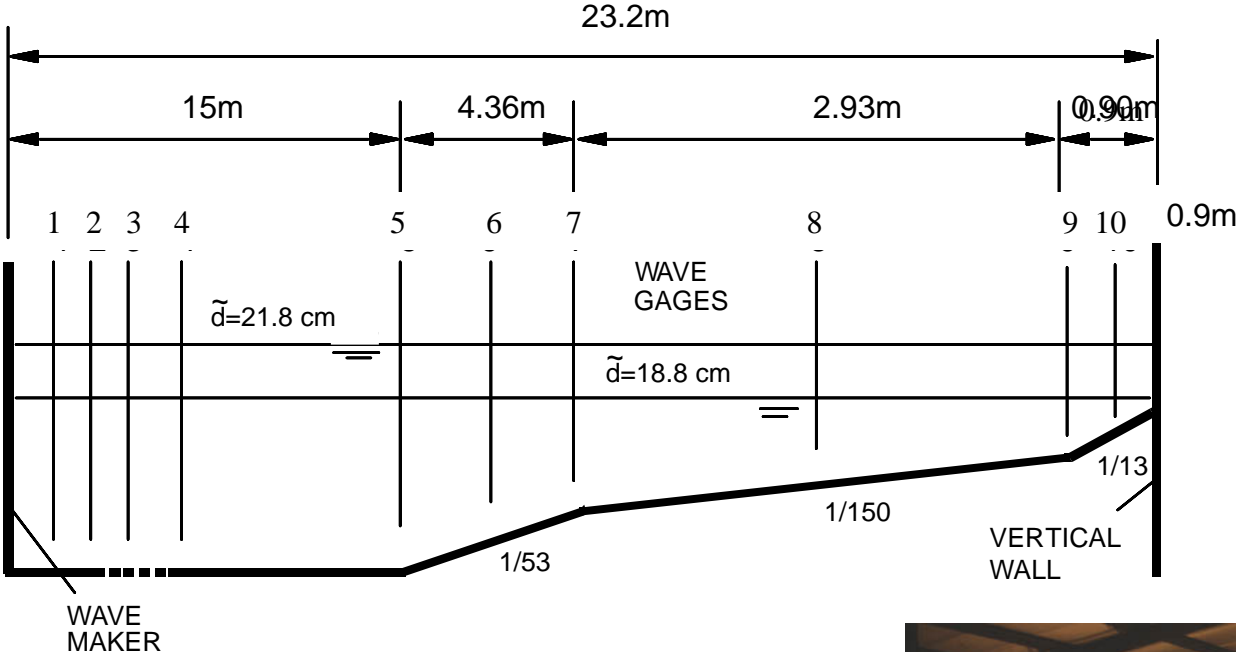
$$\mathcal{R}(t) = 8\sqrt{\pi} 3^{1/4} H^{5/4} \sum_{n=1}^{+\infty} (-1)^{n+1} n^{3/2} e^{-\frac{n\pi}{\alpha}(x_s - x_2 - t + 2(\frac{\sqrt{h_1}}{m_1} + \frac{1 - \sqrt{h_1}}{m_2}))}.$$

$$R = 2.831 (1/m_1)^{1/2} H^{1/4}$$

Maximum Runup of Solitary Wave Over Continental Slope and Shelf Bathymetry



Revere Beach



Kanoglu and Synolakis, 1998

Revere Beach, Analytical Solution

The following matrix equation must be solved to find the time histories of surface elevation or maximum runup

$$\begin{pmatrix} J_1\left(\frac{\omega\sqrt{h_0}}{m_1}\right) & Y_1\left(\frac{\omega\sqrt{h_0}}{m_1}\right) & 0 & 0 & 0 & 0 & 0 \\ J_0\left(\frac{\omega\sqrt{h_0}}{m_1}\right) & J_0\left(\frac{\omega\sqrt{h_0}}{m_1}\right) & -J_0\left(\frac{\omega\sqrt{h_0}}{m_1}\right) & -Y_0\left(\frac{\omega\sqrt{h_0}}{m_1}\right) & 0 & 0 & 0 \\ J_1\left(\frac{\omega\sqrt{h_0}}{m_1}\right) & Y_1\left(\frac{\omega\sqrt{h_0}}{m_1}\right) & -J_1\left(\frac{\omega\sqrt{h_0}}{m_1}\right) & -Y_1\left(\frac{\omega\sqrt{h_0}}{m_1}\right) & 0 & 0 & 0 \\ 0 & 0 & J_0\left(\frac{\omega\sqrt{h_0}}{m_2}\right) & Y_0\left(\frac{\omega\sqrt{h_0}}{m_2}\right) & -J_0\left(\frac{\omega\sqrt{h_0}}{m_2}\right) & -Y_0\left(\frac{\omega\sqrt{h_0}}{m_2}\right) & 0 \\ 0 & 0 & J_1\left(\frac{\omega\sqrt{h_0}}{m_2}\right) & Y_1\left(\frac{\omega\sqrt{h_0}}{m_2}\right) & -J_1\left(\frac{\omega\sqrt{h_0}}{m_2}\right) & -Y_1\left(\frac{\omega\sqrt{h_0}}{m_2}\right) & 0 \\ 0 & 0 & 0 & 0 & J_0\left(\frac{\omega\sqrt{h_0}}{m_3}\right) & Y_0\left(\frac{\omega\sqrt{h_0}}{m_3}\right) & -\frac{h_0}{c\sqrt{h_0}} \\ 0 & 0 & 0 & 0 & J_1\left(\frac{\omega\sqrt{h_0}}{m_3}\right) & Y_1\left(\frac{\omega\sqrt{h_0}}{m_3}\right) & \frac{h_0}{ic\sqrt{h_0}} \end{pmatrix} \begin{pmatrix} A_1 \\ B_1 \\ A_2 \\ B_2 \\ A_3 \\ B_3 \\ A_+ \end{pmatrix} = \begin{pmatrix} 0 \\ 0 \\ 0 \\ 0 \\ 0 \\ \frac{h_0}{c\sqrt{h_0}} \\ \frac{h_0}{ic\sqrt{h_0}} \end{pmatrix} A_+$$

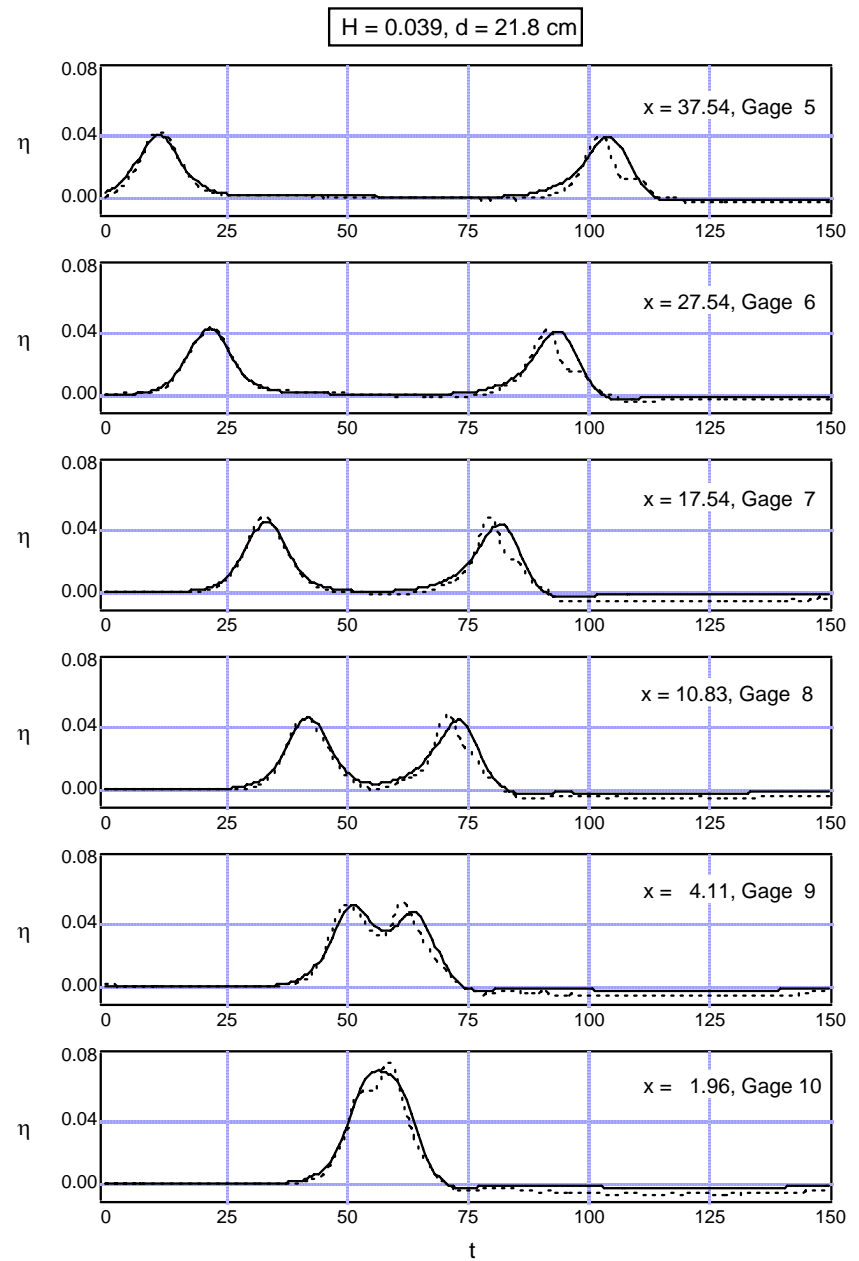
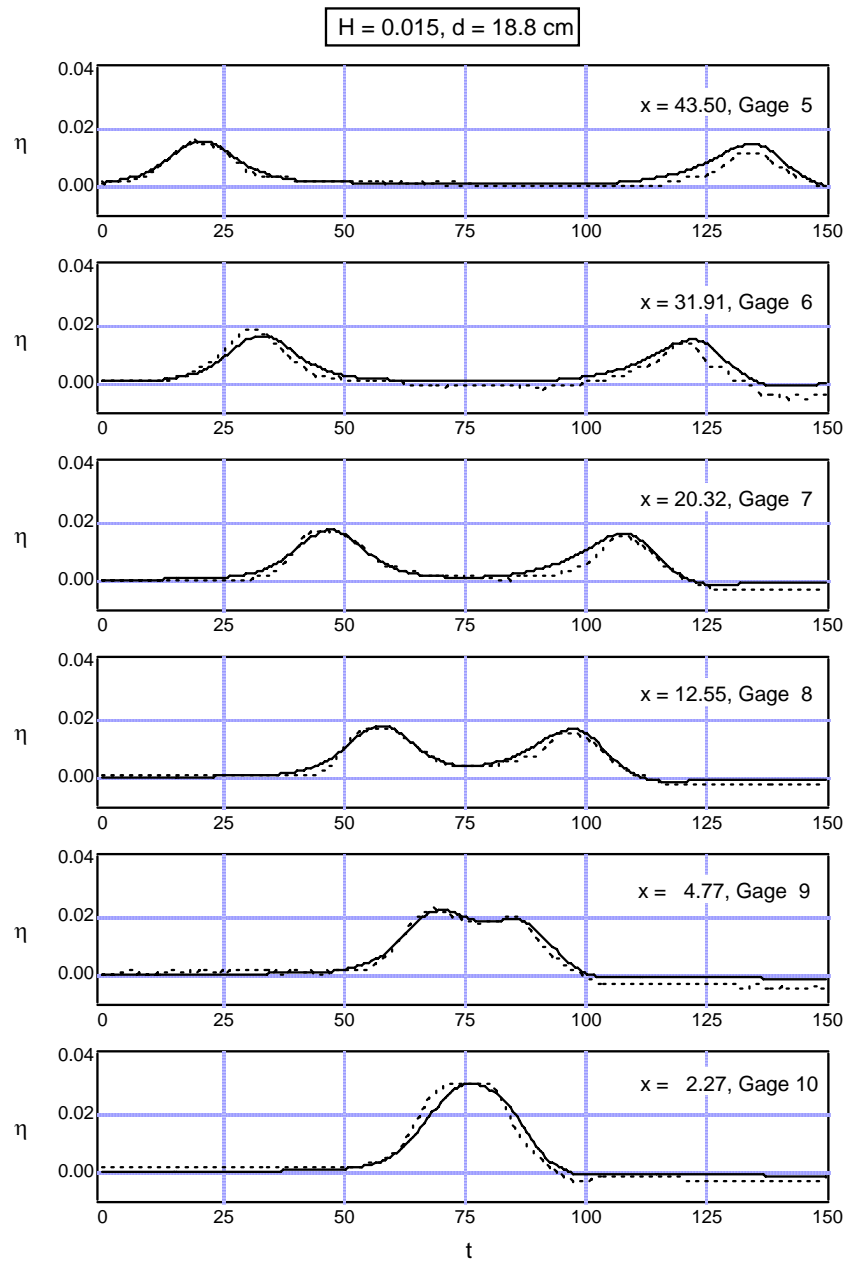
Alternatively, using the new general methodology

$$\begin{pmatrix} 1 \\ -J_1\left(\frac{\omega\sqrt{h_0}}{m_3}\right)/Y_1\left(\frac{\omega\sqrt{h_0}}{m_3}\right) \end{pmatrix} A_+ = \begin{pmatrix} J_0\left(\frac{\omega\sqrt{h_0}}{m_0}\right) & Y_0\left(\frac{\omega\sqrt{h_0}}{m_0}\right) \\ J_1\left(\frac{\omega\sqrt{h_0}}{m_0}\right) & Y_1\left(\frac{\omega\sqrt{h_0}}{m_0}\right) \end{pmatrix}^{-1} \begin{pmatrix} J_0\left(\frac{\omega\sqrt{h_0}}{m_0}\right) & Y_0\left(\frac{\omega\sqrt{h_0}}{m_0}\right) \\ J_1\left(\frac{\omega\sqrt{h_0}}{m_0}\right) & Y_1\left(\frac{\omega\sqrt{h_0}}{m_0}\right) \end{pmatrix} \begin{pmatrix} J_0\left(\frac{\omega\sqrt{h_0}}{m_0}\right) & Y_0\left(\frac{\omega\sqrt{h_0}}{m_0}\right) \\ J_1\left(\frac{\omega\sqrt{h_0}}{m_0}\right) & Y_1\left(\frac{\omega\sqrt{h_0}}{m_0}\right) \end{pmatrix}^{-1} \begin{pmatrix} J_0\left(\frac{\omega\sqrt{h_0}}{m_0}\right) & Y_0\left(\frac{\omega\sqrt{h_0}}{m_0}\right) \\ J_1\left(\frac{\omega\sqrt{h_0}}{m_0}\right) & Y_1\left(\frac{\omega\sqrt{h_0}}{m_0}\right) \end{pmatrix} \begin{pmatrix} J_0\left(\frac{\omega\sqrt{h_0}}{m_0}\right) & Y_0\left(\frac{\omega\sqrt{h_0}}{m_0}\right) \\ J_1\left(\frac{\omega\sqrt{h_0}}{m_0}\right) & Y_1\left(\frac{\omega\sqrt{h_0}}{m_0}\right) \end{pmatrix}^{-1} \begin{pmatrix} \frac{h_0}{c\sqrt{h_0}} & \frac{h_0}{c\sqrt{h_0}} \\ \frac{h_0}{ic\sqrt{h_0}} & -\frac{h_0}{ic\sqrt{h_0}} \end{pmatrix} \begin{pmatrix} A_+ \\ A_+ \end{pmatrix}$$

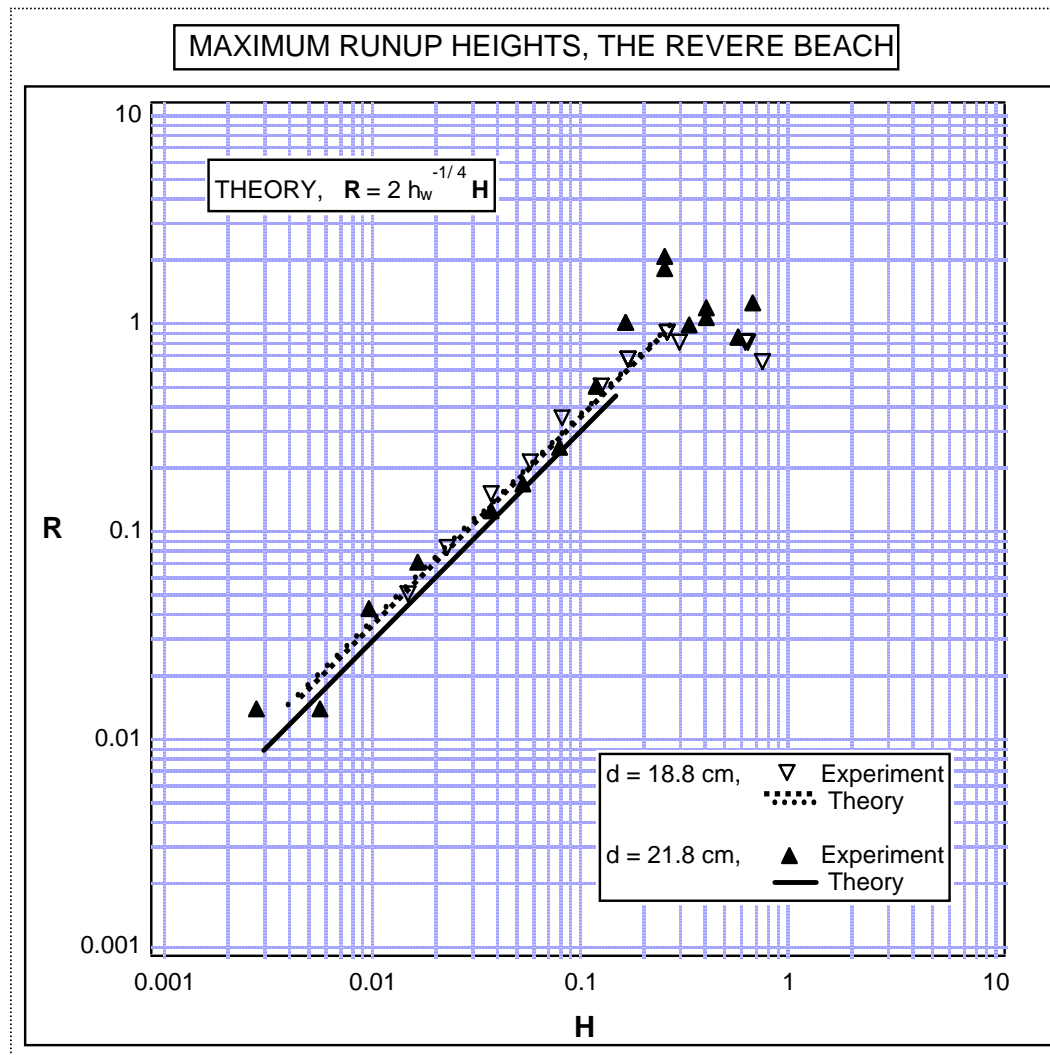
After extensive algebra

$$R = 2 h_w^{-1/4} H$$

Revere Beach, Time Histories of Surface Elevations



Revere Beach, Maximum Runup



Note how small change of depth at seawall produces large change in runup

Milestones: December 12, 1992 Flores Island, Indonesia



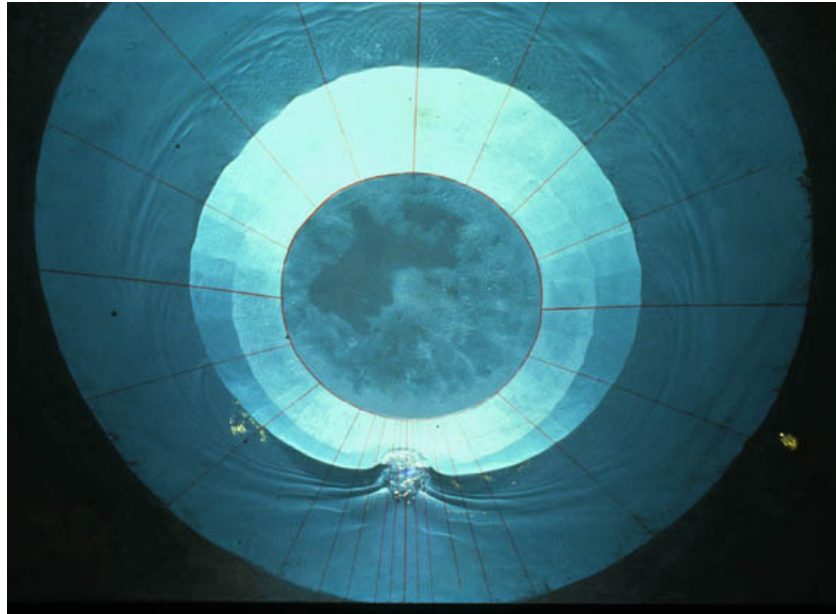
*Enhanced runup on
the lee side of Babi
Island.*

*Realization of flow
pattern in the
laboratory.*

*Validation of first
2+1 D runup codes.*

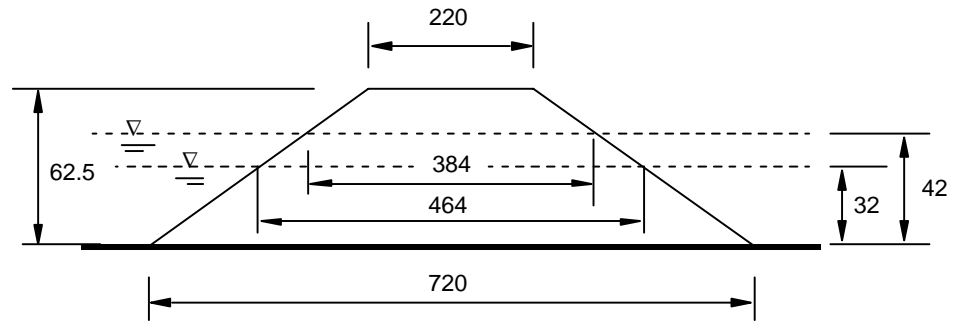


Wave Evolution Around the Conical Island

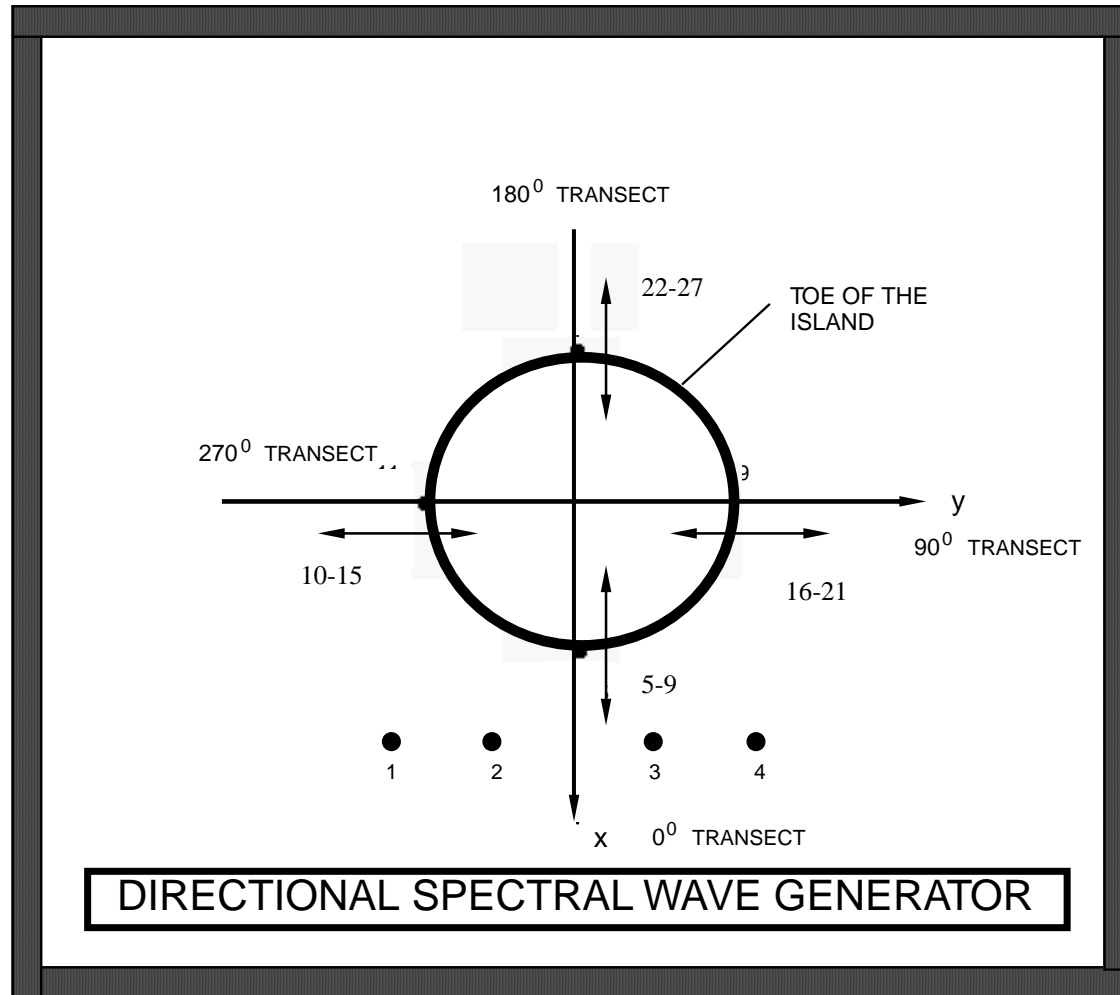


US Army Corps of Engineers
Coastal Engineering Research Center (CERC)
Vicksburg, Mississippi

C
o
n
i
c
a
l
i
s
l
a
n
d



E
x
p
e
r
i
m
e
n
t
s



Conical Island, Analytical Solution

The linearized equation of motion, $\frac{\partial^2 \eta}{\partial t^2} = h \nabla^2 \eta + \nabla h \cdot \nabla \eta,$

Consider circular bottom contours, $h(r), \eta(r, \theta) = R(r)e^{i(n\theta - \omega t)},$

$$R'' + \left(\frac{1}{r} + \frac{h'}{h}\right)R' + \left(\frac{\omega^2}{h} - \frac{n^2}{r^2}\right)R = 0.$$

- In the case of conical island, $h = \alpha(r - a),$ the differential equation can not be solved in term of known functions;
- In the case of the constant depth, $h(r) = h_0,$ the solution is

$$\eta(r, \theta, t) = \sum_{n=-\infty}^{+\infty} \{A_n J_n(kr) + B_n Y_n(kr)\} e^{i(n\theta - \omega t)}, \quad k = \omega / \sqrt{h_0}.$$

Outside toe of the island:

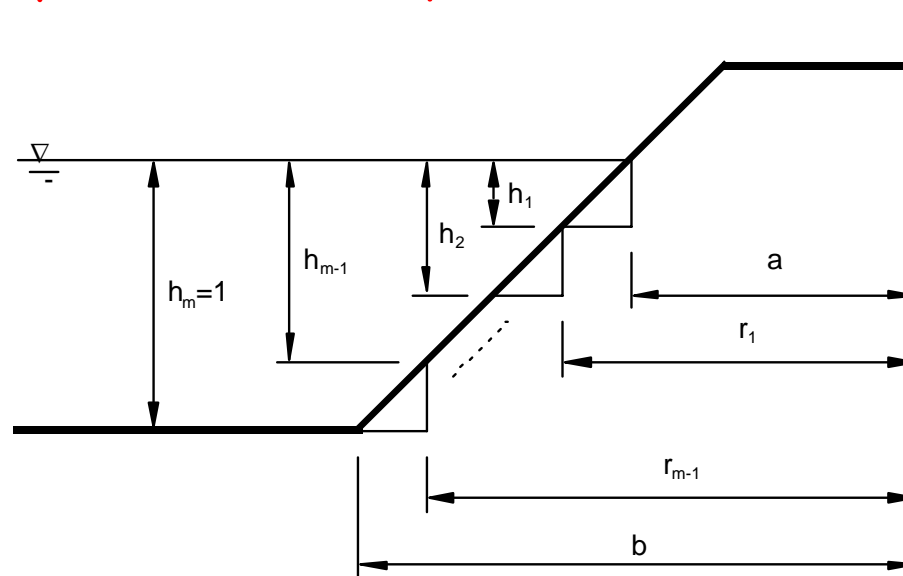
The incident wave approaching from infinity;

$$\eta_i = A^i e^{-i(kx + \omega t)} = \sum_{n=-\infty}^{\infty} A_n^i J_n(kr) e^{in(\theta - \pi/2)} e^{-i\omega t}.$$

The outgoing scattered wave to infinity;

$$\eta_s = \sum_{n=-\infty}^{\infty} A_n^r H_n^{(1)}(kr) e^{i(n\theta - \omega t)}.$$

Given the singularity of the field equation consider stepwise topography;



The solution in each individual region is known as,

$$\eta = \sum_{n=-\infty}^{\infty} e^{i(n\theta - \omega t)} \begin{cases} \{A_n^i e^{-in\pi/2} J_n(kr) + A_n^r H_n^{(1)}(kr)\} & r \geq b, \\ \{A_n J_n(kr) + B_n Y_n(kr)\} & b \leq r_j \leq a. \end{cases}$$

Boundary conditions are

$$\frac{\partial \eta}{\partial r} \Big|_{r=a} = 0 \quad \eta_j \Big|_{r=r_j} = \eta_{j+1} \Big|_{r=r_j}, \quad h_j \frac{\partial \eta_j}{\partial r} \Big|_{r=r_j} = h_{j+1} \frac{\partial \eta_{j+1}}{\partial r} \Big|_{r=r_j}.$$

For brevity, define

$$\kappa_j = k_j r_j = \frac{\omega}{\sqrt{h_j}} r_j, \quad \epsilon_j = \frac{k_{j+1}}{k_j} = \sqrt{\frac{h_j}{h_{j+1}}}.$$

A system of $(2m-1)$ equations must be solved. Instead of solving this system of equations, rank two matrices will again be used to get the solution.

The boundary conditions imply that

$$\begin{aligned}
 A_{m2} J'_n(\epsilon_0 \kappa_0) + B_{m2} Y'_n(\epsilon_0 \kappa_0) &= 0, \\
 A_{m2} J_n(\kappa_1) + B_{m2} Y_n(\kappa_1) &= A_{m2} J_n(\epsilon_1 \kappa_1) + B_{m2} Y_n(\epsilon_1 \kappa_1), \\
 A_{m2} \epsilon_1 J'_n(\kappa_1) + B_{m2} \epsilon_1 Y'_n(\kappa_1) &= A_{m2} J'_n(\epsilon_1 \kappa_1) + B_{m2} Y'_n(\epsilon_1 \kappa_1), \\
 A_{m2} J_n(\kappa_2) + B_{m2} Y_n(\kappa_2) &= A_{m2} J_n(\epsilon_2 \kappa_2) + B_{m2} Y_n(\epsilon_2 \kappa_2), \\
 A_{m2} \epsilon_2 J'_n(\kappa_2) + B_{m2} \epsilon_2 Y'_n(\kappa_2) &= A_{m2} J'_n(\epsilon_2 \kappa_2) + B_{m2} Y'_n(\epsilon_2 \kappa_2), \\
 &\vdots \\
 A_{m2} J_n(\kappa_{m-1}) + B_{m2} Y_n(\kappa_{m-1}) &= A_{m2} e^{-\frac{i\omega \kappa}{c}} J_n(\epsilon_{m-1} \kappa_{m-1}) + A_{m2} H_n^{(1)}(\epsilon_{m-1} \kappa_{m-1}), \\
 A_{m2} \epsilon_{m-1} J'_n(\kappa_{m-1}) + B_{m2} \epsilon_{m-1} Y'_n(\kappa_{m-1}) &= A_{m2} e^{-\frac{i\omega \kappa}{c}} J'_n(\epsilon_{m-1} \kappa_{m-1}) + A_{m2} H_n^{(1)'}(\epsilon_{m-1} \kappa_{m-1}).
 \end{aligned}$$

To determine time histories of surface elevation and maximum runup system of $(2m-1)$ equations must be solved.
Again alternatively in closed form;

$$\begin{pmatrix} 1 \\ -J'_n(\epsilon_0 \kappa_0) / Y'_n(\epsilon_0 \kappa_0) \end{pmatrix} A_{n,1} = \begin{pmatrix} J_n(\kappa_1) & Y_n(\kappa_1) \\ \epsilon_1 J'_n(\kappa_1) & \epsilon_1 Y'_n(\kappa_1) \end{pmatrix}^{-1} \begin{pmatrix} J_n(\epsilon_1 \kappa_1) & Y_n(\epsilon_1 \kappa_1) \\ J'_n(\epsilon_1 \kappa_1) & Y'_n(\epsilon_1 \kappa_1) \end{pmatrix} \begin{pmatrix} J_n(\kappa_2) & Y_n(\kappa_2) \\ \epsilon_2 J'_n(\kappa_2) & \epsilon_2 Y'_n(\kappa_2) \end{pmatrix}^{-1} \begin{pmatrix} J_n(\epsilon_2 \kappa_2) & Y_n(\epsilon_2 \kappa_2) \\ J'_n(\epsilon_2 \kappa_2) & Y'_n(\epsilon_2 \kappa_2) \end{pmatrix} \\
 \vdots \\
 \begin{pmatrix} J_n(\kappa_{m-1}) & Y_n(\kappa_{m-1}) \\ \epsilon_{m-1} J'_n(\kappa_{m-1}) & \epsilon_{m-1} Y'_n(\kappa_{m-1}) \end{pmatrix}^{-1} \begin{pmatrix} e^{-\frac{i\omega \kappa}{c}} J_n(\epsilon_{m-1} \kappa_{m-1}) & H_n^{(1)}(\epsilon_{m-1} \kappa_{m-1}) \\ e^{-\frac{i\omega \kappa}{c}} J'_n(\epsilon_{m-1} \kappa_{m-1}) & H_n^{(1)'}(\epsilon_{m-1} \kappa_{m-1}) \end{pmatrix} \begin{pmatrix} A_{n,i} \\ A_{n,1} \end{pmatrix}.
 \end{pmatrix}$$

$$S_{m-1m}^{-1} S_{m-1m-1} \cdots S_{33} S_{23}^{-1} S_{22} S_{12}^{-1} S_{11} S_1 A_{n2}^1 = V_m.$$

$$C = S_{m-1m-1} S_{m-2m-1}^{-1} \cdots S_{33} S_{23}^{-1} S_{22} S_{12}^{-1},$$

$$\Delta_{j-1j} = \frac{2h_j}{\pi r_{j-1}}, \quad j = 2, m$$

$$\varphi = \epsilon_m J'_n(\epsilon_{m-1} \kappa_{m-1}) C(1) - J_n(\epsilon_{m-1} \kappa_{m-1}) C(2),$$

$$\chi = \epsilon_m Y'_n(\epsilon_{m-1} \kappa_{m-1}) C(1) - Y_n(\epsilon_{m-1} \kappa_{m-1}) C(2).$$

The transmitted wave to the beach is given by

$$\eta = \frac{4}{3} \frac{1}{\pi \alpha} \left(\prod_{j=1}^m \Delta_{j-1j} \right) \int_{-\infty}^{\infty} \omega \operatorname{cosech}(\alpha \omega) \sum_{n=-\infty}^{\infty} \frac{e^{i\Theta}}{\varphi + i\chi} d\omega,$$

where $\Theta = n\theta + \omega(X_s - t) + (-n + 1)\pi/2$.

Using the asymptotic expansions for the large arguments of the Bessel functions;

$$S_{jj} S_{(j-1)j}^{-1} = \sqrt{\tau_{j-1}/\tau_j} \begin{pmatrix} 1 & 0 \\ 0 & 1 \end{pmatrix}.$$

Runup dependence for conical island

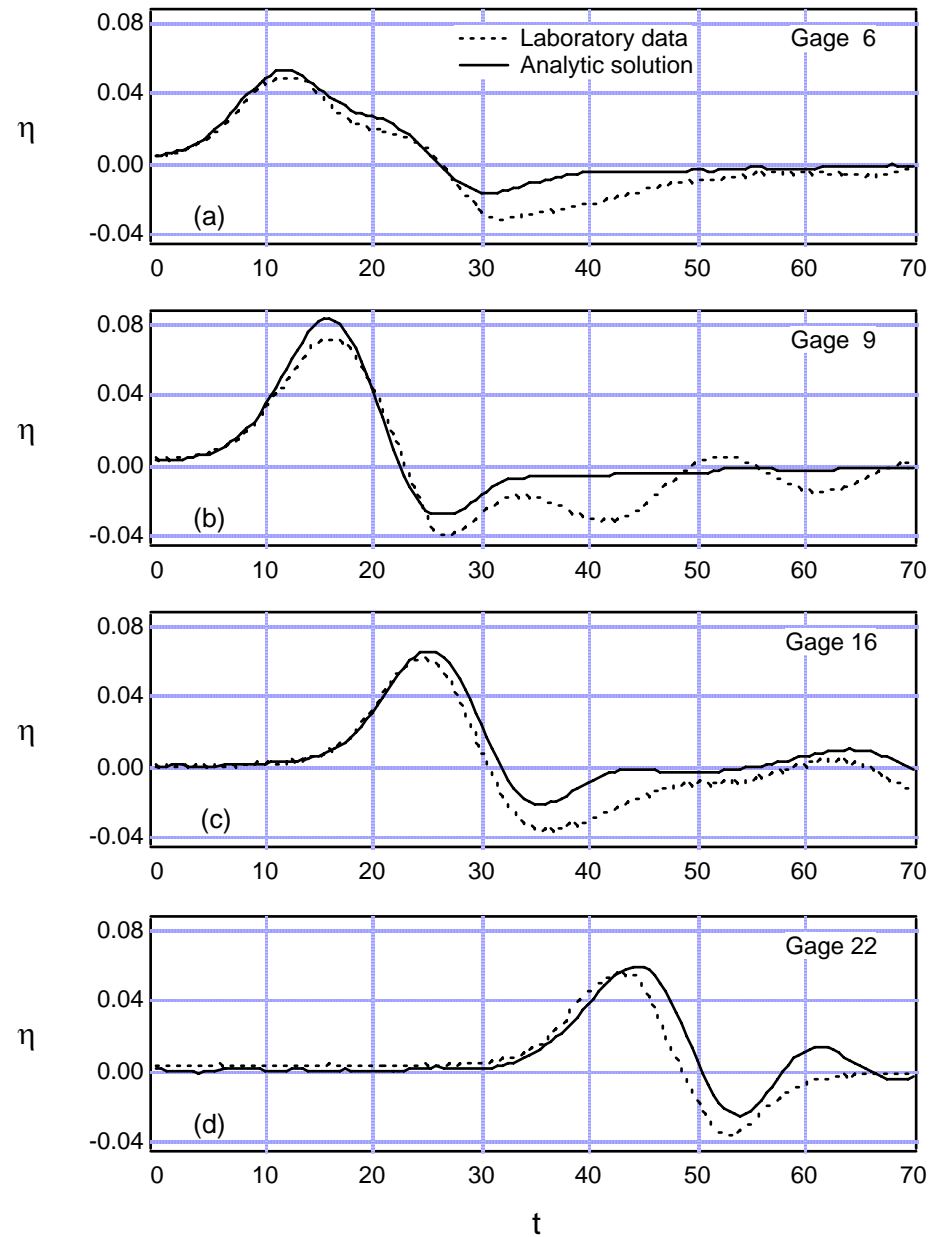
$$R(t) = \frac{4}{3\pi} \sqrt{\frac{1}{ab}} \int_{-\infty}^{+\infty} \operatorname{cosech}(\alpha\omega) \sum_{n=-\infty}^{+\infty} \frac{e^{i\Theta}}{H_n^{(1)'(\omega b)} d\omega.$$

Exact solution for sill

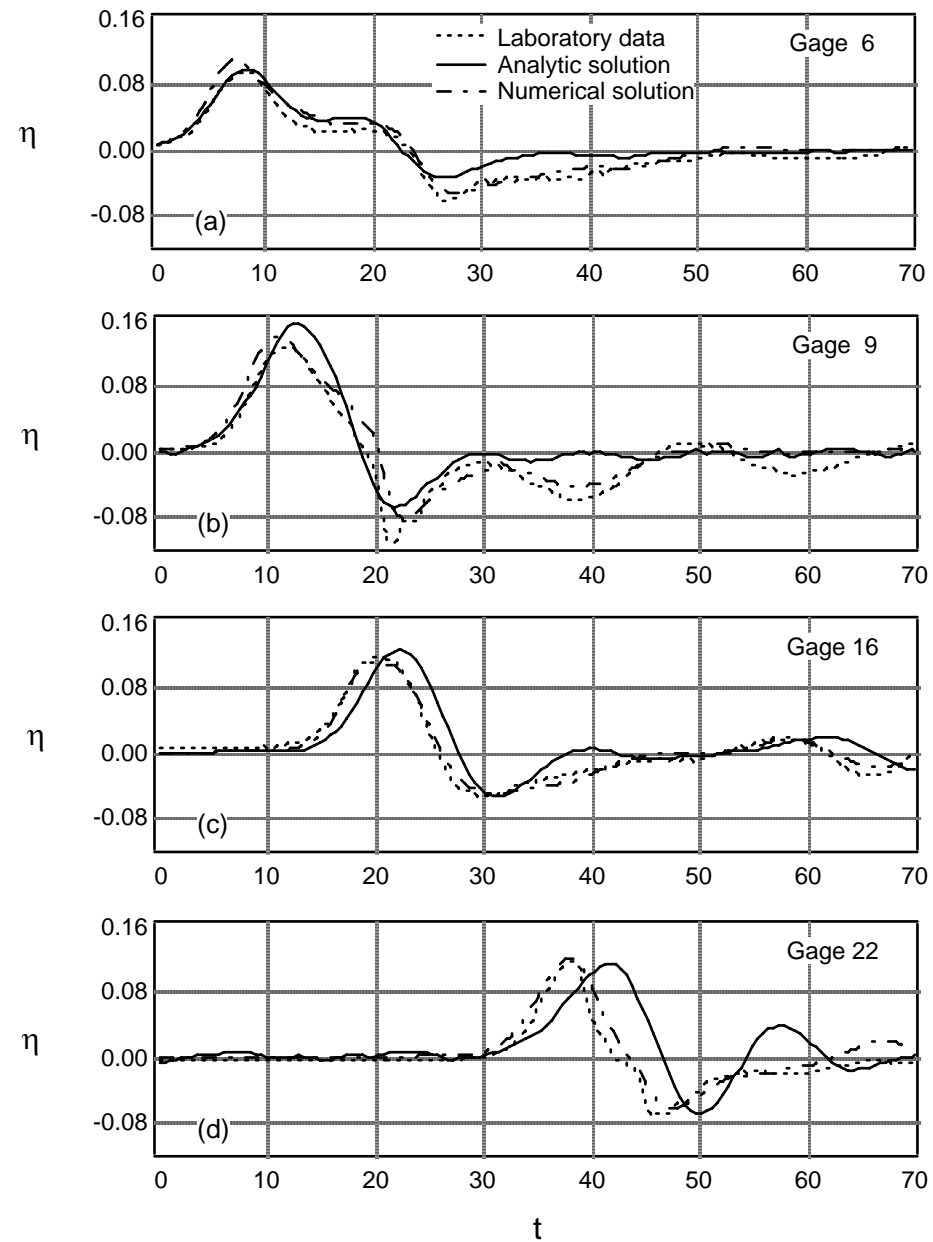
$$R(t) = \frac{4}{3\pi} \frac{1}{a} \int_{-\infty}^{+\infty} \operatorname{cosech}(\alpha\omega) \sum_{n=-\infty}^{+\infty} \frac{e^{i\Theta}}{H_n^{(1)'(\omega a)} d\omega.$$

(b ---> a, conical island turns to sill.)

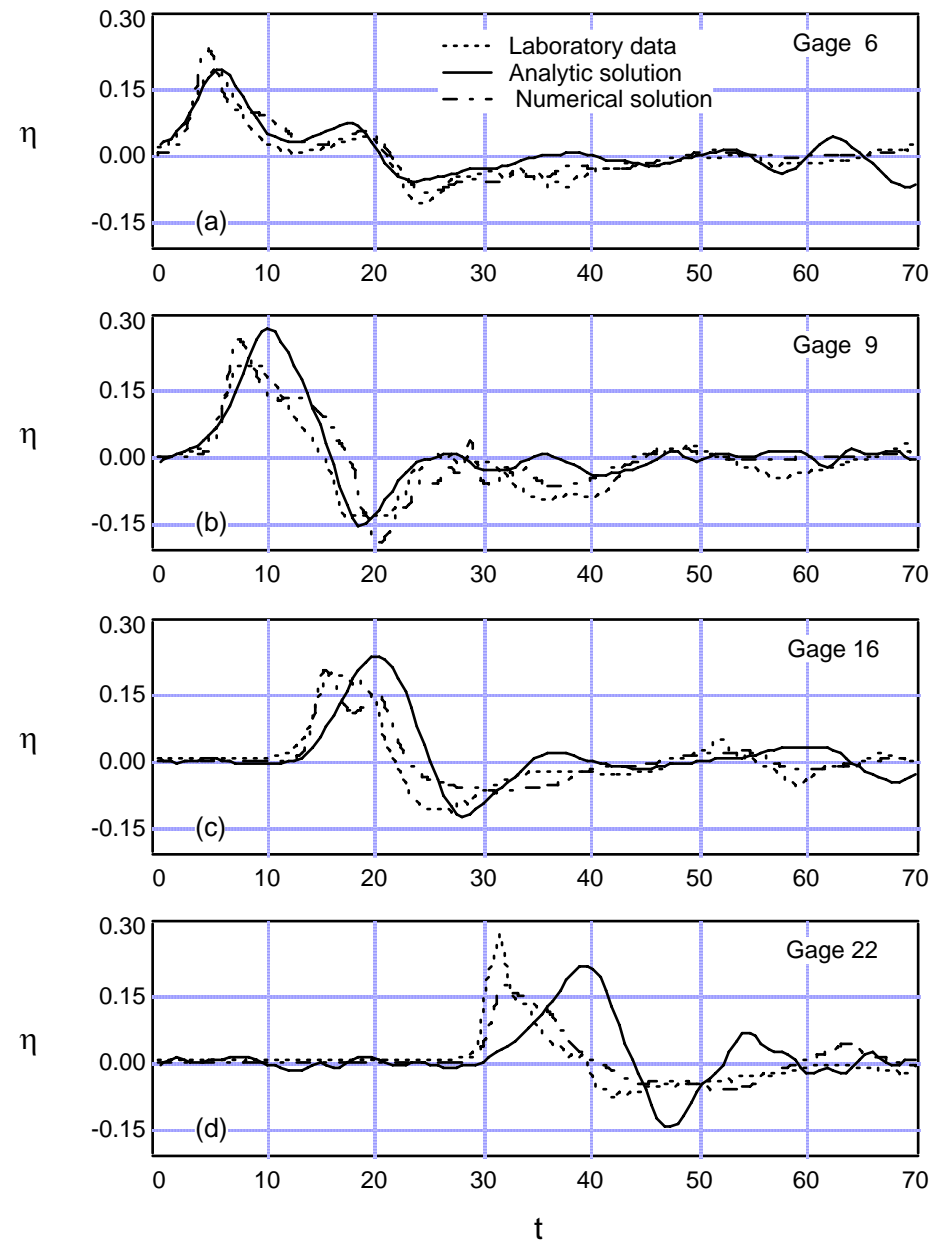
Conical Island, Time Histories of Surface Elevations, $d=32\text{cm}$, $H=0.05$



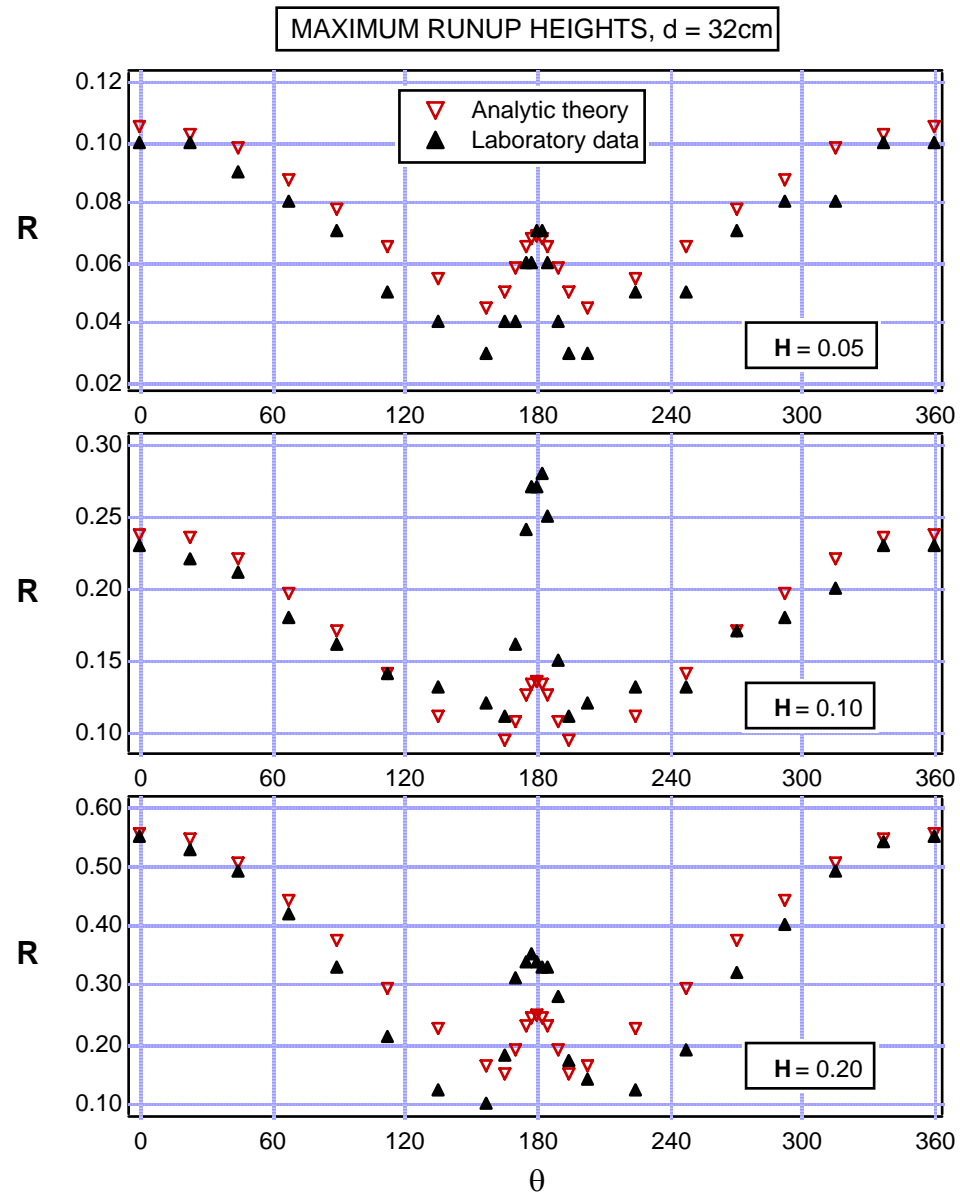
Conical Island, Time Histories of Surface Elevations, $d=32\text{cm}$, $H=0.10$



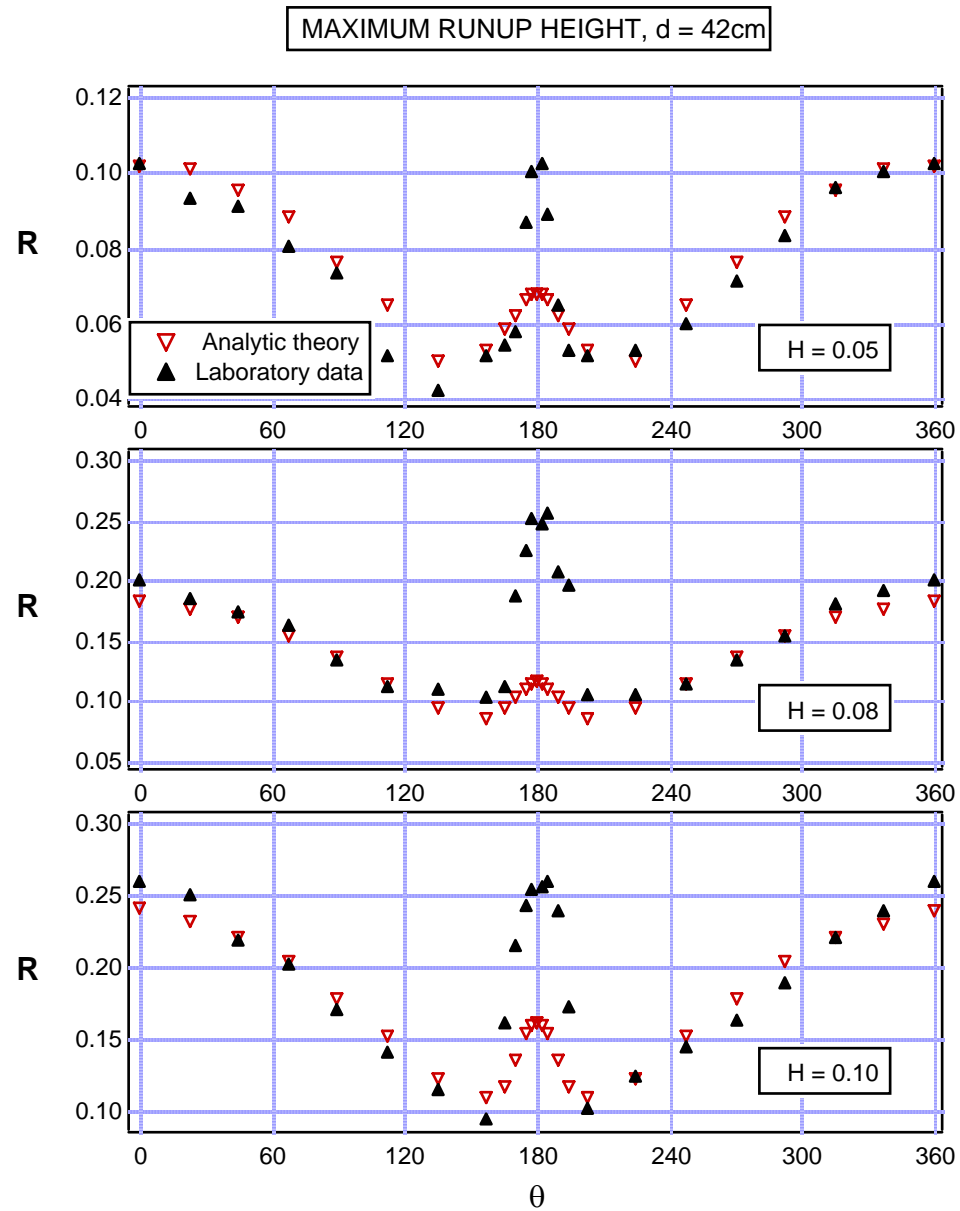
Conical Island, Time Histories of Surface Elevations, $d=32\text{cm}$, $H=0.20$



Conical Island, Maximum Runup of Solitary Wave

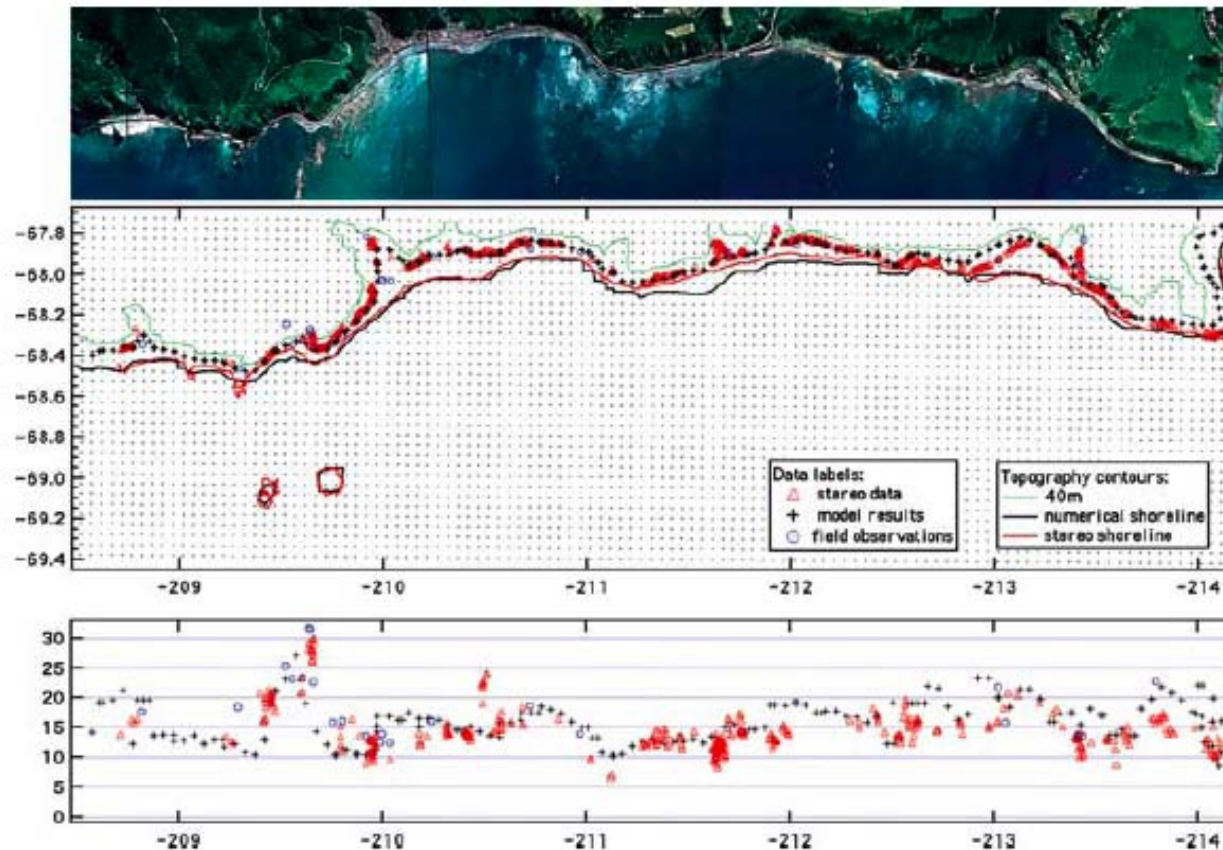


Conical Island, Maximum Runup of Solitary Wave



Milestones: Okushiri 1993

Validation of inundation codes for extreme runup and overland flows.



Comparison of MOST predictions for the extreme runup in Monai with field measurements.

Two verification/validation objectives are achieved.

The algorithm is seen to converge to the measurements as the grid size is reduced.

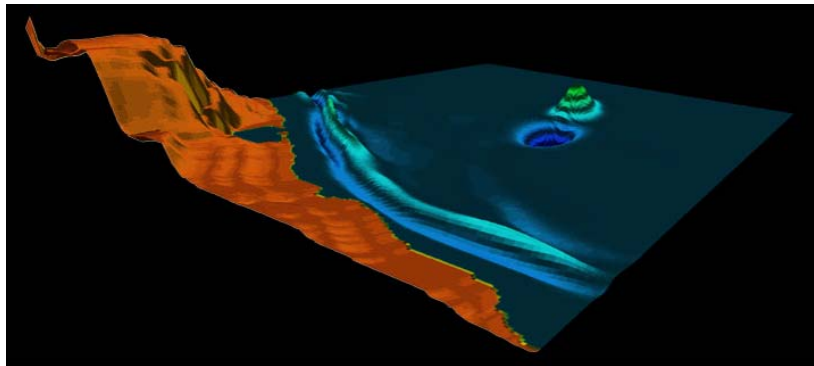
Titov and Synolakis, JWPCOE, 1998

Milestones: Papua New Guinea 1998

First evidence of *seismically generated landslide tsunami*.

Validation of numerics for overland flow into lagoons.

Leading depression dipole wave by the “wrong” earthquake..



Initial and final wave from animation of Borrero (2001)

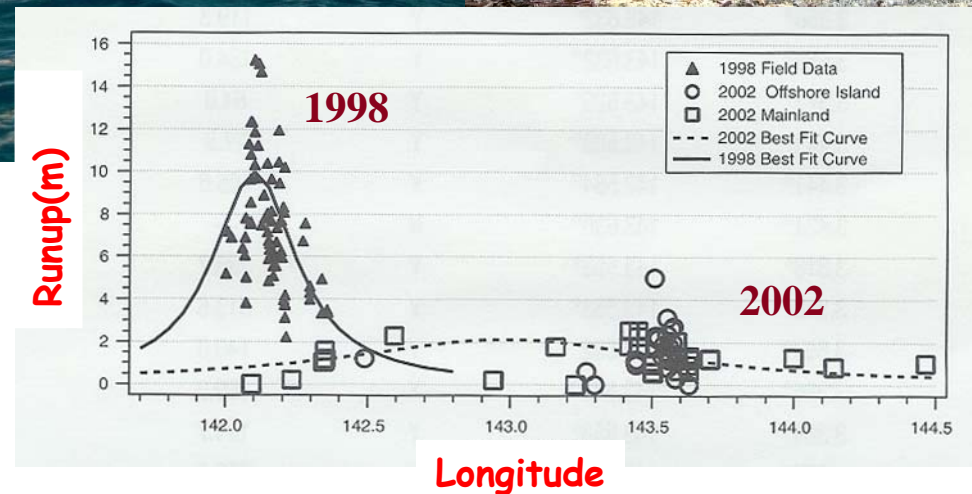
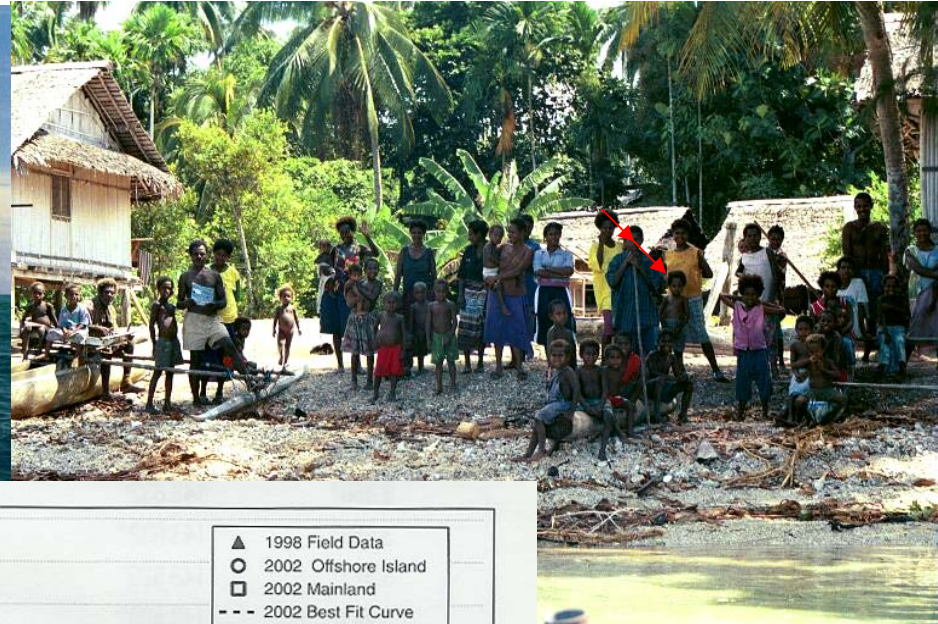
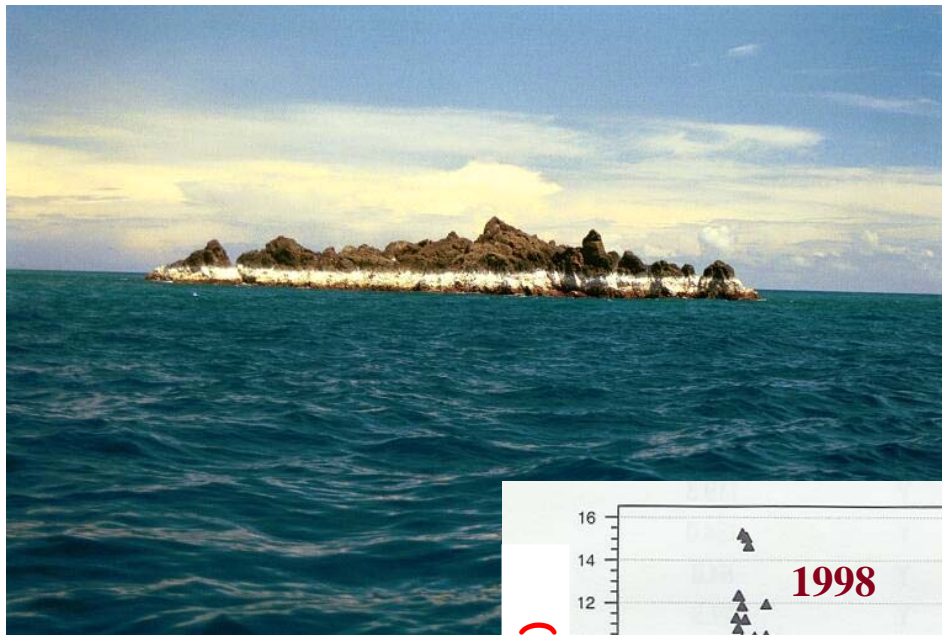


Sissano Spit

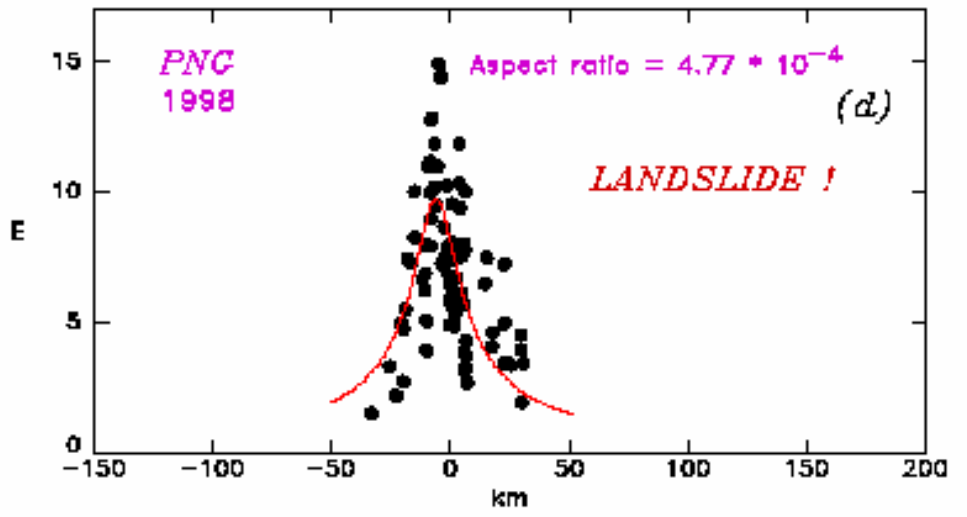
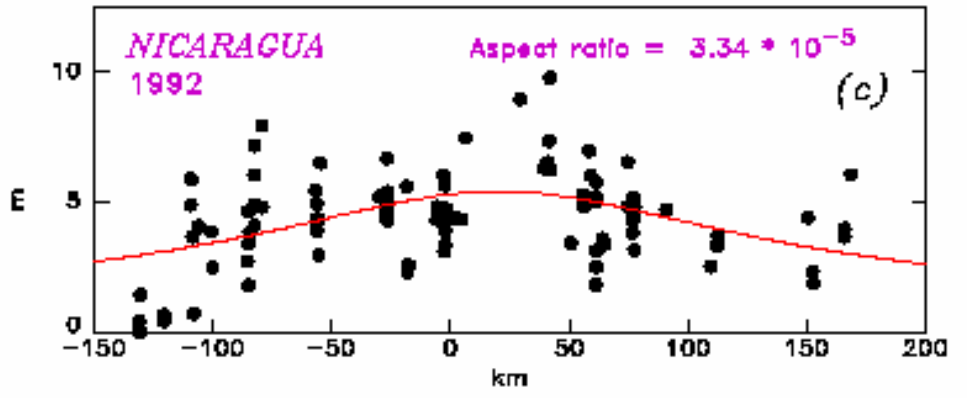
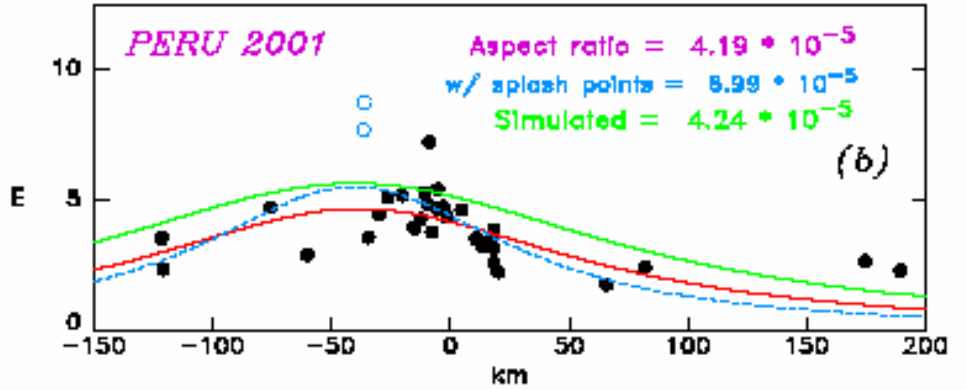
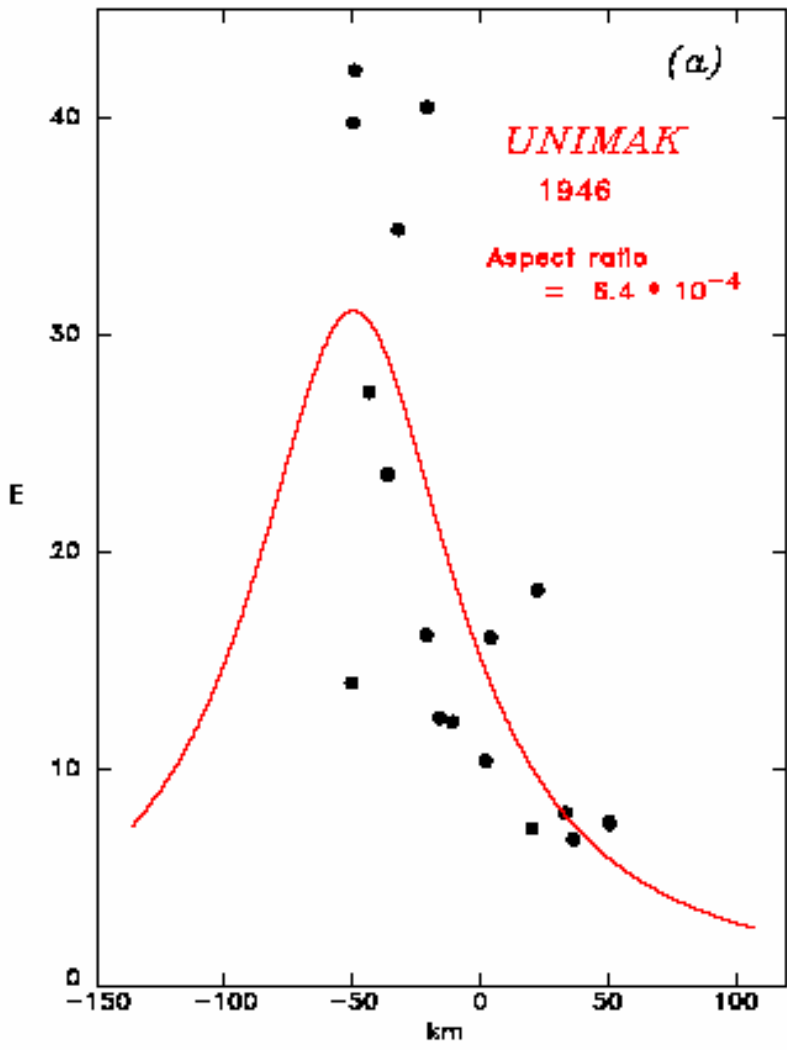


Milestones: PNG 2002

Larger earthquake than 1998, significant uplift, smaller tsunami.

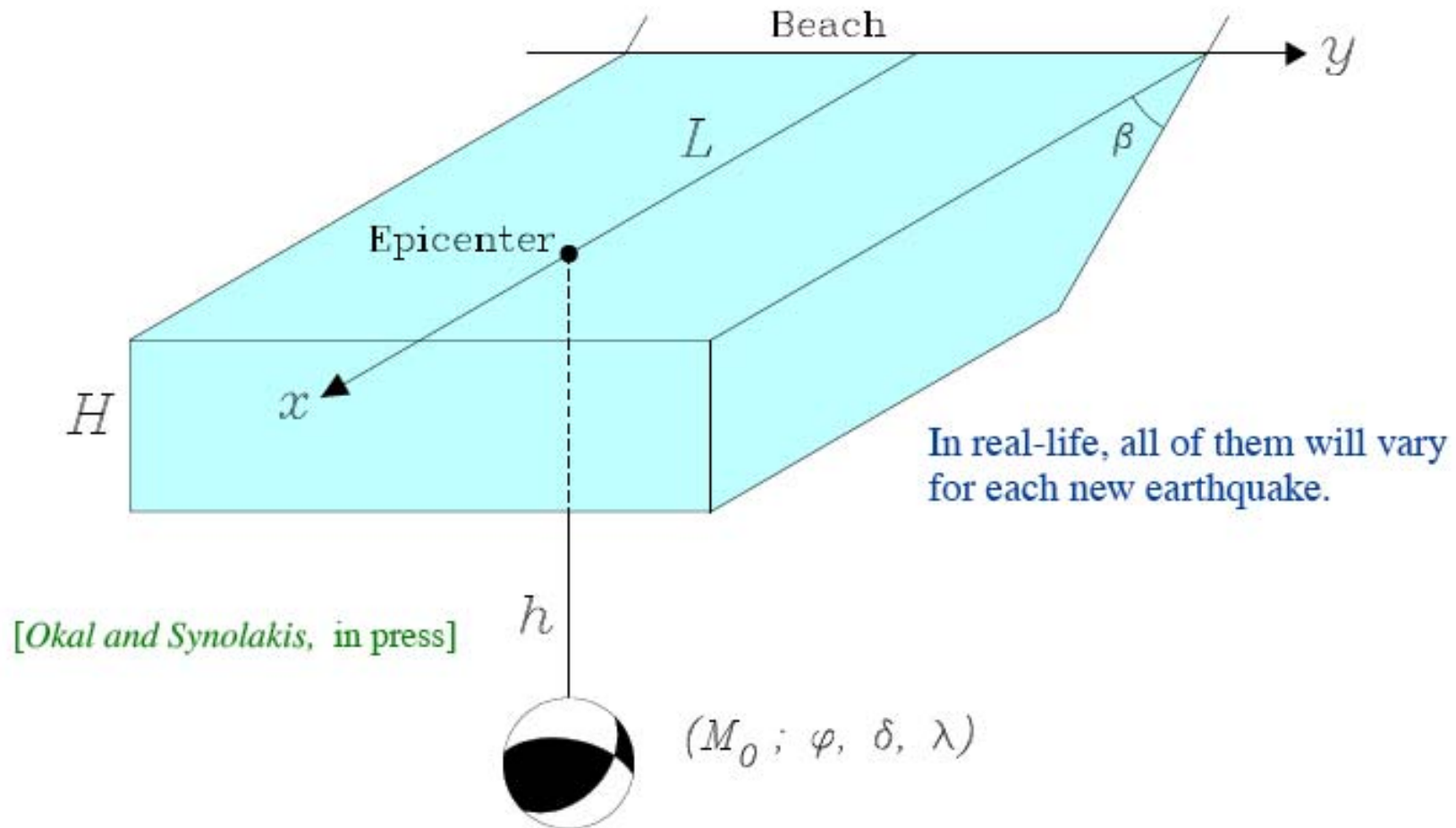


No large slump in 2002. Notice differences in runup distribution.



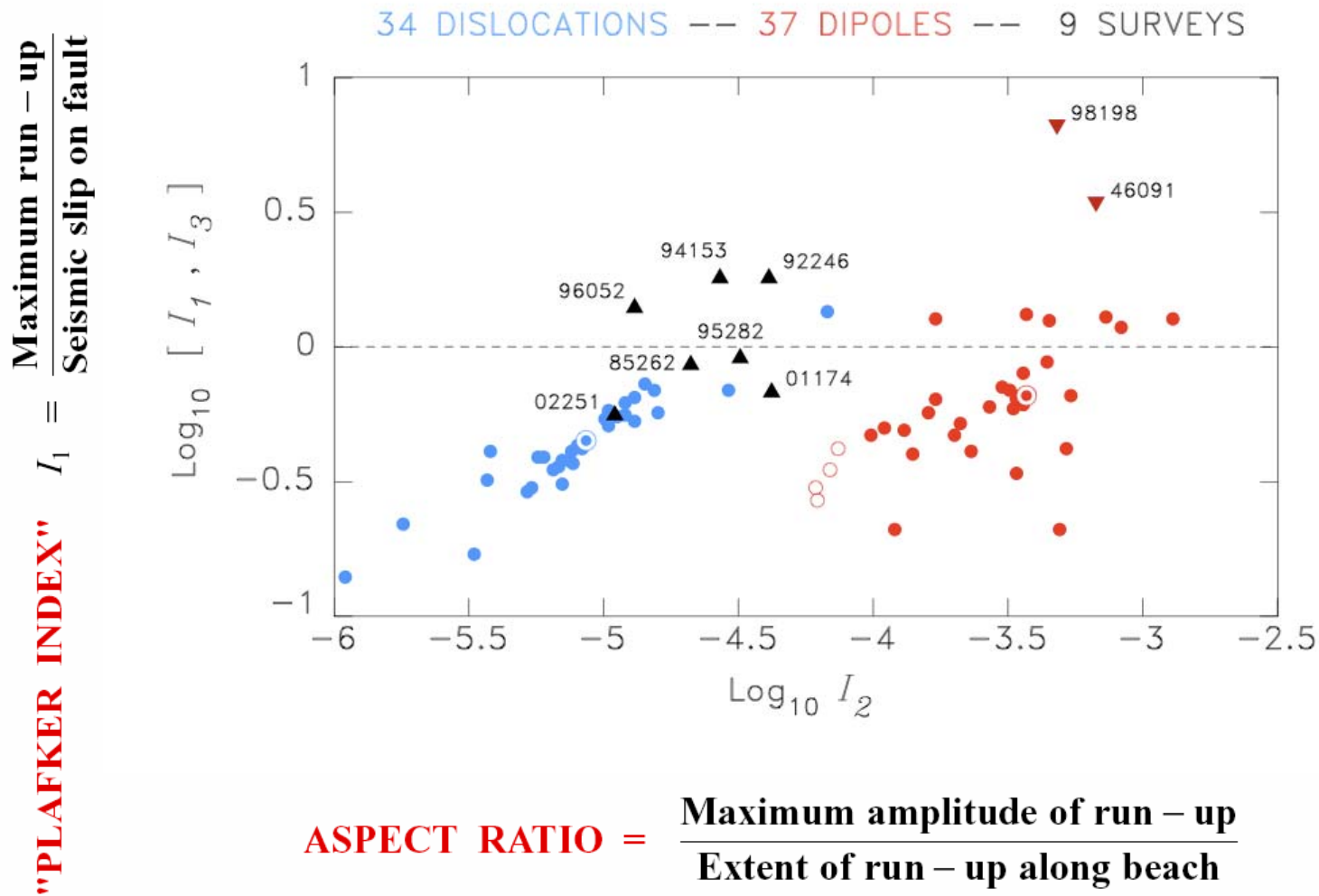
THE DISLOCATION SOURCE in the NEAR FIELD

A full description requires at least 8 parameters.



We explore systematically their influence on run-up and seek to define INVARIANTS

After 500 simulations of tsunamigenic events, a source discriminant is rediscovered and "officially" introduced for nearfield tsunami impact. (Sometimes even geophysicists test their inferences.)



Could some lives had been spared ?

Galle - headland with overland flow ?

(Wurhing, 1992, Okushiri, 1993)

Hambandota - Living sandwitched between a lagoon and the ocean ?

(Pancer, 1994, PNG 1998)

Banda Aceh - Wave attack from two sides ?

(Chimbote, 1996, Wuhring, 1992)

Banda Aceh - 3km inundation of flat land ?

(Mindoro, 1994, Chimbote, 1996)

Yale, Sri Lanka - Sand dune removal, reef mining ?

(Nicaragua, 1992, Okushiri, 1994)

Thailand, Malaysia and Sumatra - Shoreline recession as a precursor ?

(Nicaragua, 1992, Manzanillo, 1995, PNG, 1998)

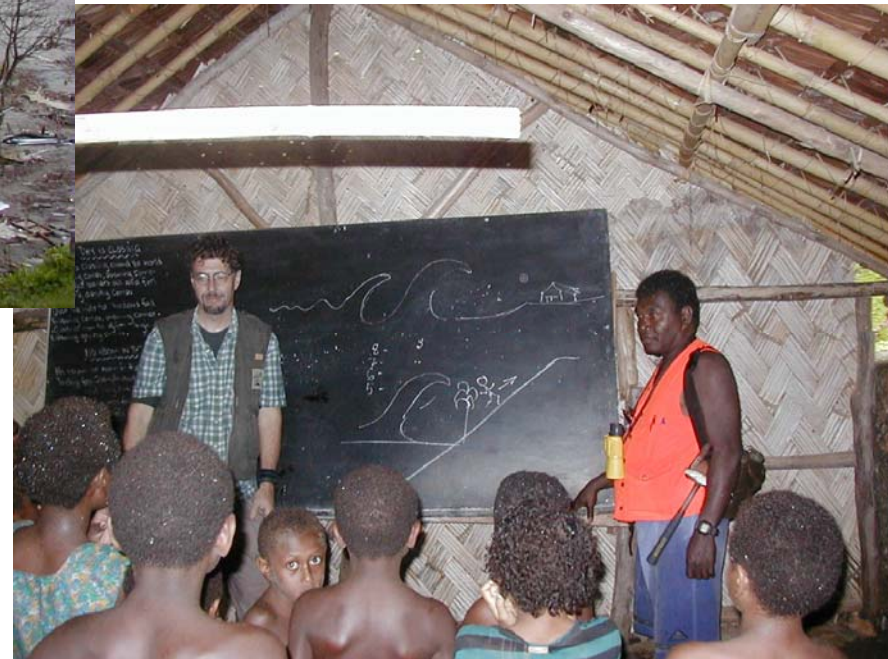
Everywhere - Well-engineered structures survived, yet no vertical evacuation ?

(All the tsunamis of 1992-2004).

Milestones: Vanuatu, 1999

Out of 500 residents in Baie Martelle, 3 died.

Education worked.



History of hydrodynamic inundation codes and the development of validation and verification standards.

- *The 1950s + 1960s*: Development of analytic solutions, first laboratory studies with experiments completely disjointed from analytical results, development of first 1+1 propagation code by Peregrine in 1966.
- *The 1970s*: Laboratory studies for tsunami generation coupled with numerical models, 2+1 directionality, the solitary wave paradigm is established, early 1+1 propagation codes and runup codes for an infinite bore.
- *The 1980s*: Laboratory studies and analytical results for the runup of solitary waves on plane beaches (NSW, LSW), first Boussinesq 2+1 propagation and runup numerical solutions.
- *1990*: 1st National Science Foundation (NSF) Workshop on Long Wave Runup - establishes how analytic solutions can be used for code validation, confirms the overall, applicability of NSW and LSW.

History of hydrodynamic inundation codes and the development of validation and verification standards.

- *The 1990s* : Rapid development of 2+1 numerical codes, large-scale laboratory experiments (Babi Island), fortuitous incidence of tsunamis, N-wave results.
- *1995* : 2nd NSF Workshop on Long Wave Runup Models, four benchmark problems for code verification.
- *Late 1990s* : NOAA tsunami forecasting capability and inversion from tsunameter (DART) data. PNG tsunami rekindles interest in modeling submarine landslides.
- *2003* : First warning cancellation in Hawaii, the first ever tsunami *inundation* forecast.

Goals of numerical simulation of tsunami inundation.

- 1) Understand the basic physics, the fundamental processes that control inundation.
- 2) Provide civil defense with guidelines for producing evacuation maps for emergency preparedness.
- 3) Provide real time forecasts.

Why it is not trivial.

- 1) Coupled nonlinear equations.
- 2) Uncertainties in nearshore bathymetry and topography affect inundation to first order.
- 3) Large variances in the parameters affect applicability of different approximations.
- 4) Large uncertainties in seismic initial condition affect predictions to first order.

*Why tsunami modeling
is a real computational challenge.*

*Tsunami floods can be very clean and also debris floods,
2nd wave carries back all the "material" that the first
wave removed.*

High-end animations

After the July 08, 2006 Java Tsunami

7 animations were posted at
the Tsunami Bulletin Board

Now the question is

How many of these numerical models are
validated rigorously?

Need for standards

There is substantial need for tsunami mitigation plans not just in the US but also world wide for the nations facing tsunami hazards.

As an outcome:

Forecasting/inundation maps might be based on older and/or untested methodology.

Unfortunately, there is no standards for modeling tools.

Benchmarks needed

Incorrectly assessing possible inundation:

- Put lives at risk
- Unnecessary evacuations
- Reduce the credibility of the system

Urgently,

standards (benchmarks) are needed to ensure a minimum level of quality and reliability for forecasting and inundation.

To calculate tsunami currents, forces and runup on coastal structures, and inundation of coastlines, one must calculate the evolution of the tsunami from the deep ocean to its coastal community, numerically.

No matter which numerical model is used, both

validation (the process of ensuring that the model solves the governing equations of motion accurately)

and

verification (the process of ensuring that the model used represents geophysical reality appropriately)

are essential parts of the model development.

While there is in principle no absolute certainty that a numerical code that has performed well in all the benchmark tests will also produce realistic inundation predictions with any given source motions, validated codes reduce the level of uncertainty in their results to the uncertainty in the geophysical initial conditions.

Further, when coupled with real-time free-field tsunami measurements from tsunameters, validated codes are the only choice for realistic forecasting of inundation: **the consequences of failure are too ghastly to take chances with less-validated numerical procedures.**

Three landmark scientific meetings that contributed to the understanding of tsunami hydrodynamics.

In the first meeting, only one dimensional data were available for idealized bathymetries, in the second, two dimensional results were presented, while in the third results for landslide waves were shown.

All three were supported by the National Science Foundation of the United States and were geared towards the development of hydrodynamics model for tsunami propagation, inundation and forecasting

1991 Catalina Island, Los Angeles, 1996 Friday Harbor, Seattle, Washington, and 2003 Catalina Island, Los Angeles Long Wave Runup Models Workshops.

Steps to take to validate and verify the numerical codes

- Basic considerations
- Analytical benchmarking
- Laboratory benchmarking
- Field data benchmarking
- Scientific evaluation
- Formal operational evaluation

Long Wave Runup Model Workshops:
1995 Friday Harbor, Washington and 2003 Catalina Island, Los Angeles

Basic consideration

Mass conservation

A most basic step in ensuring that a numerical model works for predicting evolution, before even checking its inundation results, is ensuring that the model conserves mass.

While the conservation of mass equation is part of the equations of motion that are solved in any numerical procedure, cumulative numerical approximations can sometimes produce results that violate mass conservation.

This is particularly the case when friction factors are used, or smoothing to stabilize inundation computations for breaking waves. The total volume at the end of the computation, i.e., when the initial wave is entirely reflected and offshore.

Basic consideration

Convergence

The next basic step is checking convergence of the numerical code to a certain asymptotic limit, presumably the actual solution of the equations solved.

The optimal locations to check convergence are the extreme runup and rundown. The numerical predictions should be seen to converge to a certain value, and further reductions in step sizes should not change the results.

Analytical benchmarking

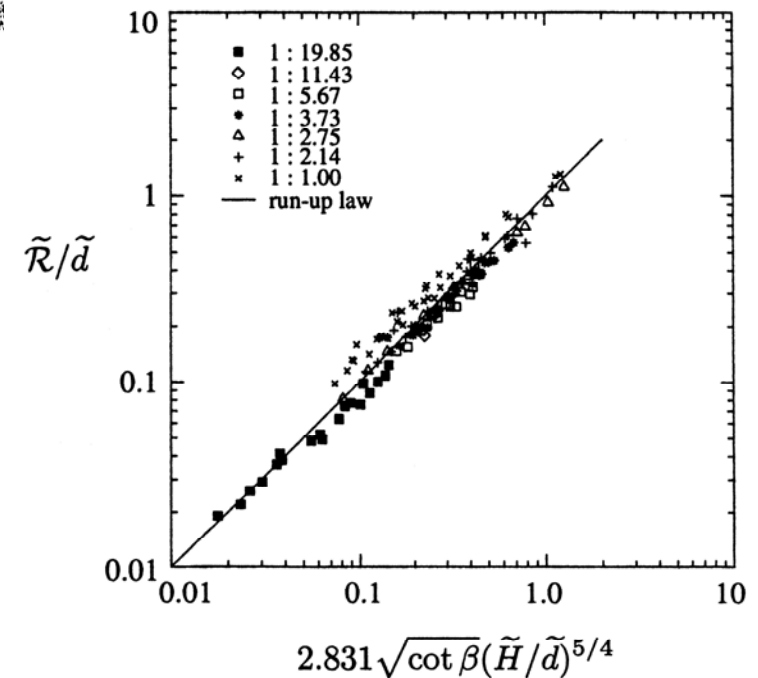
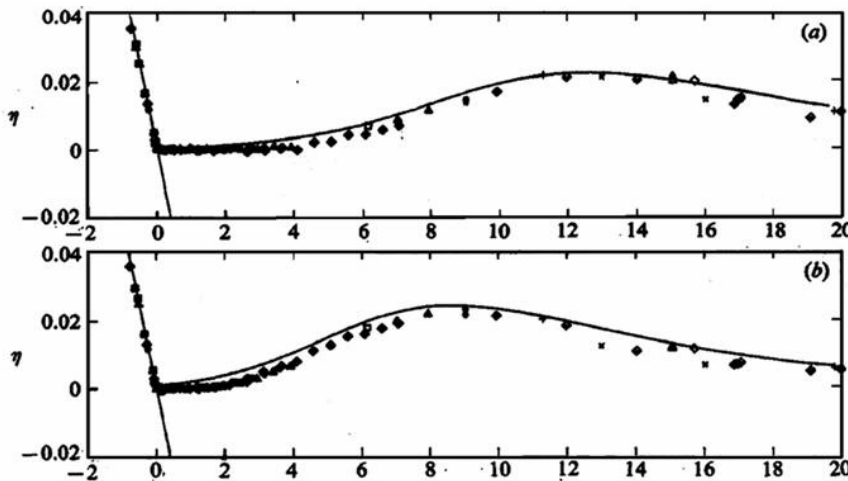
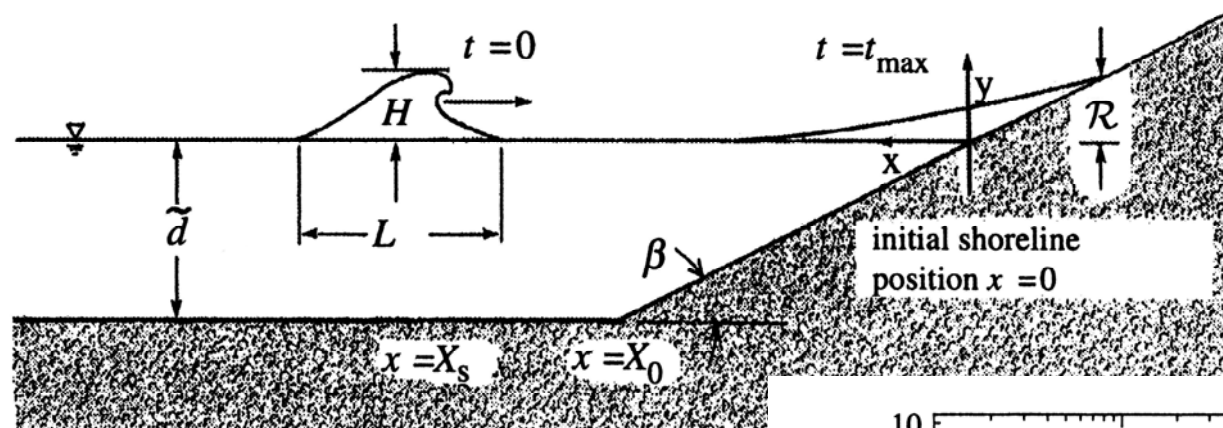
Why is analytical benchmarking important?

Exact solutions of the SW equations are useful for validating the complex numerical models which are used for final design and which often involve adhoc assumptions, particularly during inundation computations when grid points are introduced and withdrawn during the runup process on what was dry land.

Comparisons of numerical predictions with analytical solutions can identify systematic errors, as when using friction factors or dissipative terms to augment the idealized equations of motion.

Analytical benchmarking

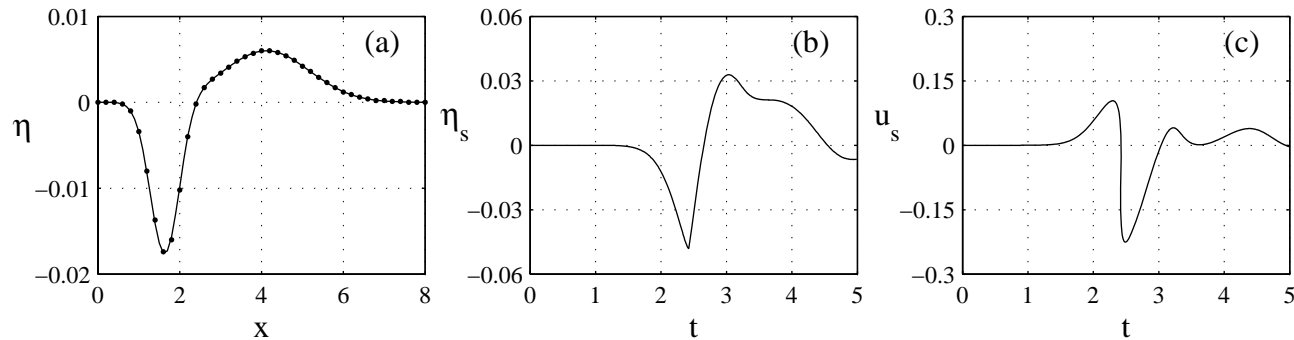
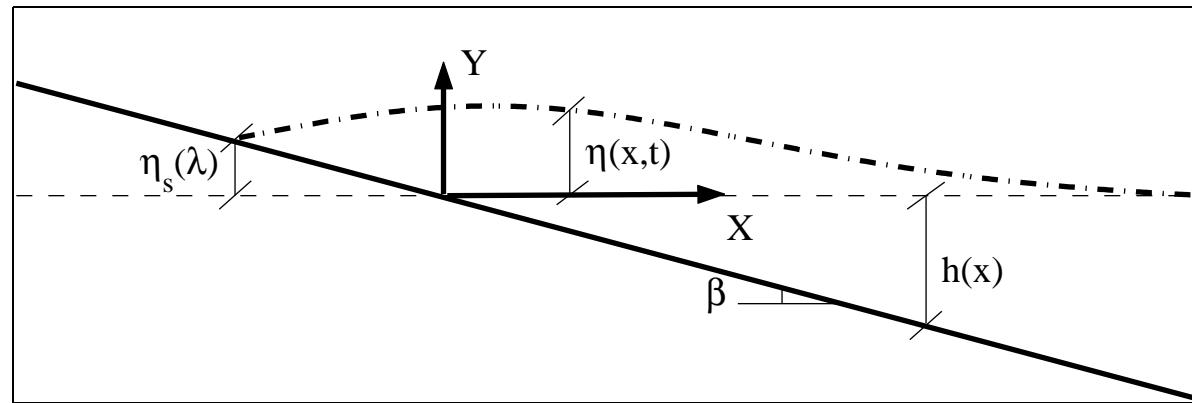
Solitary wave evolution over a sloping beach and runup



Synolakis, JFM, 1987

Analytical benchmarking

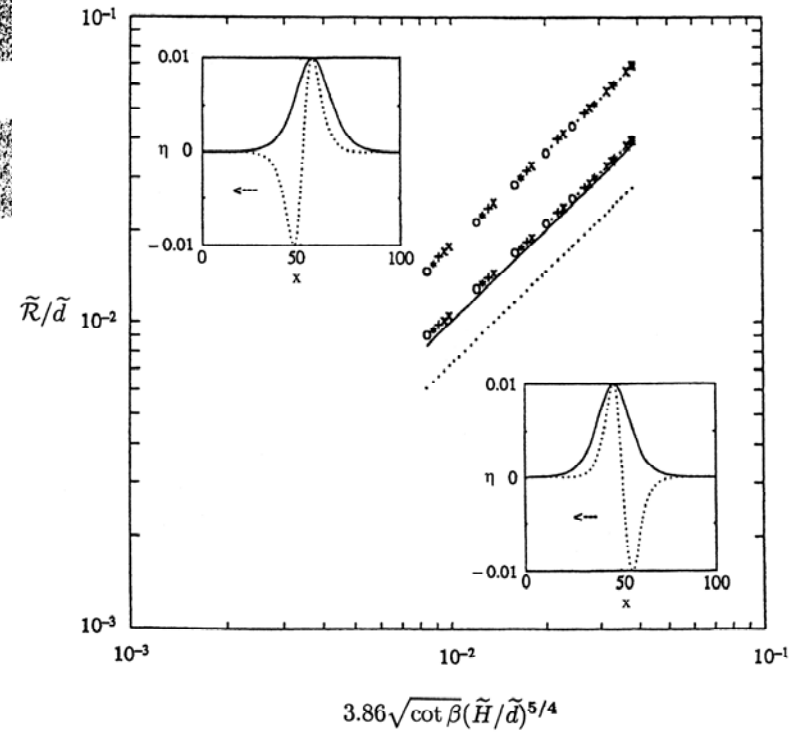
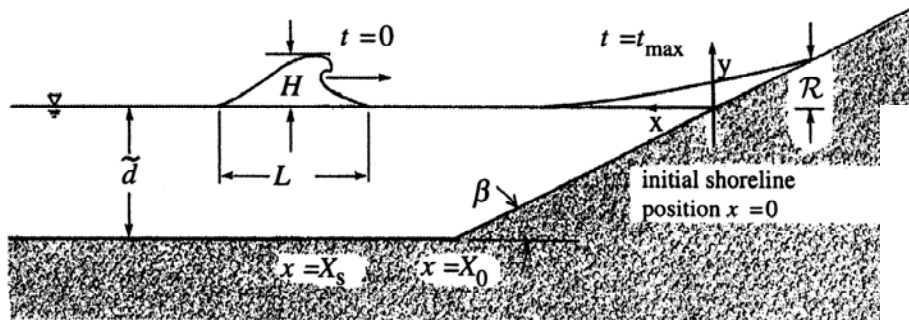
Initial value problem over a sloping beach



Kanoglu, JFM, 2004; Kanoglu and Synolakis, PRL, 2006

Analytical benchmarking

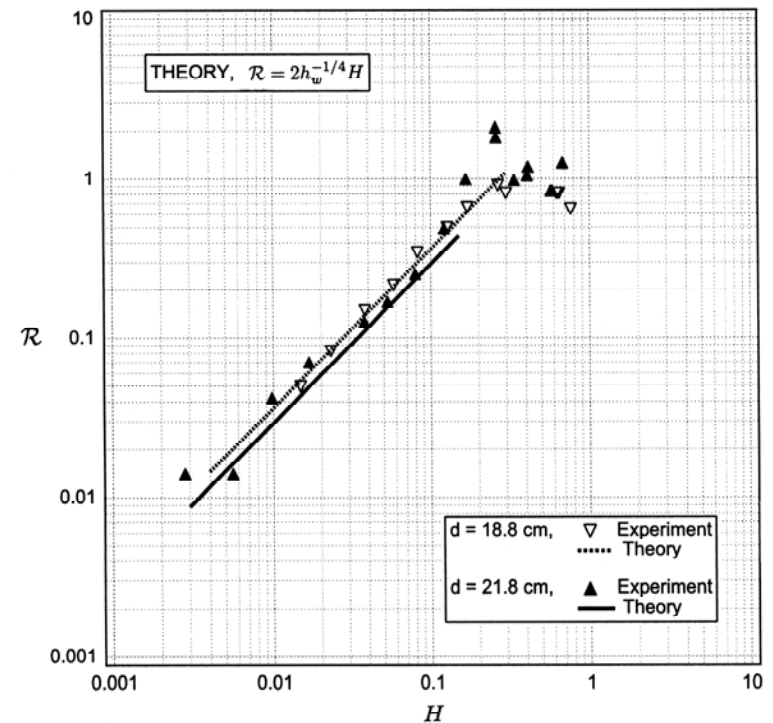
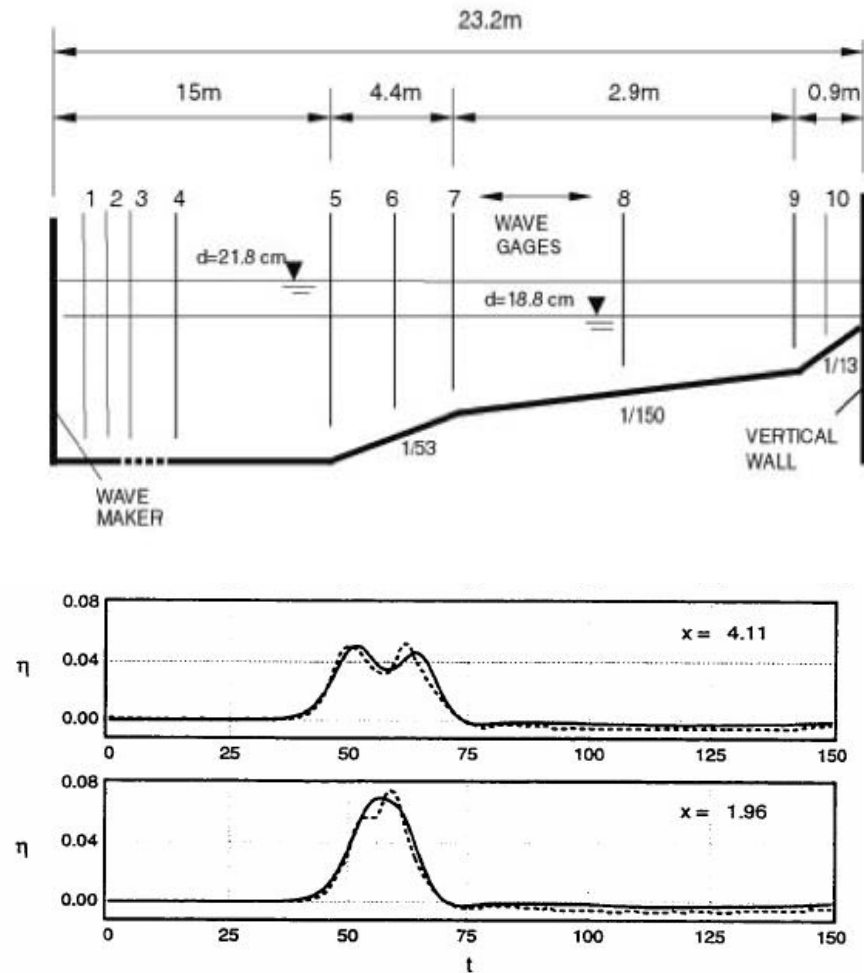
N-wave runup over a sloping beach



Tadepalli and Synolakis, Proc. Royal. Soc., 1994

Analytical benchmarking

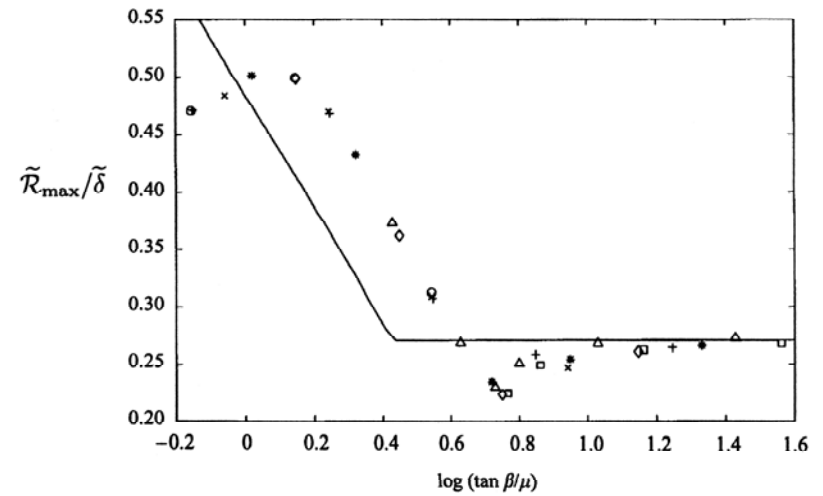
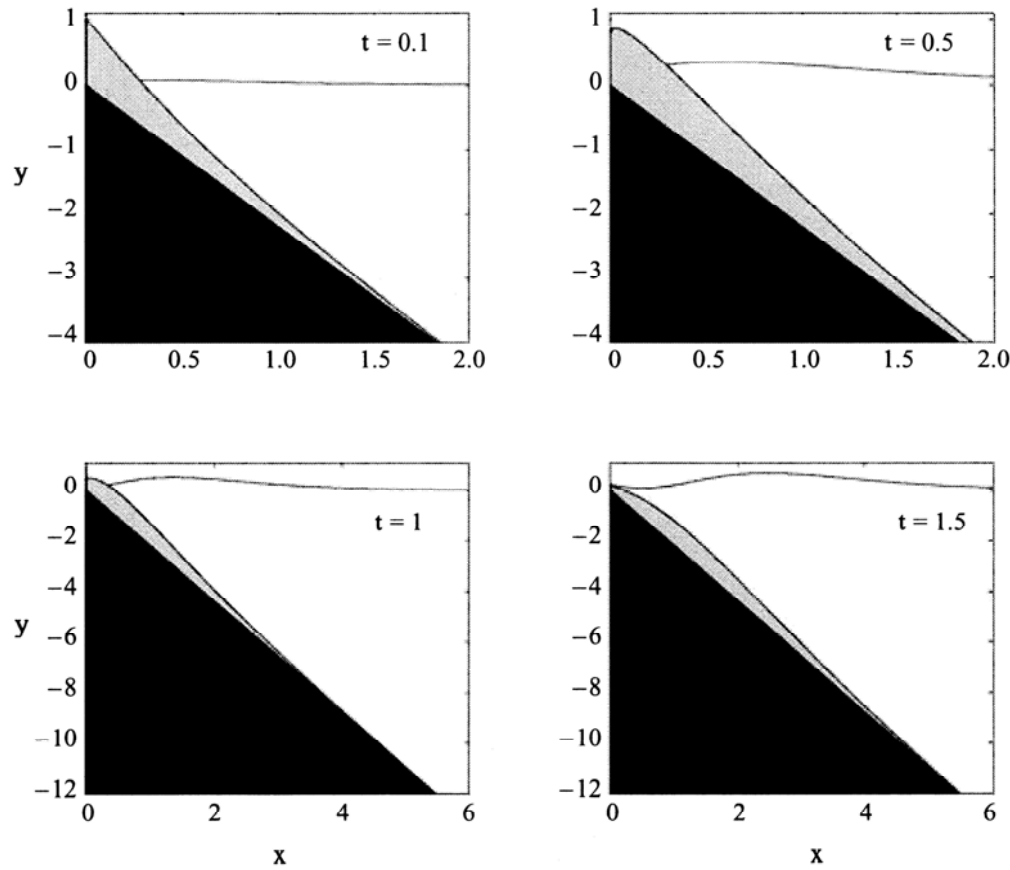
Solitary wave on a composite beach



Kanoglu and Synolakis, JFM, 1998

Analytical benchmarking

Subaerial landslide over a sloping beach



Liu, Lynett and Synolakis, JFM, 2003

Analytical benchmarking

Subaerial landslide over a sloping beach

Can the forced LSW be revisited and derive an analytical solution for a landslide to help validate models?

The **forced linear** (FLSW) equation for a sloping beach of angle β and forcing h_0 is

$$\frac{\partial^2 \zeta}{\partial t^2} - \frac{\tan \beta}{\mu} \frac{\partial}{\partial x} \left(x \frac{\partial \zeta}{\partial x} \right) = \frac{\partial^2 h_0}{\partial t^2},$$

Let

$$\xi = 2\sqrt{\frac{\mu x}{\tan \beta}},$$

Astonishingly, a particular solution of the FLSW for a forcing $h_0 = \exp(i\omega(\xi-t))$ is exactly

$$\zeta_p(\xi, t) = \frac{1}{3}[1 + 2\xi(\xi - t)]e^{(\xi-t)^2}.$$

Liu, Lynett and Synolakis, JFM, 2003

Laboratory benchmarking

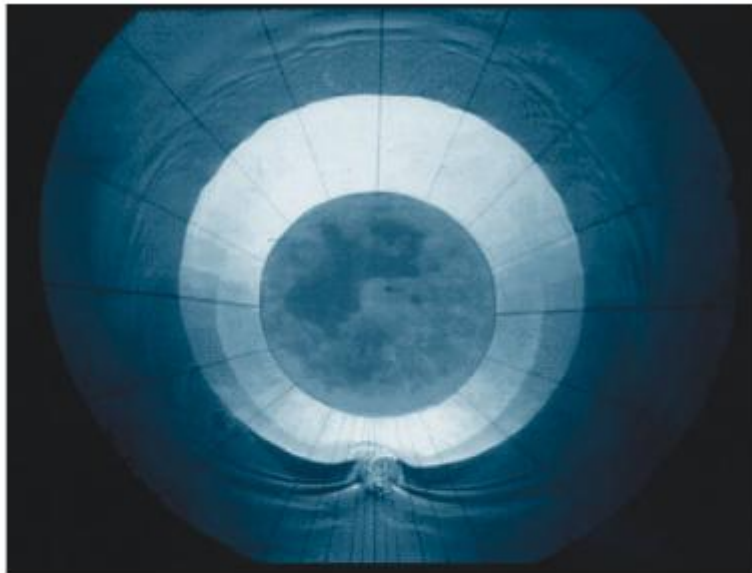
Why is laboratory benchmarking important?

For the purpose of validating inundation models, the scale differences are not believed to be important.

Numerical codes developed in the last decade that produce predictions in excellent agreement with measurements from small-scale laboratory experiments have been shown to model geophysical scale tsunamis well.

For example, a numerical code that models quantitatively adequately the inundation in a 1 m-deep model is also expected to model the inundation in the 1 km-deep geophysical geometry, as the grid sizes are adjusted accordingly and in relationship to the scale of the problem. Scale models, in general, do not have bottom friction characteristics similar to real ocean floors or sandy beaches, but this has proven not to be a severe limitation.

Laboratory benchmarking



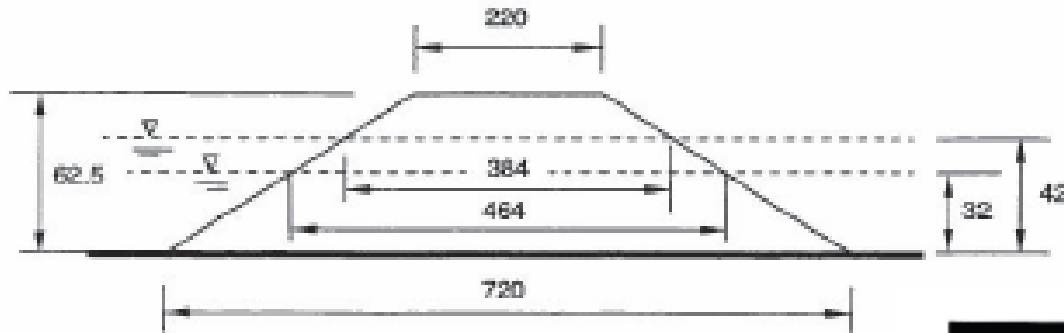
Solitary wave evolution over a sloping beach and runup
Synolakis, JFM, 1987

Solitary wave on a composite beach
Kanoglu and Synolakis, JFM, 1998

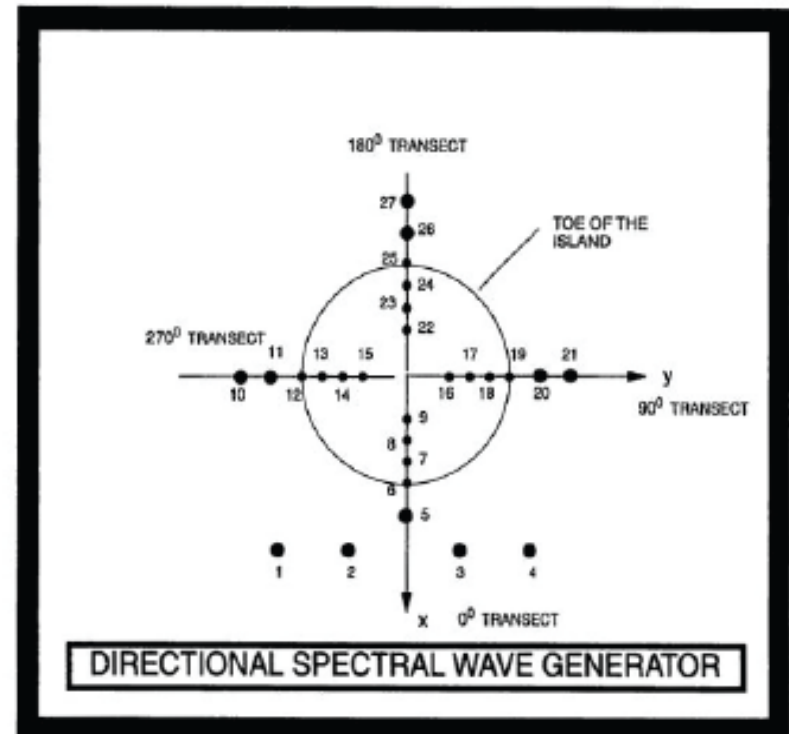


Solitary wave on a conical island
Kanoglu and Synolakis, JFM, 1998
and
Liu et al., JFM, 1995

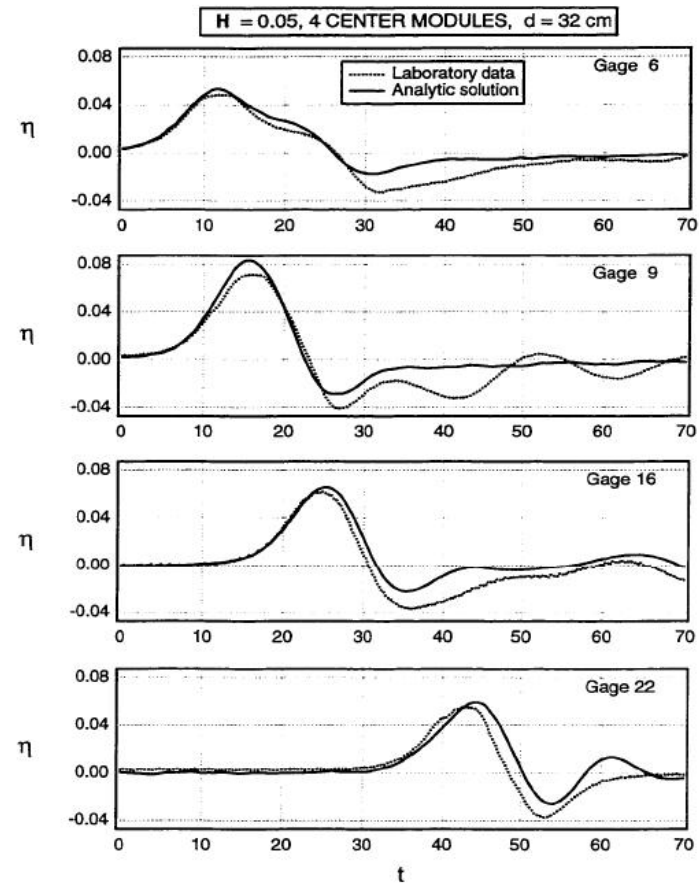
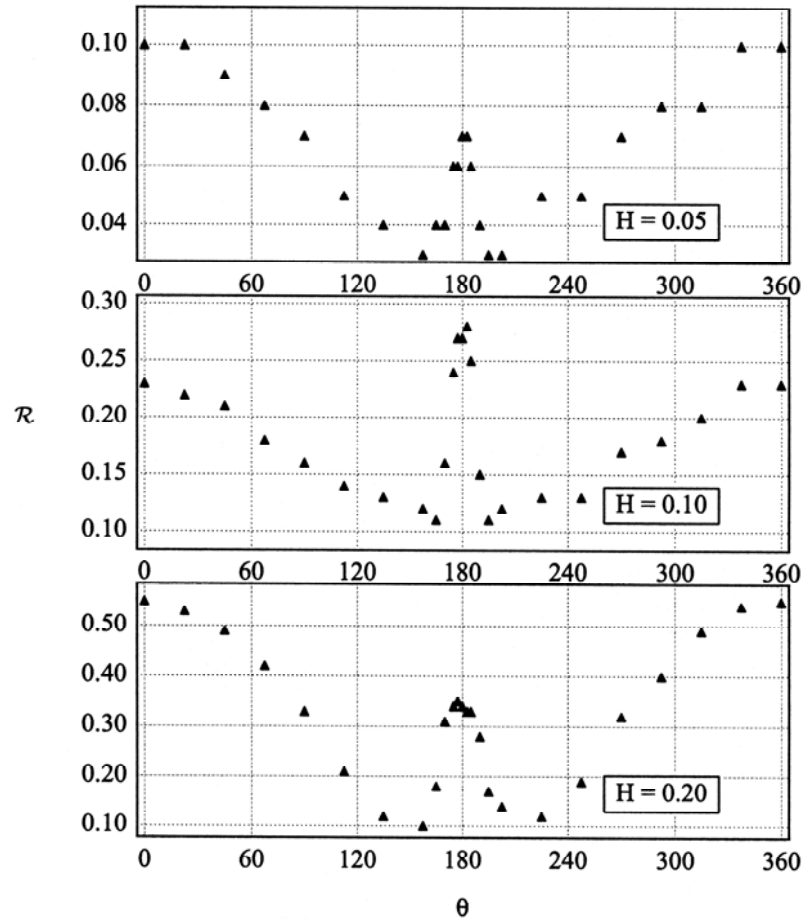
Laboratory benchmarking



Kanoglu and Synolakis, JFM, 1998
Liu et al., JFM, 1995



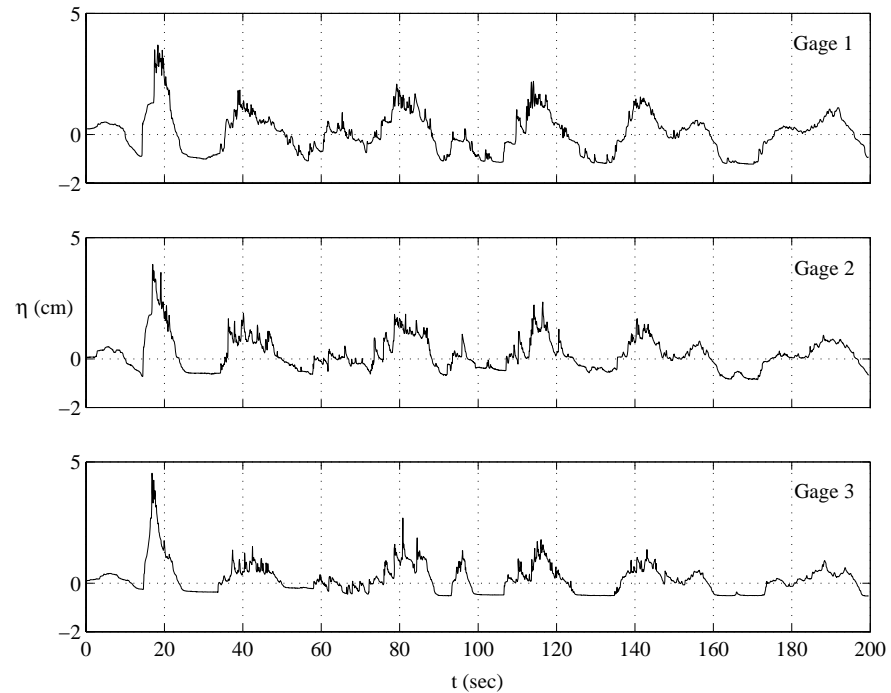
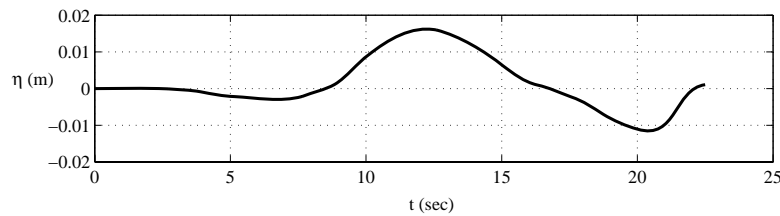
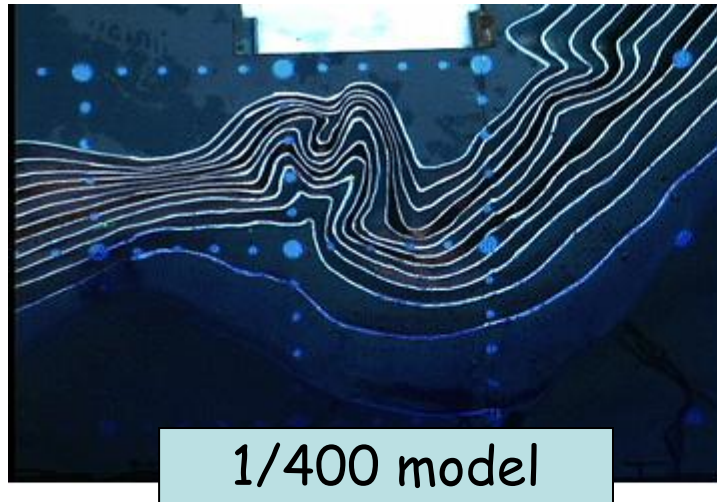
Laboratory benchmarking



Kanoglu and Synolakis, JFM, 1998; Liu et al., JFM, 1995

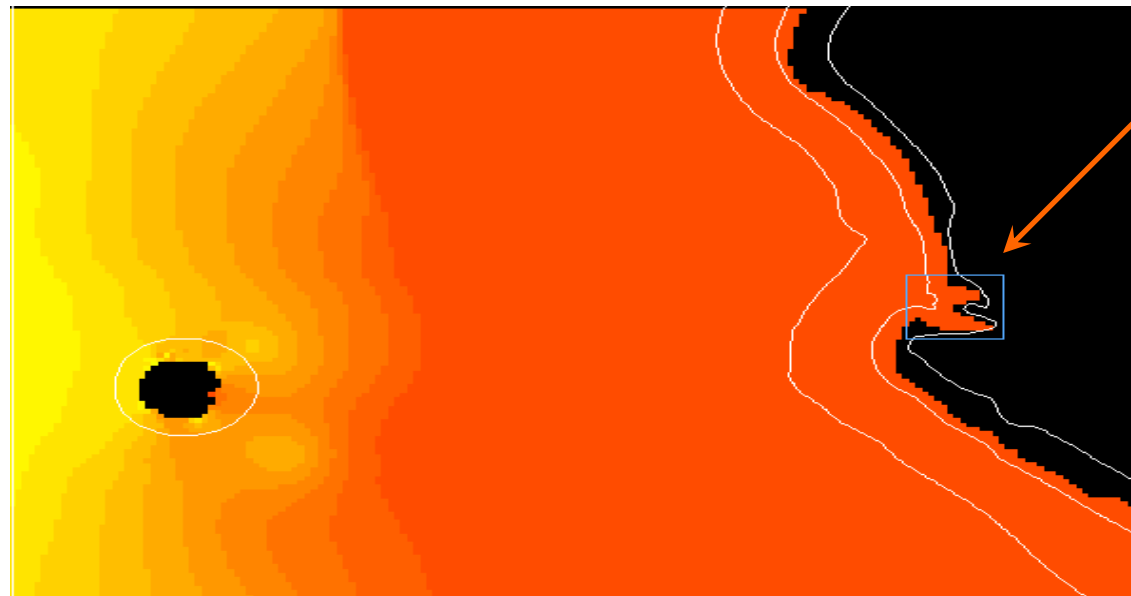
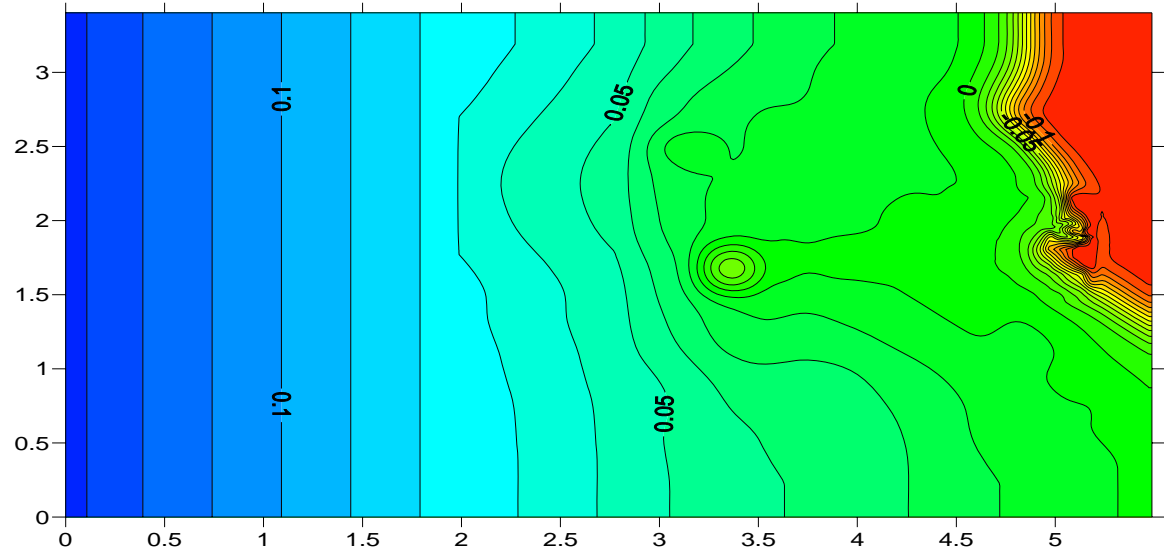
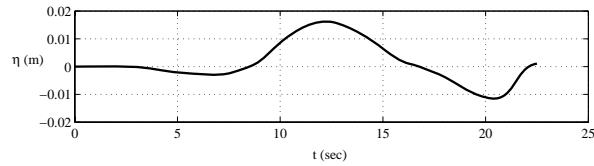
Laboratory benchmarking

Tsunami runup onto a complex three-dimensional beach; Monai Valley, Okushiri Island



Central Research Institute for Electric Power Industry, Abiko, Japan

Calculation of maximum runup in the Okushiri laboratory data



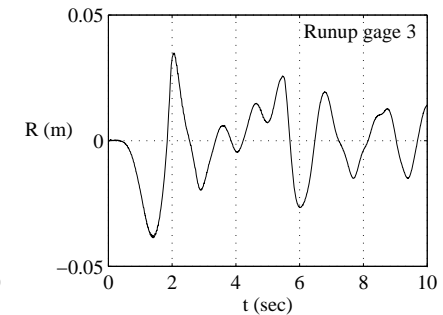
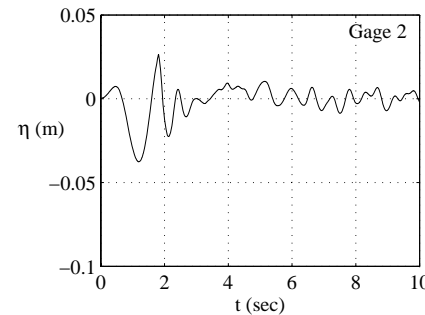
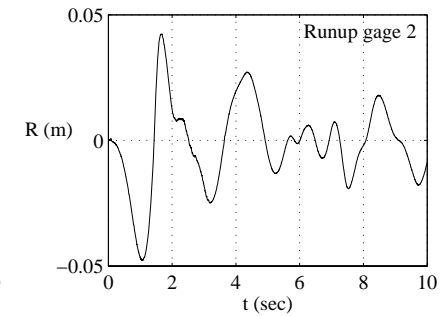
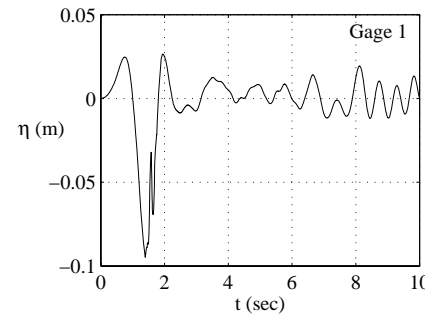
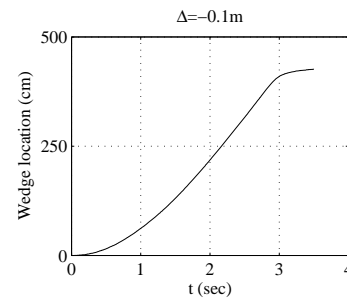
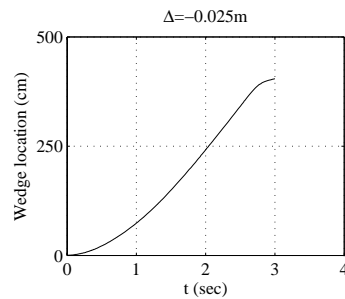
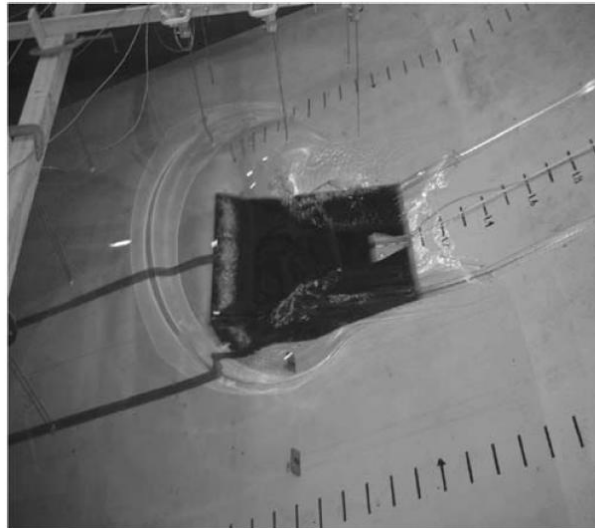
Maximum height:
7.10cm

Yasuda, 2004

2004 NSF Catalina Long Wave Runup Verification Workshop, Liu, Yeh and Synolakis

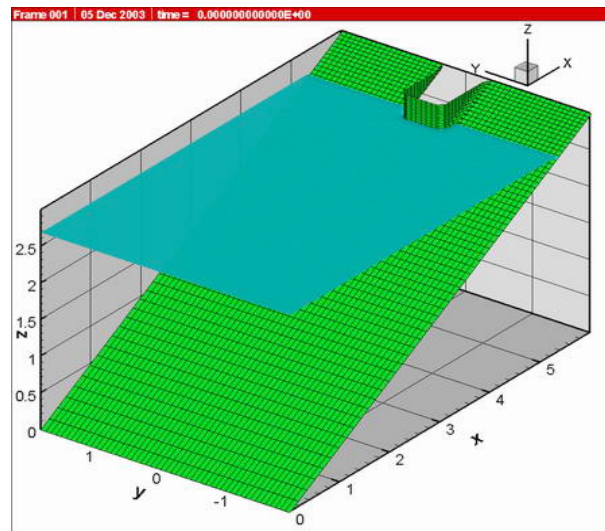
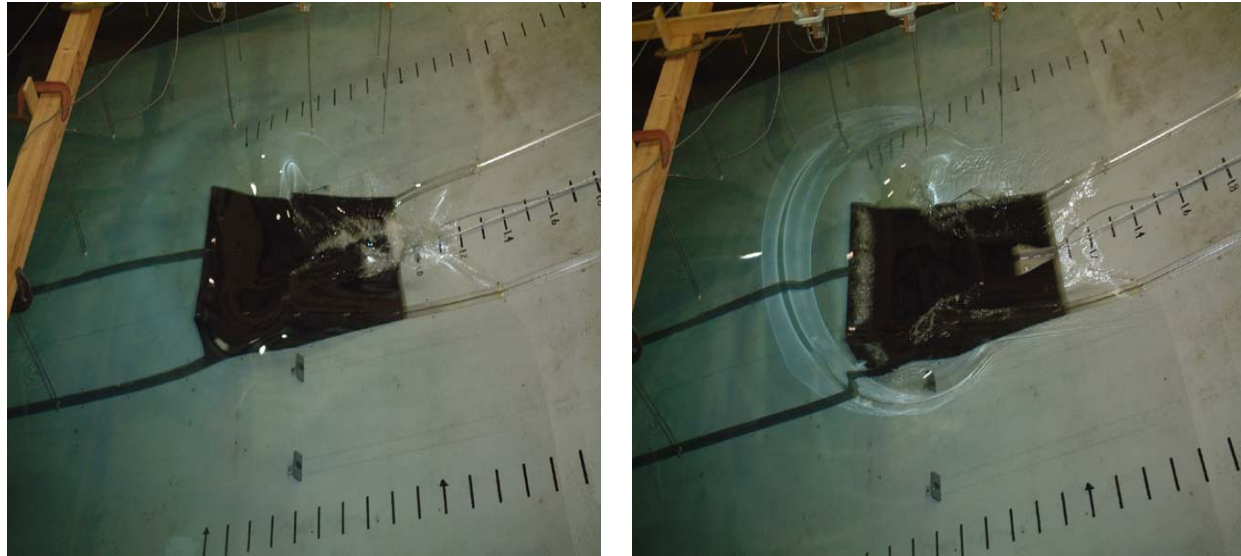
Laboratory benchmarking

Tsunami generation and runup due to three-dimensional landslide



Liu, Raichlen, Borrero, Wu and Synolakis, JFM, 2006

Large scale laboratory experiments on "landslide" tsunami generation. Liu, Raichlen, Borrero, Wu and Synolakis (2004)



Field benchmarking

Why is field benchmarking important?

Verification of a model in a real-world setting is an important part of model validation, especially for an operational model validation.

No analytical or laboratory data comparisons (or any limited number of tests, for that matter) can assure robust model performance in the operational environment.

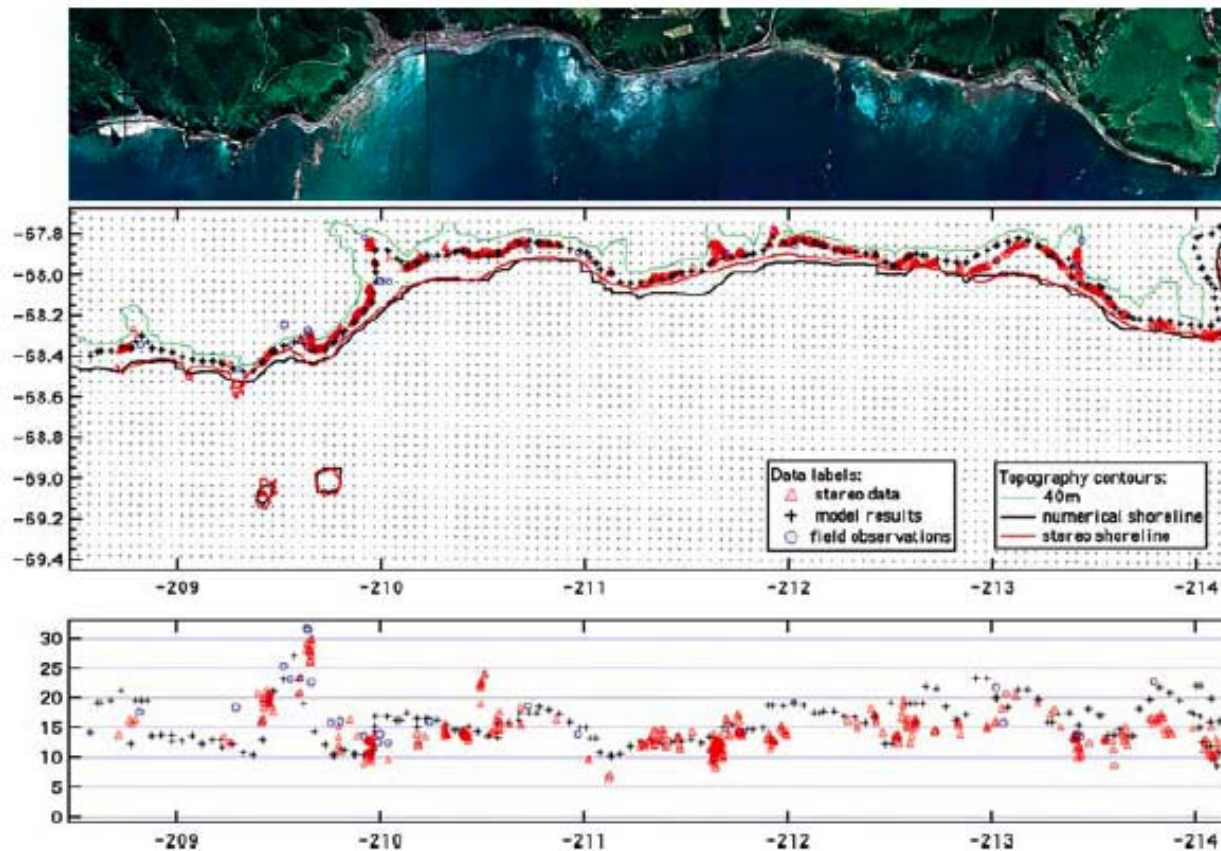
Test comparisons with real-world data provide an additional important step in the validation of a model to perform well during operation implementation.

The main challenge of testing a model against real-world events is to overcome uncertainties of the tsunami source. While the source of the wave is very deterministic in the controlled setting of the laboratory experiment and can be reproduced precisely, field data would always have uncertainties about the source.

Comparison of MOST predictions for the extreme runup in Monai with field measurements.

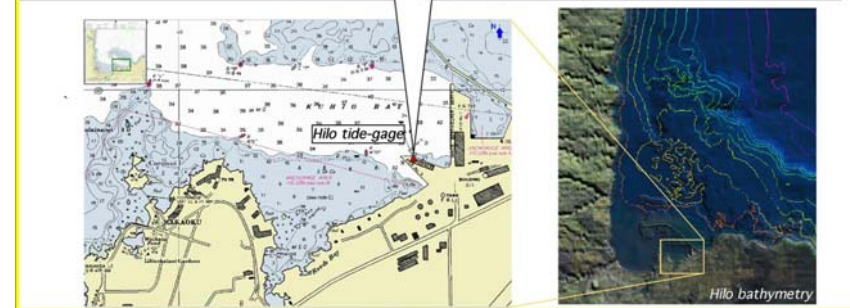
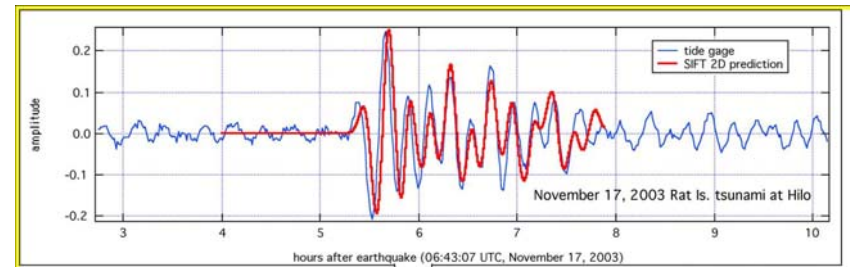
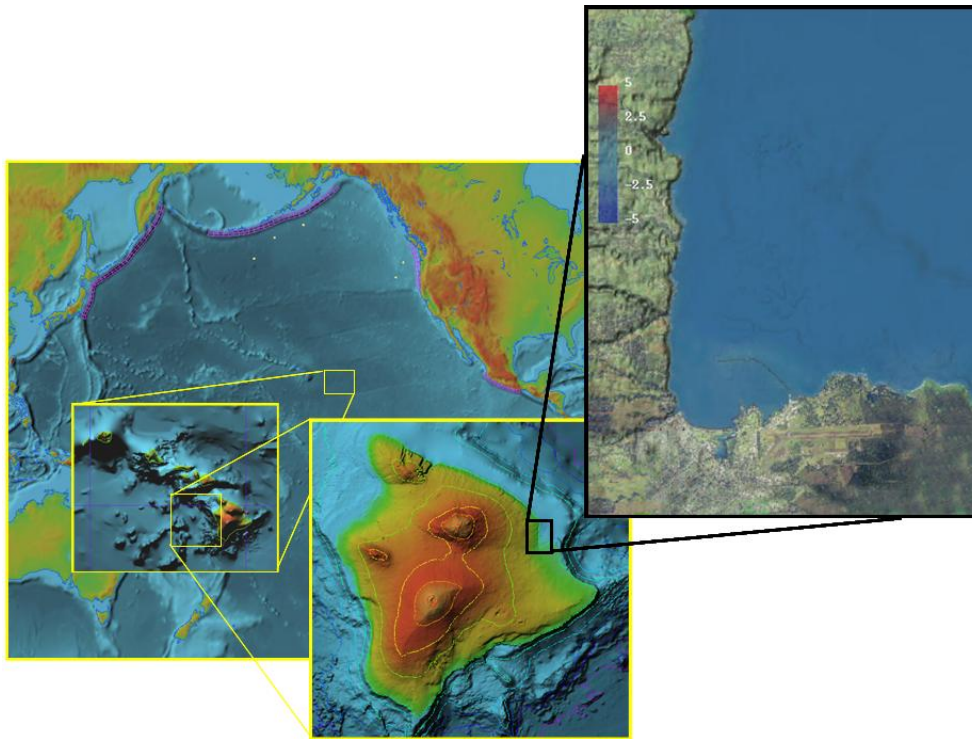
Two verification/validation objectives are achieved.

The algorithm is seen to converge to the measurements as the grid size is reduced.



Field benchmarking

17 November 2003 Rat Island tsunami



Titov et al., Natural Hazards, 2005

Scientific evaluation

Peer-review documentation

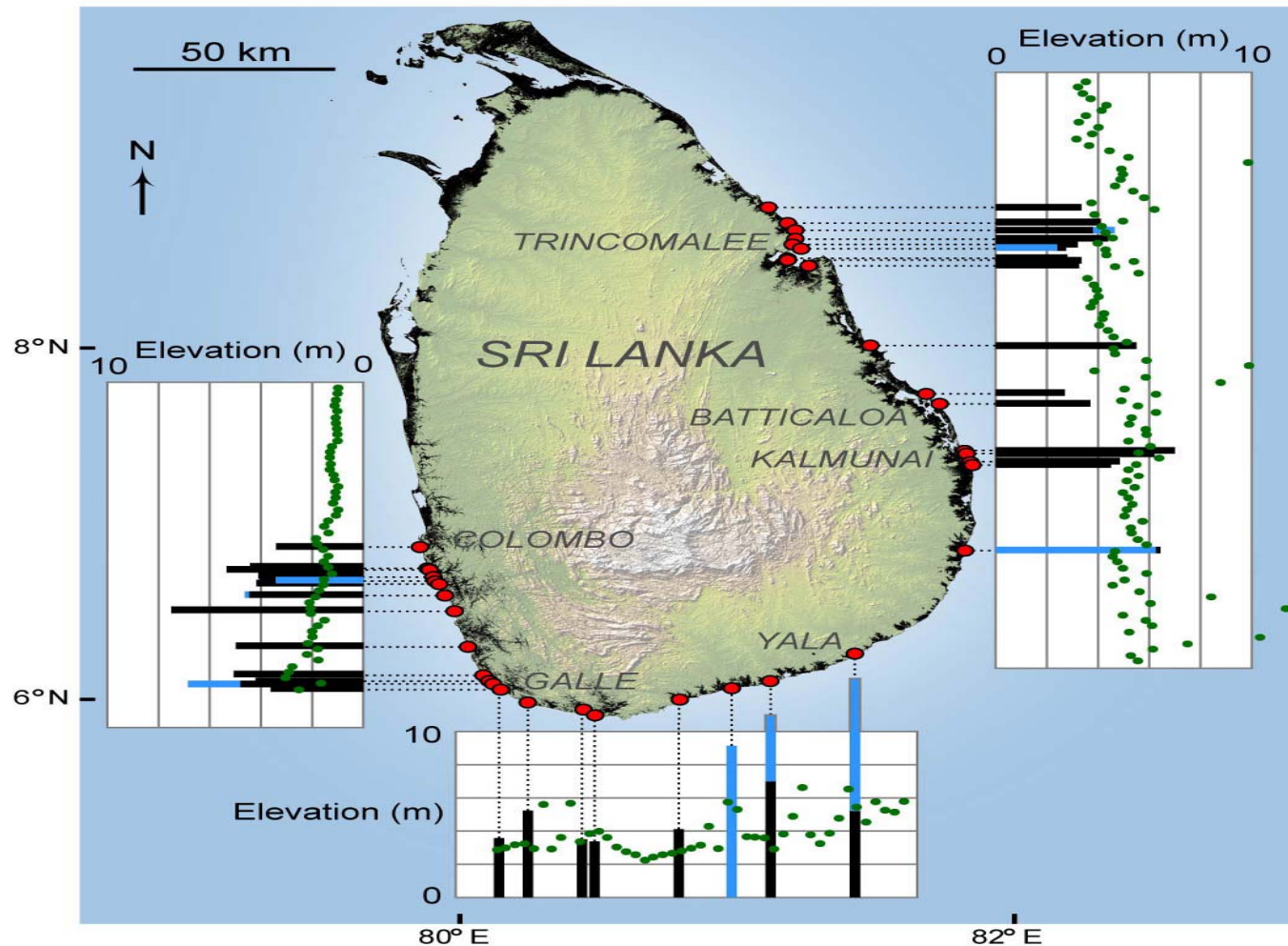
Model validation and verification is a continuing process. Any model used for inundation mapping or operational forecasts needs to be presented in peer-reviewed scientific journals. The publications need to include comparisons of the model predictions with all the above benchmarks (or equivalents).

Formal scientific evaluation

A formal evaluation process of individual models needs to be established to avoid ad hoc decisions as to the suitability of any given model. This process may include solicitation of additional reviews of the model's veracity by experts, or the requirement that additional testing be performed. This process will set the standard for the best available practice at any given time, and it will hopefully eliminate the liability to code developing institutes, states, engineers, and geophysicists who collaborate on the development of inundation maps.

What confidence can we have in verified and validated inundation models ?

Sri Lanka Inundation : Measurements and Model Predictions



Liu et al, SCIENCE, in press.

Operational evaluation

Pacific Environmental Laboratory/Tsunami Warning Centers
National Oceanic and Atmospheric Administration, Seattle, Washington

The operational evaluation should be done by a test-bed consisting of research and operational parts of NOAA.

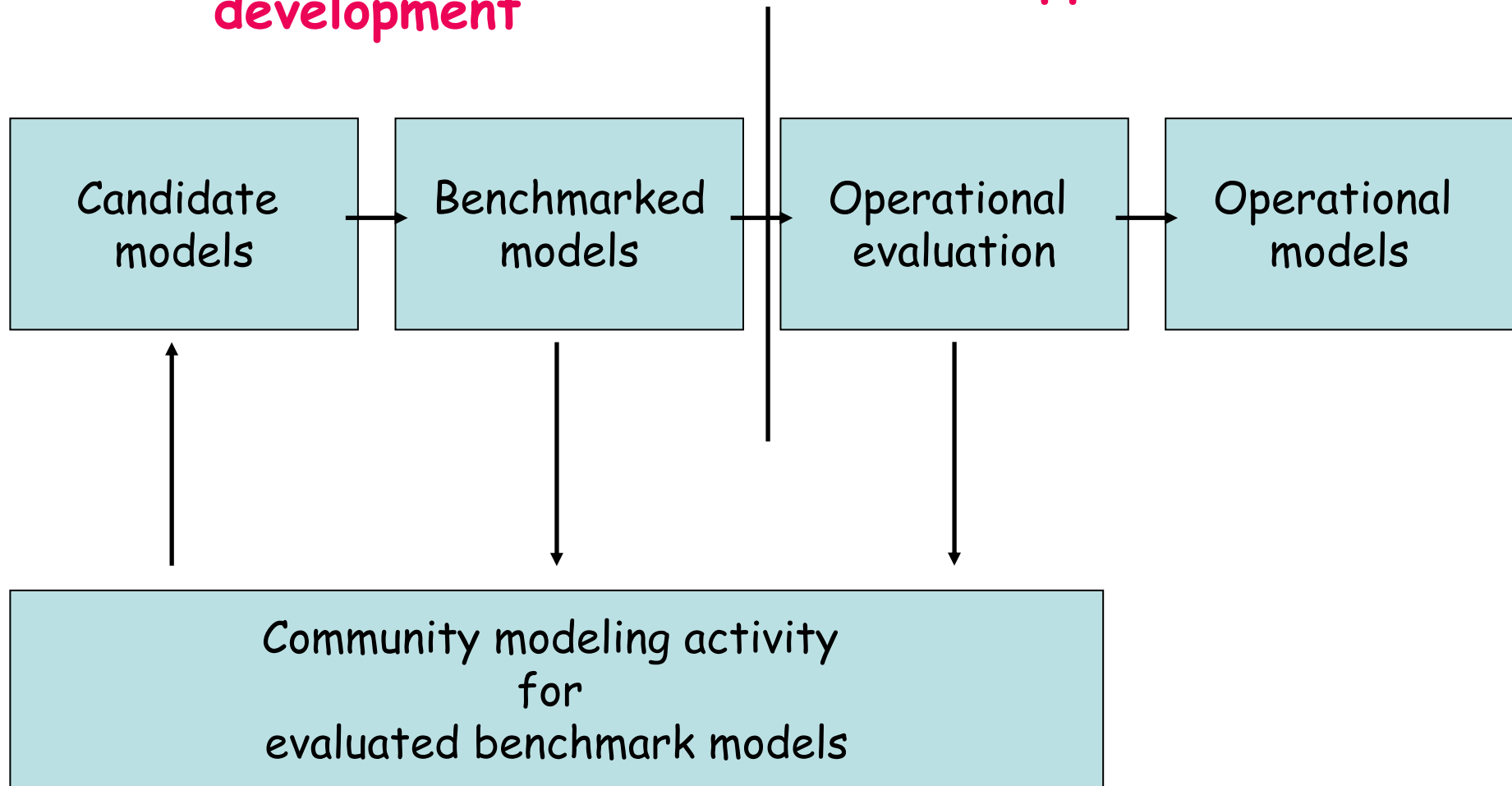
While the scientific evaluation process may identify models that are realistic and computationally correct, some of them may not be sufficiently versatile for inundation mapping or operational applications, as is often the case with university-based research codes.

An additional evaluation process needs to be established to assess operational factors of the model, such as special implementation hardware/software issues, ease of use, computation time, etc.

Developing NOAA operational model

Research and development

Application



Conclusion

State-of-the-art inundation codes in use today have evolved from first principles through a painstaking process of careful validation and verification.

However, every new event poses a diminishing challenge.

1. Establishment of standards for model validation and verification;
2. Scientific evaluation of individual models;
3. Operational evaluation of individual models;
4. Development of operational applications for forecasting;
5. Procedures for transfer of technology to operations.

Only through parallel testing of models under identical conditions, as when there is a tsunami emergency and an operation forecast is performed, can the community determine the relative merits of different computational formulations, an important step to further improvements in speed, accuracy, and reliability.

NOAA report is published.

TSUNAMI MITIGATION — *Early Attempts*

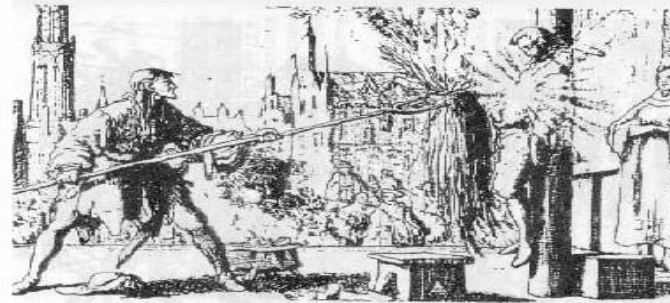
Medieval Japan



Kashima restrains Namazu

The Enlightenment

(Lisbon Tsunami — 01 November 1755)



Committee of Experts from Coimbra University recommends Auto-da-fe

[Voltaire, *Candide ou l'Optimisme*, 1759]

More Modern Approach

- *Protection:* The walls of the Japanese coastline.

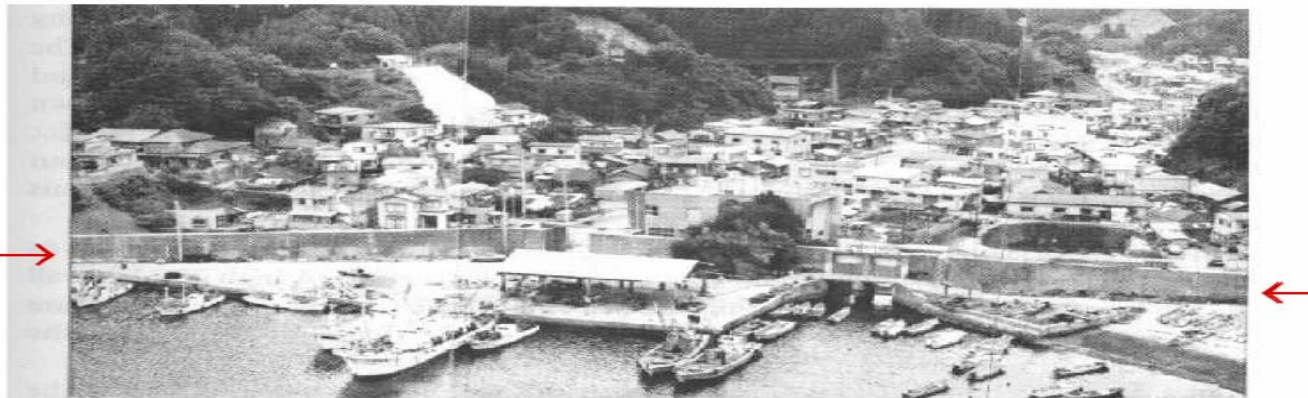


Photo 2. Typical fishing village, (Ryoishi), on the Sanriku coast.

[Fukuchi and Mitsuhashi, 1983]



Tsunami Forecast Modeling & Mapping

Methodologies and Strategy based on:

- Titov, Vasily V., Frank I. Gonzalez, E. N. Bernard, Marie C. Eble, Harold O. Mofjeld, Jean C. Newman, Angie J. Venturato (2005): Real-Time Tsunami Forecasting: Challenges and Solutions, *J. Natural Hazards*, 35, 1, 35-41
- González, Frank I., Vasily V. Titov, Harold O. Mofjeld, Angie J. Venturato, R. Scott Simmons, Roger Hansen, Rodney Combellick, Richard K. Eisner, Don F. Hoirup, Brian S. Yanagi, Sterling Yong, Mark Darienzo, George R. Priest, George L. Crawford, Timothy J. Walsh (2005): Progress in NTHMP Hazard Assessment, *J. Natural Hazards*, 35, 1, 89-110.
- González, Frank I., Eddie N. Bernard, Christian Meinig, Marie C. Eble, Harold O. Mofjeld, Scott Stalin, (2005): The NTHMP Tsunameter Network, *J. Natural Hazards*, 35, 1, 25-39
- Titov, V.V., and C.E. Synolakis (1998): Numerical Modeling of tidal wave runup. *J. Waterw. Port Coastal Ocean Eng.*, 124(4), 157-171.



Operational Tsunami Forecasting

- Essential to Improve Warning Speed and Reliability
- Vast Ocean Areas with **No Tsunami Measurements**
- Must Integrate Real-time **Measurement** and **Modeling**
 - *Measurement: NOAA DART Network*
 - *Modeling: NOAA Tsunami Forecast Model*



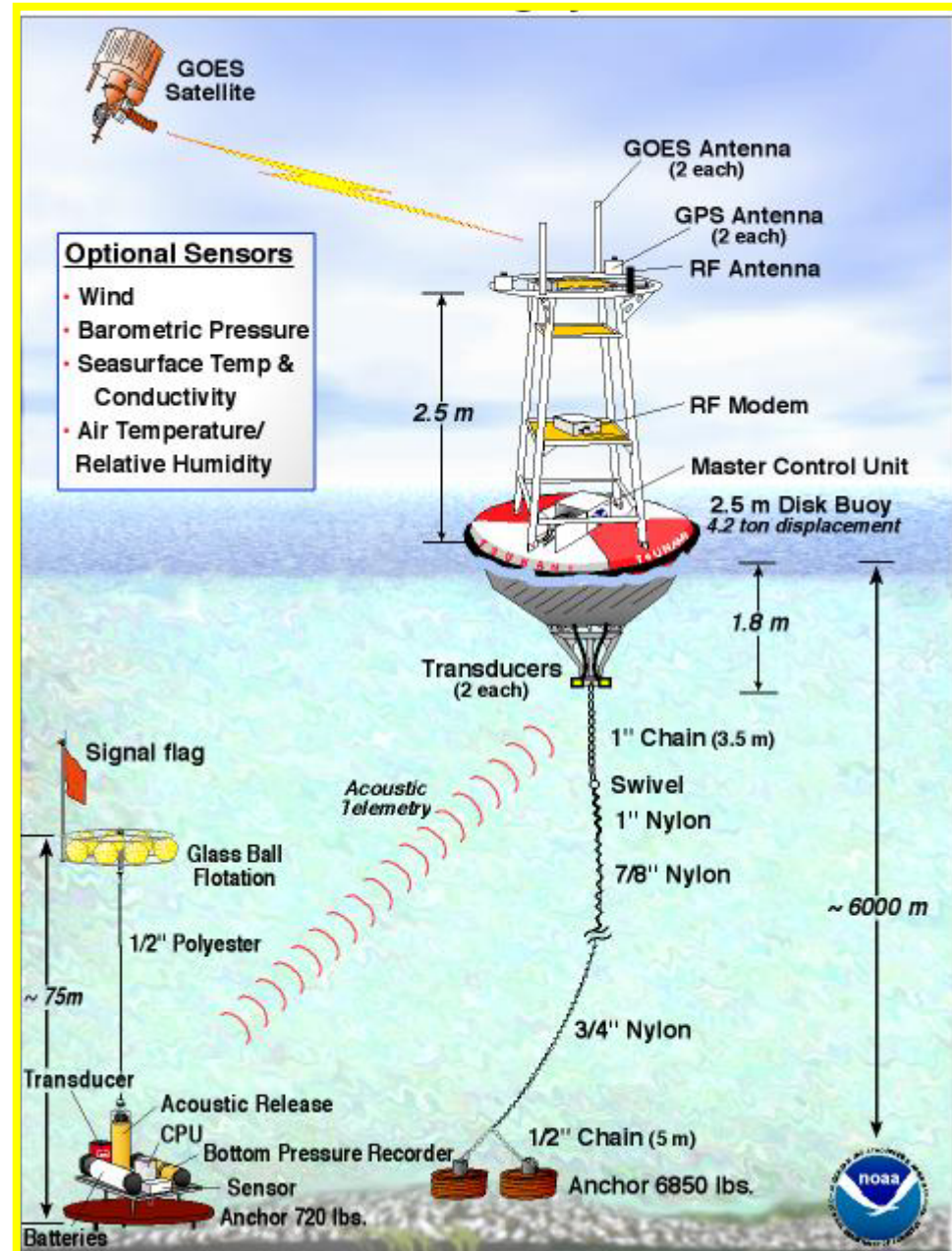
DART Concept

BPR measures small changes in pressure at the seafloor. Data sent acoustically to surface buoy, then via satellite to the TWSs (Tsunami Warning Centers).

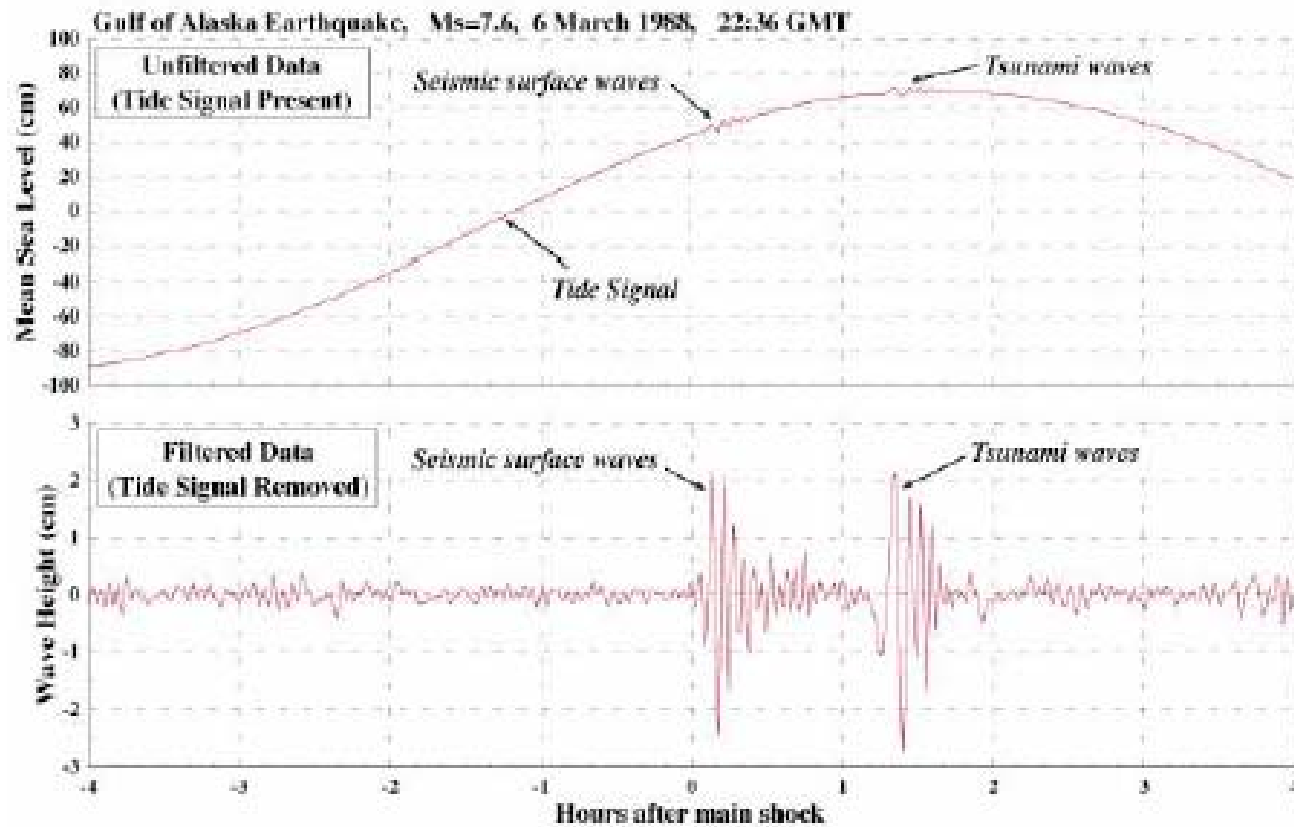
Normal transmissions: Hourly reporting of 15 minute data to confirm system readiness.

Two Event Modes:

- **Automatic:** Triggered by seismic or tsunami wave
- **Request:** Warning Center triggers data stream

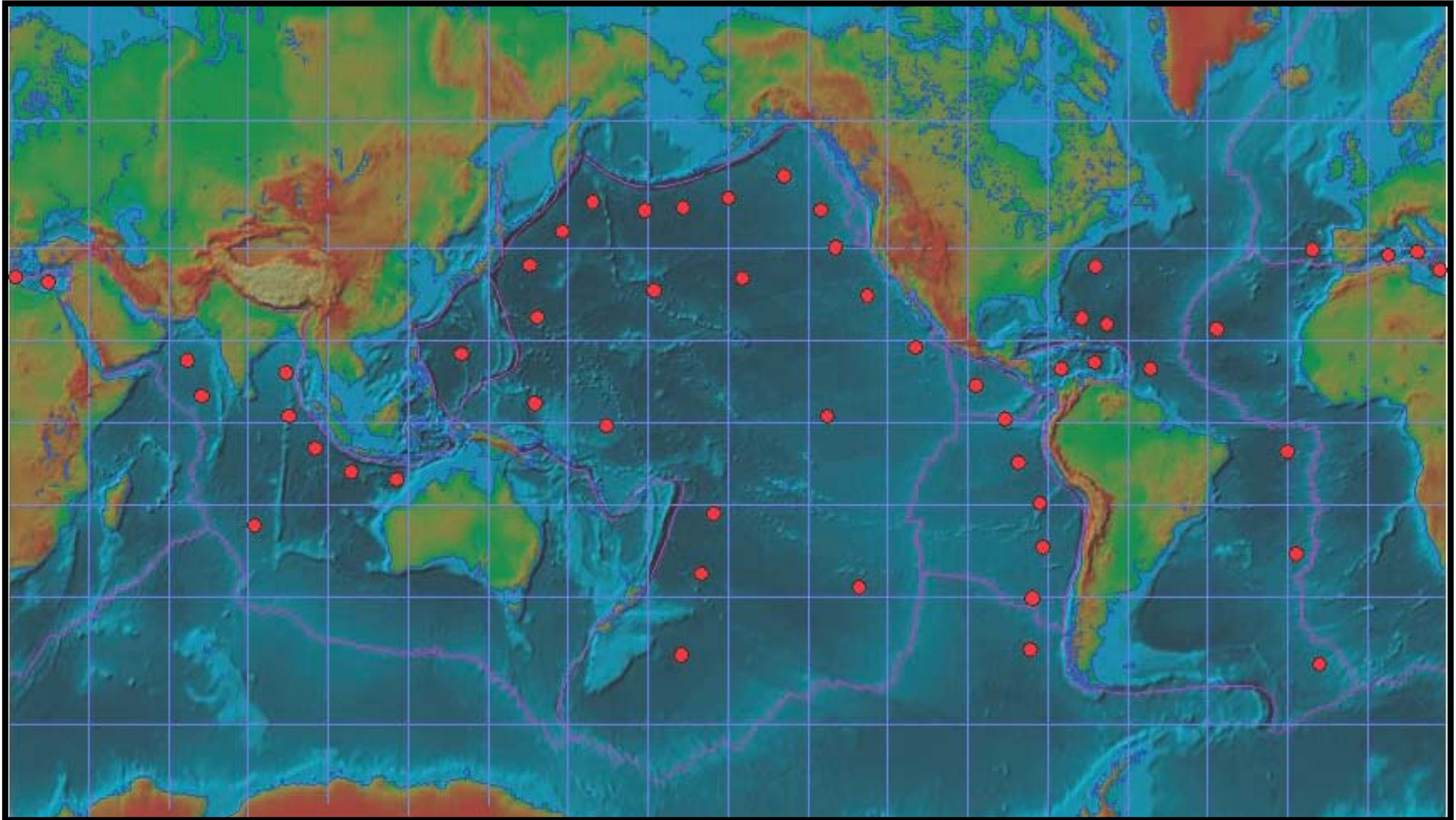


It is not trivial to identify tsunami





Measurement: Global DART Network

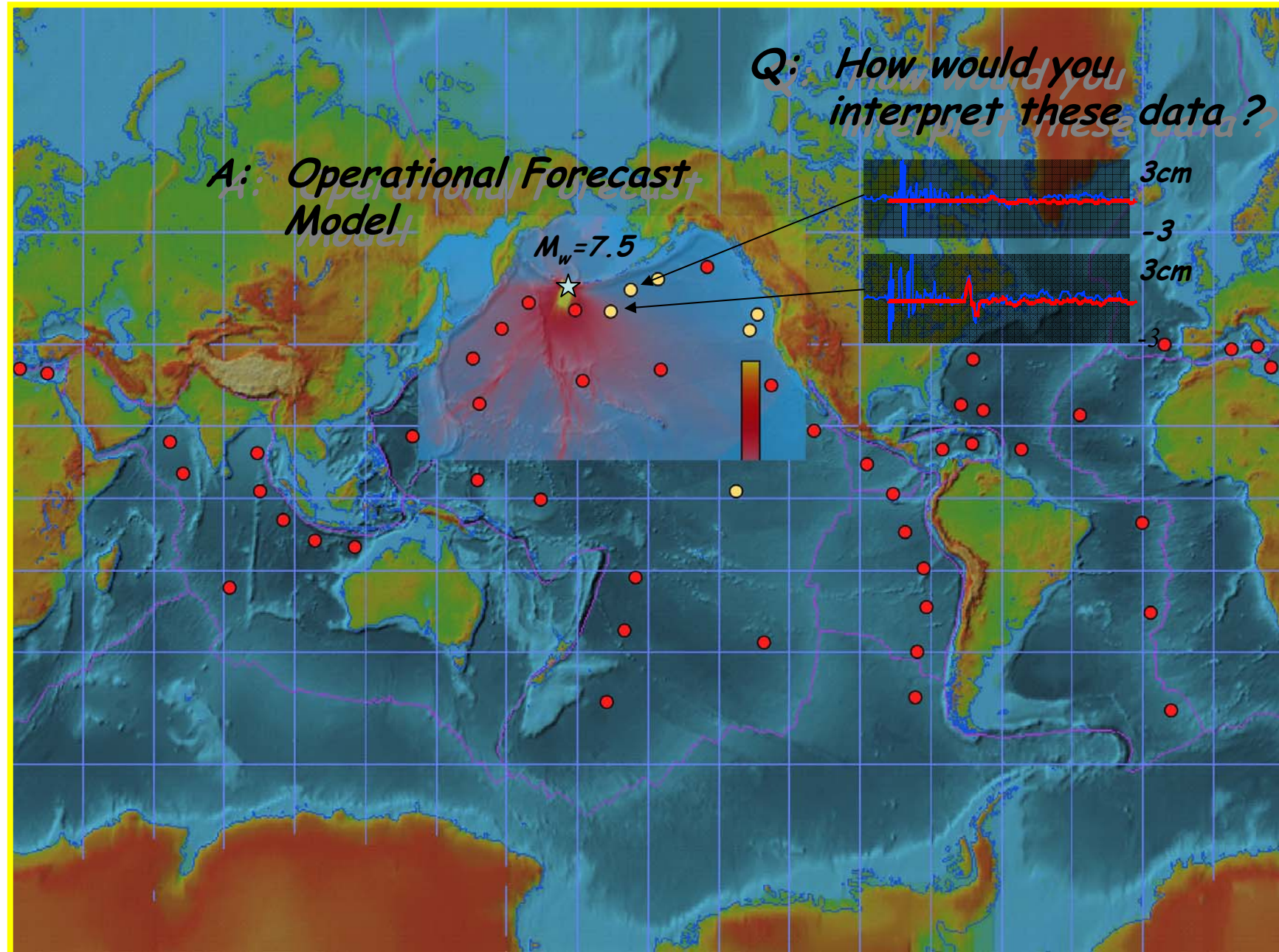




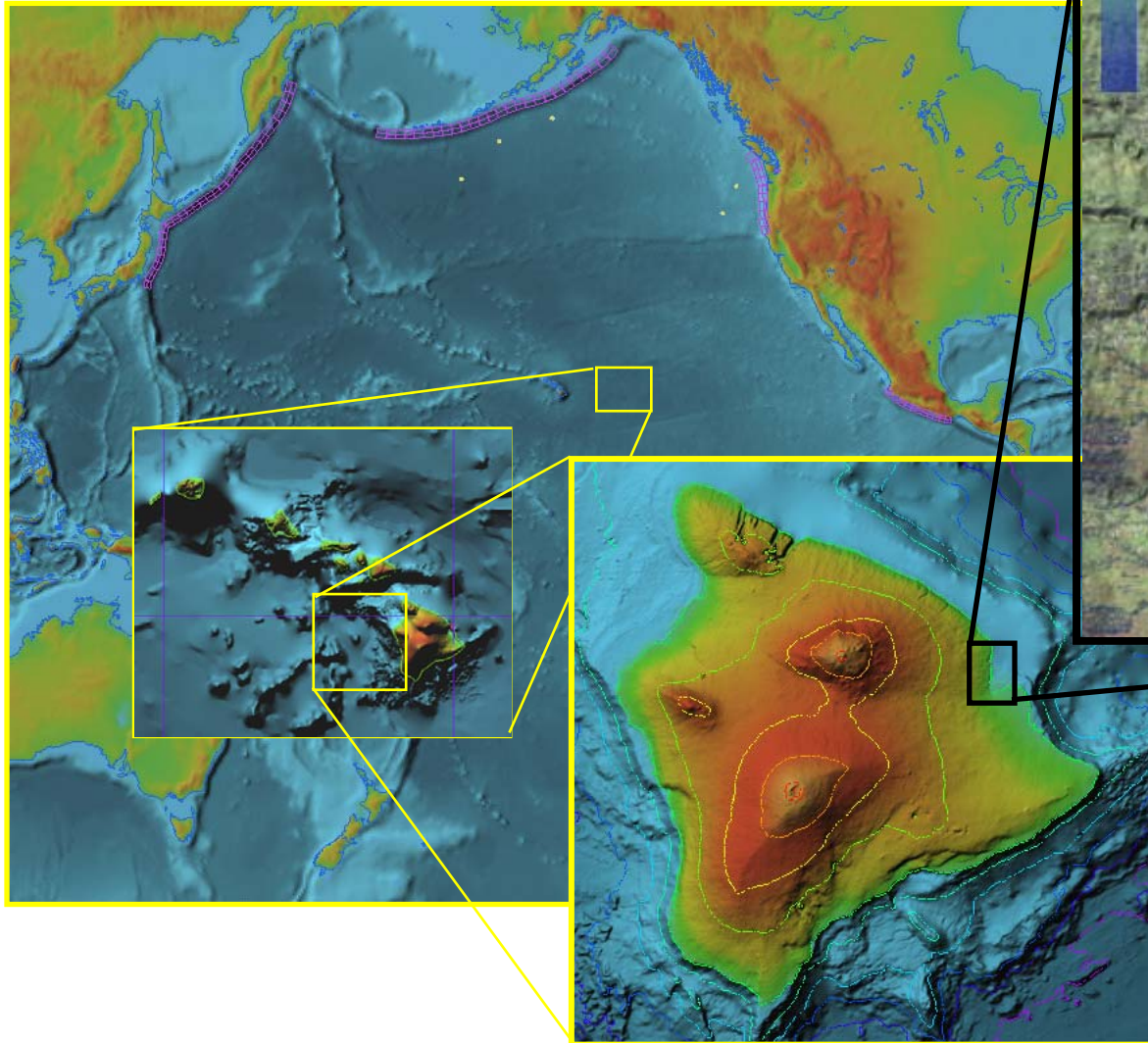
Operational Tsunami Forecasting

- **Must Integrate Real-time Measurement and Modeling**
 - *Measurement: NOAA DART Network*
 - *Modeling: NOAA Tsunami Forecast Model*
- **Real-time Methodologies**
 - *Inversion: Force Model to Match Real-time Data*
 - *Interpolation: Model Values for Areas with No Data*
 - *Forecast: Real-time Inundation Simulations*
- **International Modeling Network**
 - Transfer, Maintain, and Improve Tsunami Forecast Models*

Example of Tsunami Forecast: 17 Nov 2003

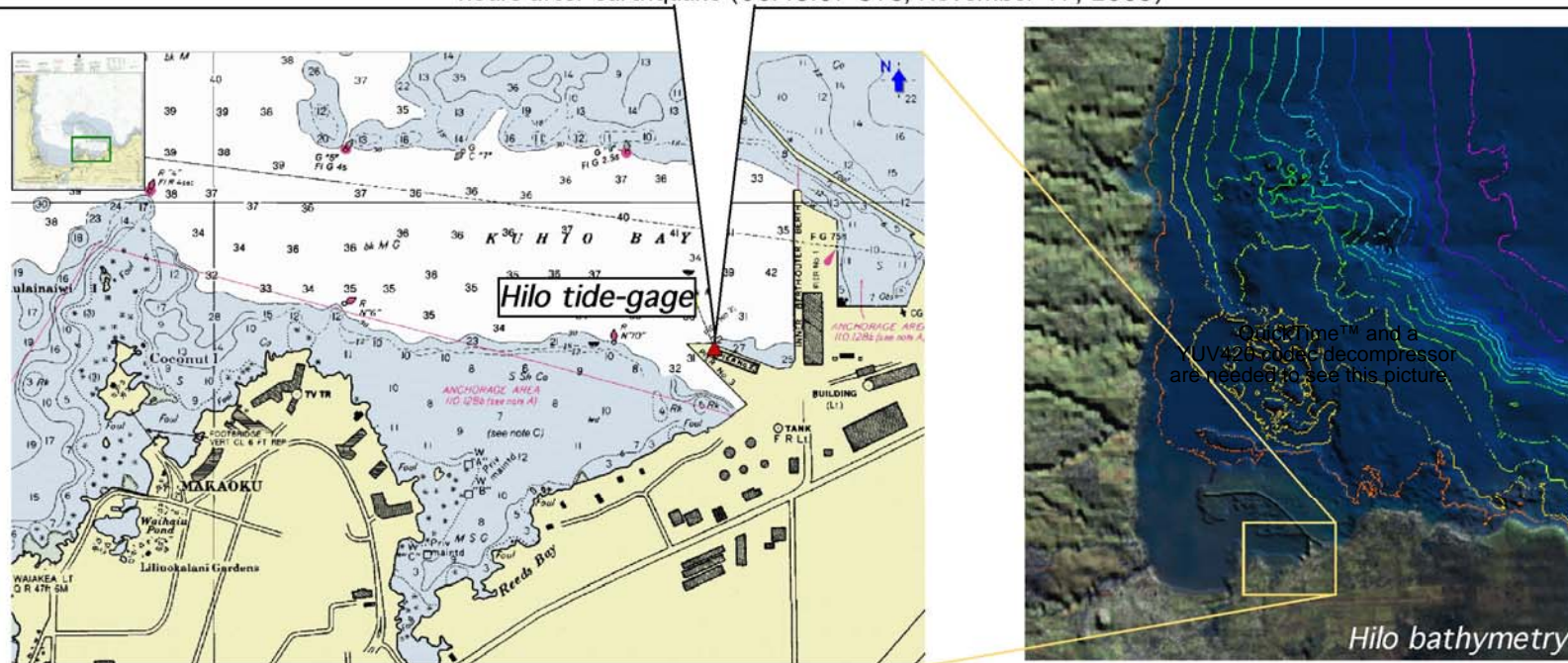
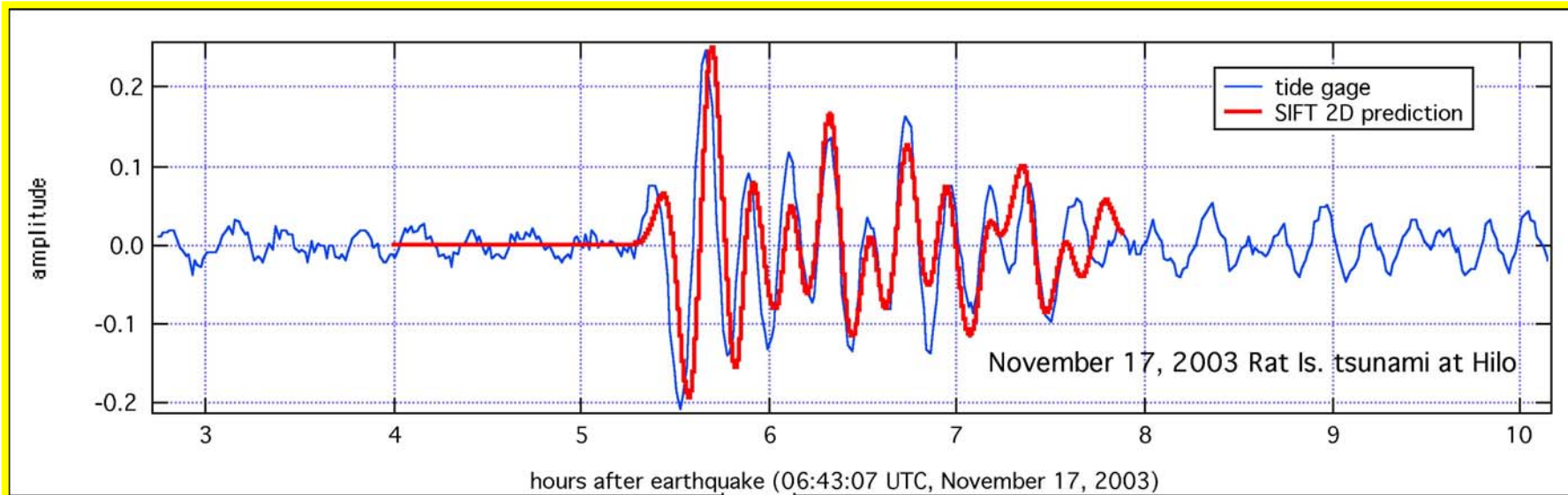


1. Pre-computed Nested Grid Database of Offshore Values



2. Provides initial conditions for real time inundation simulation (~10min to run)

Result: Tsunami Forecast at Hilo





Site-Specific Hazard Assessment: Inundation Modeling & Mapping

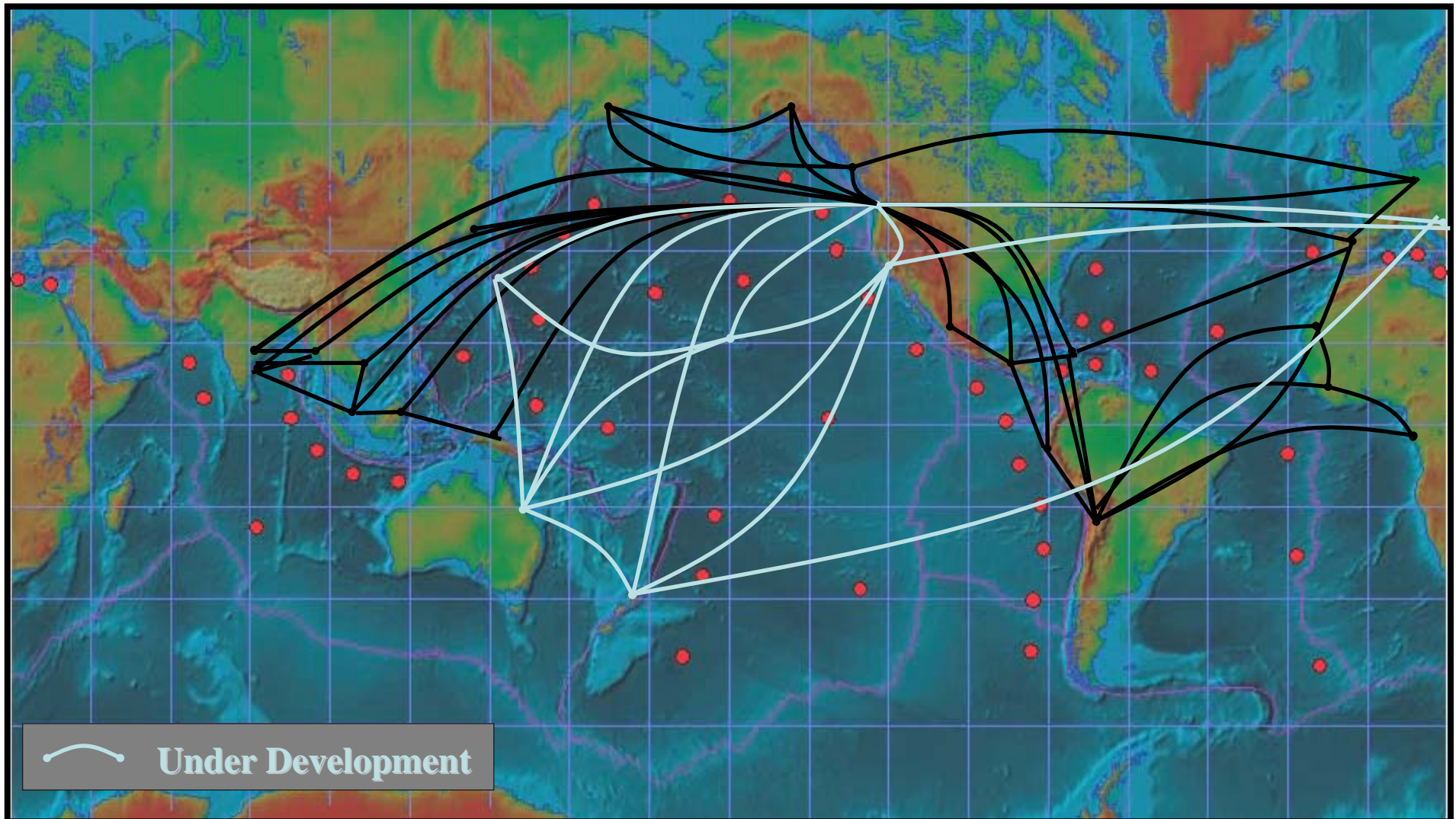
Strategy

- Develop Site-Specific Operational Forecast Model
- Exploit Commonality and Overlap Between Forecast Modeling and Hazard Assessment Modeling
 - *Embedded Bathy/Topo Grid System*
 - *Numerical Model*
- Transfer Model to State
- State Conducts Modeling Studies
 - *"Credible Worst Case" Source*
 - *Probabilistic Source Ensembles*
 - *Output for Engineering, Human Impact Studies*

International Modeling Network

Transfer, Maintain, & Improve Forecast & Hazard Assessment Models

Network Nodes Will Share: Models, R&D Tools, Databases, ...



What do we need beyond DART?

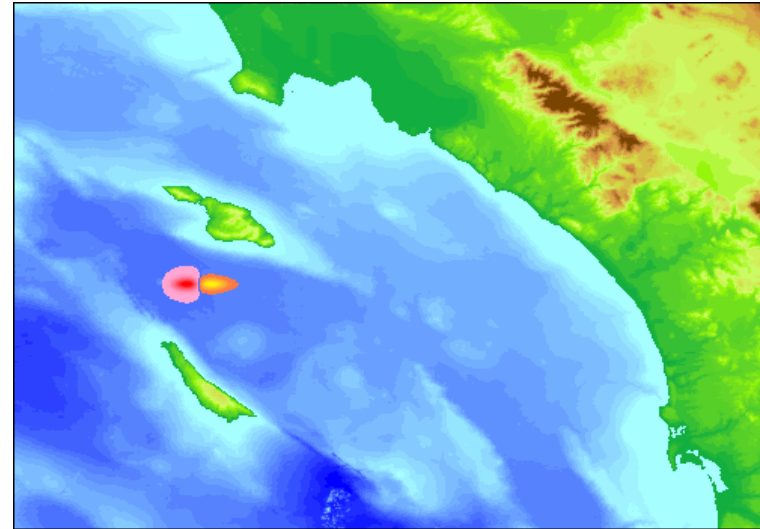
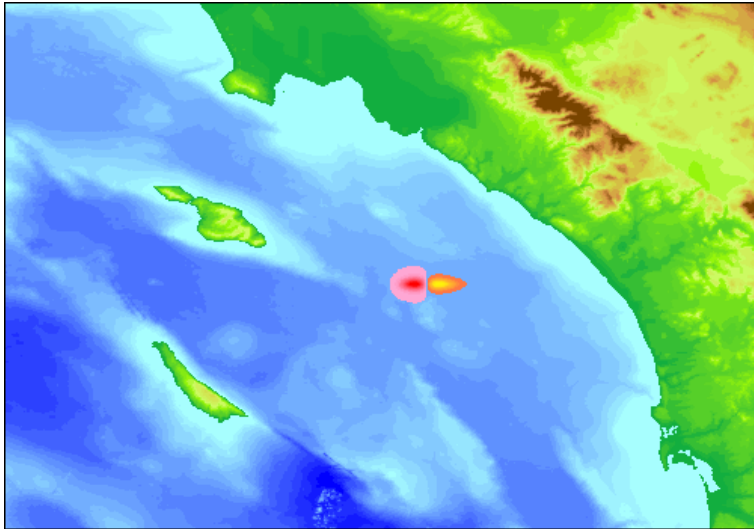
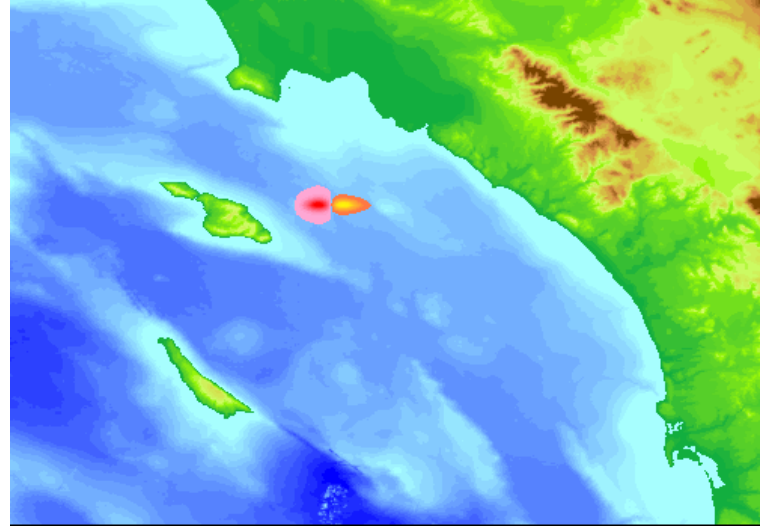
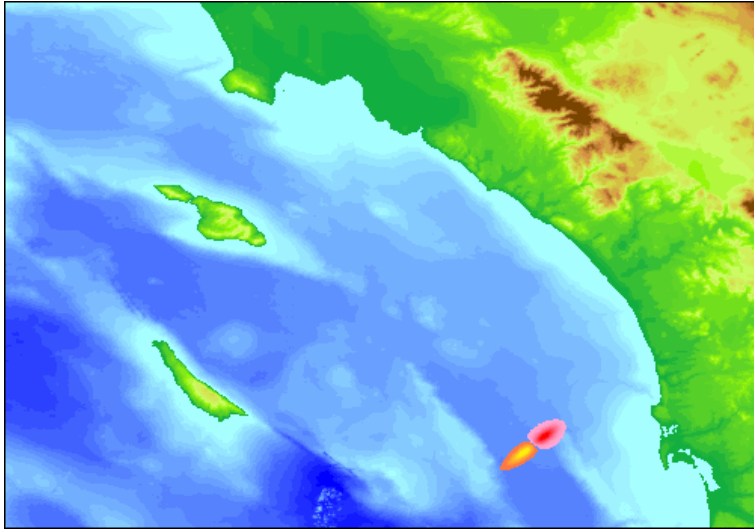
Realistic inundation maps to complement the warnings.

Education and training for self-evacuation based on evacuation maps and evacuation drills.

Training of scientists to update inundation maps and evacuation scenarios based on updated hazard information as it becomes available.

Design waves for likely events - one can build probabilistic maps with design waves.

Early inundation maps



SIMULATION OF TSUNAMI ATTACK FROM UNDERWATER LANDSLIDE OFF L.A.-L.B. HARBOR

[Borrero et al., 2003]

320

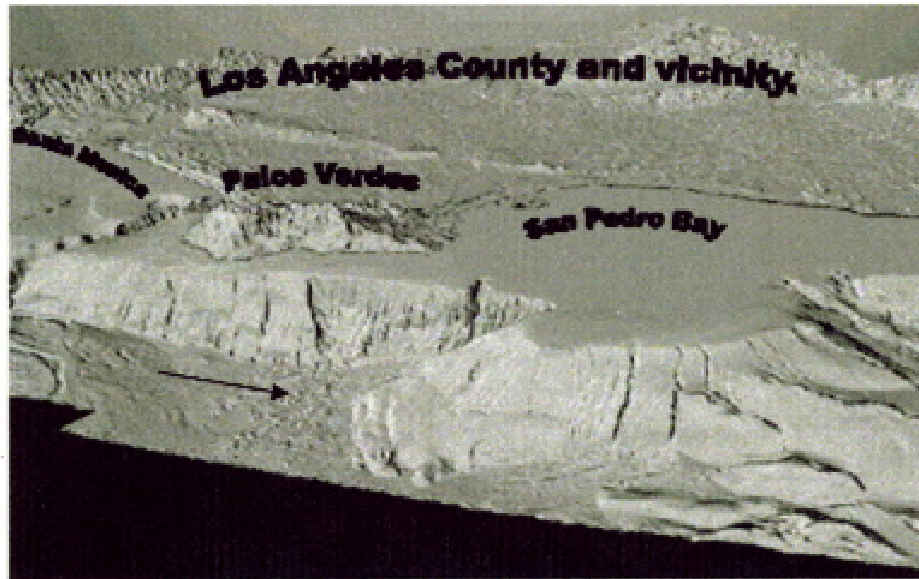
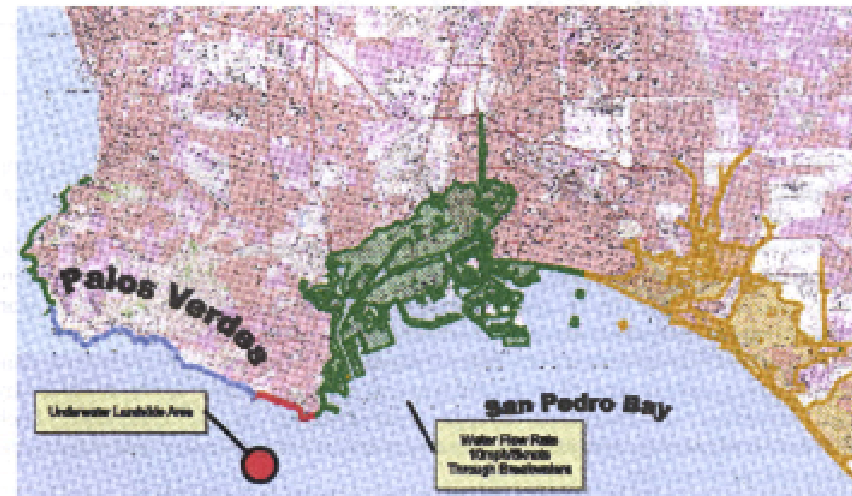
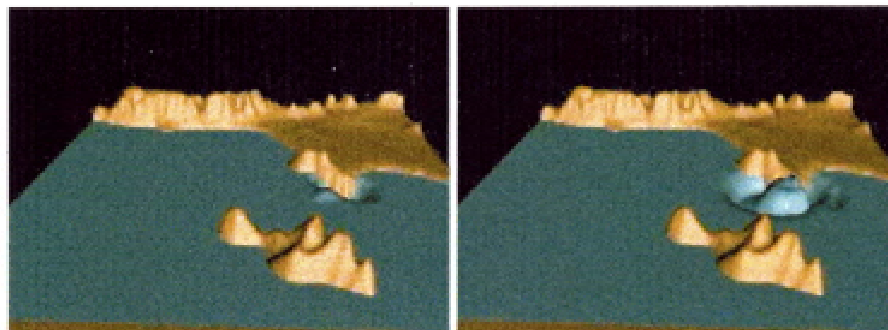
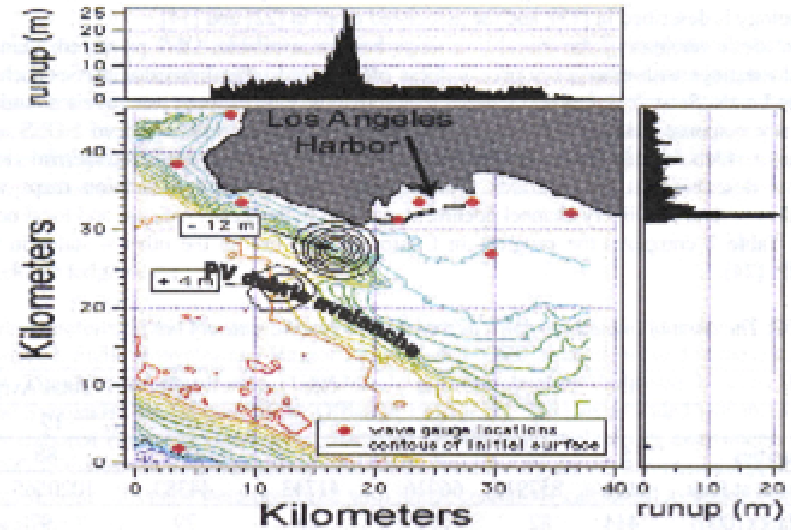
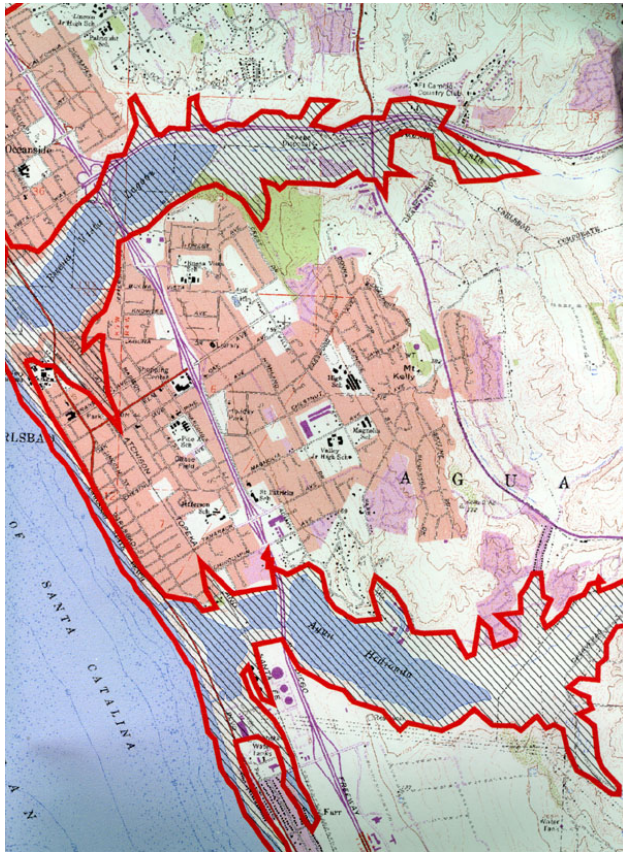


Figure 3. The bathymetry off Los Angeles, California. The Palos Verdes peninsula is seen on the left separating Santa Monica Bay and San Pedro bays (right). Various seeps suggestive of potential tsunami slides are shown including the PV debris avalanche.





Complete hazard assessment

Regions of high wave heights frequently do not correspond to regions of high currents.

Lack of correspondence between maximum wave height and maximum current means that inundation maps of maximum wave height could be dangerously misleading.

Even though some areas might experience with modest wave heights, high currents in these areas might increase tsunami hazard and destructive potential.

For a more complete hazard assessment impact metrics must be employed.

Impact metrics

Impact metrics should take account both potential and kinetic energy.

At the front surface of a perfectly reflecting wall instantaneous dynamic force is:

$$M_t(x, t) = p_d(\eta_p + h) + \rho u^2(\eta_p + h)$$

Force on a cylindrical pile:

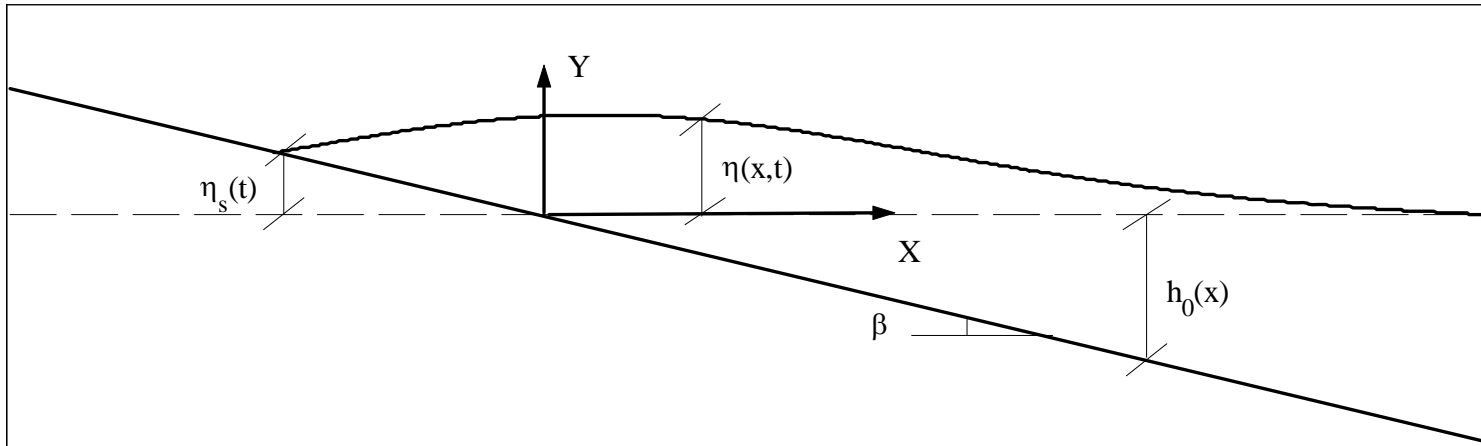
$$F_T(t) = C_M \rho R^2 \frac{dV}{dt}(\eta_p + h) + C_D \rho R V |V|(\eta_p + h)$$

Impact metrics

Damage metrics must reflect the distribution of the force over the entire impacted area and identify areas of exceptional force.

- The water depth: h
(not wave height with respect to undisturbed water level)
- The velocity: $V^2 = v^2 + u^2$
- The acceleration: dV/dt
- The inertial component: hdV/dt
- The momentum flux: hV^2

Nonlinear shallow water wave equations



$$[u (\eta + h_0)]_x + \eta_t = 0$$

$$u_t + u u_x + \eta_x = 0$$

$$x = \tilde{x} / \tilde{l}, \quad h_0 = \tilde{h}_0 / (\tilde{l} \tan \beta), \quad \eta = \tilde{\eta} / (\tilde{l} \tan \beta), \quad u = \tilde{u} / \sqrt{g \tilde{l} \tan \beta}, \quad \text{and} \quad t = \tilde{t} / \sqrt{\tilde{l} / g \tan \beta}$$

$u(x,t)$ horizontal depth-averaged velocity

$\eta(x,t)$ free-surface elevation

$h(x) = x \tan \beta$

Carrier & Greenspan

(1958 Water waves of finite amplitude on a sloping beach. JFM 4, 97-109)

Nonlinear shallow water wave equations

**Hodograph
transformation**
 $(x, t) \rightarrow (\sigma, \lambda)$

$$u = \frac{\varphi_\sigma}{\sigma}, \quad x = \frac{\sigma^2}{16} - \eta, \quad \eta = \frac{\varphi_\lambda}{4} - \frac{u^2}{2}, \quad t = u - \frac{\lambda}{2}$$

Second order ODE

$$\sigma \varphi_{\lambda\lambda} - (\sigma \varphi_\sigma)_\sigma = 0$$

Shoreline is at $\sigma = 0$ in the transform space

$$\varphi(\sigma, \lambda) = -\int_0^\infty \int_0^\infty (1/\omega) \zeta^2 J_0(\omega\sigma) \sin(\omega\lambda) J_1(\omega\zeta) \Phi(\zeta) d\omega d\zeta \quad \text{where} \quad \Phi(\zeta) = u_\lambda(\sigma, 0) = \frac{4}{\sigma} \eta_\sigma(\sigma, 0)$$

$$\eta(x, 0) \xrightarrow{\quad ? \quad} \eta(\sigma, 0)$$

Major difficulty

To derive equivalent initial condition over the transform space given the initial condition in the physical space.

Carrier, Wu & Yeh

(2003 Tsunami run-up and draw-down on a plane beach. JFM 475, 79-97)

Nonlinear shallow water wave equations

**Hodograph
transformation**
Tuck & Hwang (1972 JFM)
 $(x, t) \rightarrow (\sigma, \lambda)$

$$u = -\frac{\varphi_\sigma}{2\sigma}, \quad x = \sigma^2 - \eta, \quad \eta = \varphi_\lambda - \frac{u^2}{2}, \quad t = u + \lambda$$

Second order ODE

$$4\sigma\varphi_{\lambda\lambda} - (\sigma\varphi_\sigma)_\sigma = 0$$

$$\varphi(\sigma, \lambda) = \left[\int_0^\infty F(b)G(b, \sigma, \lambda)db + \int_0^\infty P(b)G_\lambda(b, \sigma, \lambda)db \right] \text{ where } P(\sigma) = \varphi(\sigma, 0) \text{ and } F(\sigma) = \varphi_\lambda(\sigma, 0)$$

$$G(b, \sigma, \lambda) = b \int_0^\infty J_0(\rho\lambda) \sin(\rho\lambda/2) J_0(\rho b) d\rho = \begin{cases} 0 & \frac{1}{2}\lambda < |\sigma - b| \\ \frac{1}{\pi} \sqrt{\frac{b}{\sigma}} K\left(\frac{\lambda^2 - 4(\sigma - b)^2}{16\sigma b}\right) & |\sigma - b| < \frac{1}{2}\lambda < |\sigma + b| \\ \frac{4}{\pi} \frac{b}{\lambda^2 - 4(\sigma - b)^2} K\left(\frac{16\sigma b}{\lambda^2 - 4(\sigma - b)^2}\right) & \frac{1}{2}\lambda > |\sigma + b| \end{cases}$$

where complete elliptic integral $K(k) = \int_0^{\pi/2} d\nu / \sqrt{1 - k \sin^2 \nu}$

Proposed solution

(2004 Nonlinear evolution and runup-rundown of long waves over a sloping beach. Accepted for publication in JFM)

$$\eta(x,0) \xrightarrow{x = \frac{\sigma^2}{16} + \frac{u^2}{2} - \frac{\varphi_\lambda}{4} \rightarrow x \cong \frac{\sigma^2}{16}} \eta(\sigma,0)$$

$$\varphi(\sigma, \lambda) = -\int_0^\infty \int_0^\infty (1/\omega) \zeta^2 J_0(\omega\sigma) \sin(\omega\lambda) J_1(\omega\zeta) \Phi(\zeta) d\omega d\zeta \quad \text{where} \quad \Phi(\sigma) = u_\lambda(\sigma,0) = \frac{4}{\sigma} \eta_\sigma(\sigma,0)$$

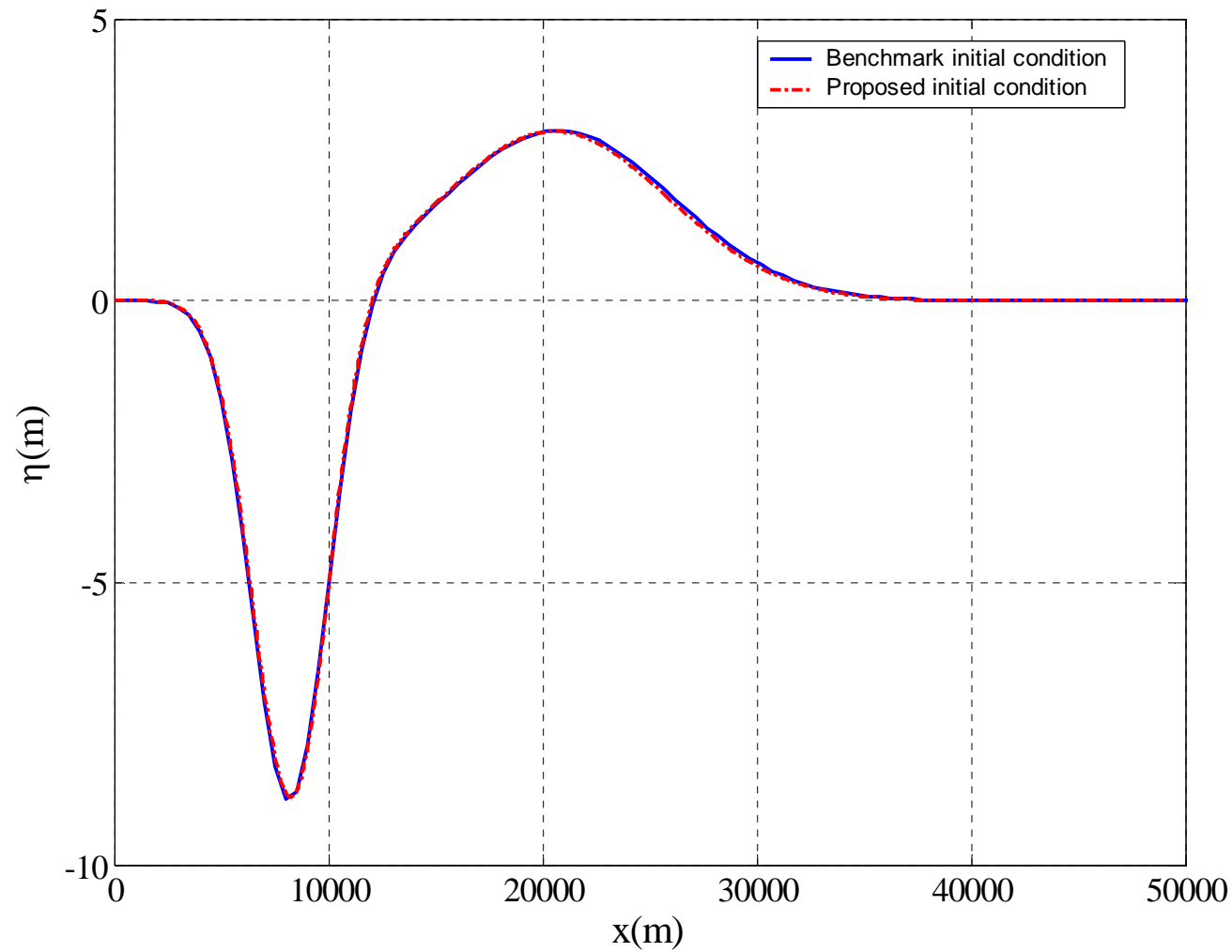
$$\begin{aligned} \eta(\sigma, \lambda) = \frac{\varphi_\lambda}{4} - \frac{u^2}{2} = & -\frac{1}{4} \int_0^\infty \zeta^2 \Phi(\zeta) \left[\int_0^\infty J_0(\omega\sigma) J_1(\omega\zeta) \cos(\omega\lambda) d\omega \right] d\zeta \\ & - \frac{1}{2} \left\{ \int_0^\infty \zeta^2 \Phi(\zeta) \left[\int_0^\infty \frac{1}{\sigma} J_1(\omega\sigma) J_1(\omega\zeta) \sin(\omega\lambda) d\omega \right] d\zeta \right\}^2 \end{aligned}$$

Solution for a particular time t^* or a location x^* Synolakis (1987 JFM)

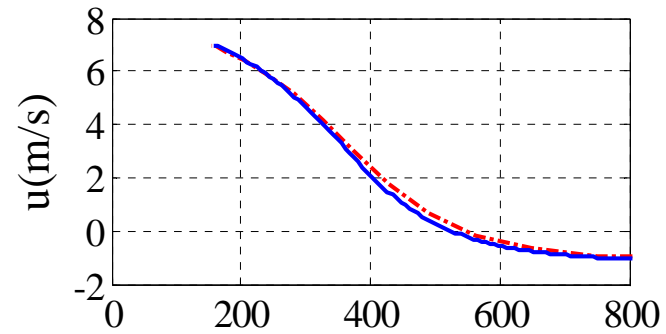
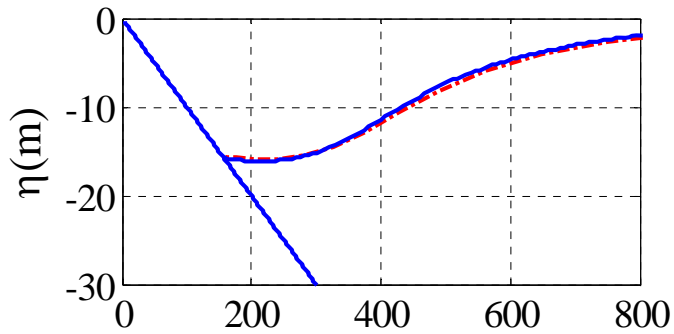
$$\lambda_{i+1} = \lambda_i + \frac{t^* - t_i}{\frac{\varphi_{\sigma\lambda}}{\sigma} - \frac{1}{2}} \quad \sigma_{i+1} = \sigma_i + \frac{x^* - x_i}{\frac{\sigma}{8} - \frac{\varphi_{\sigma\lambda}}{4} + u u_\sigma}$$

Comparison of the initial wave profiles

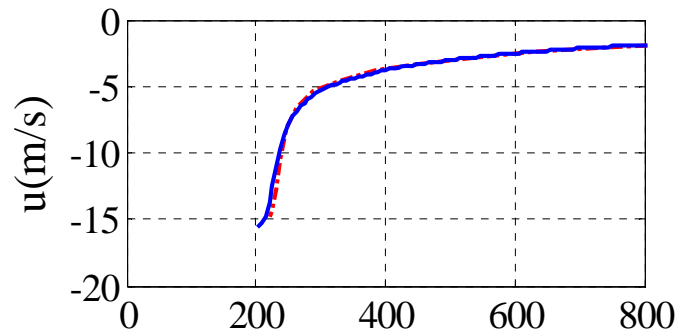
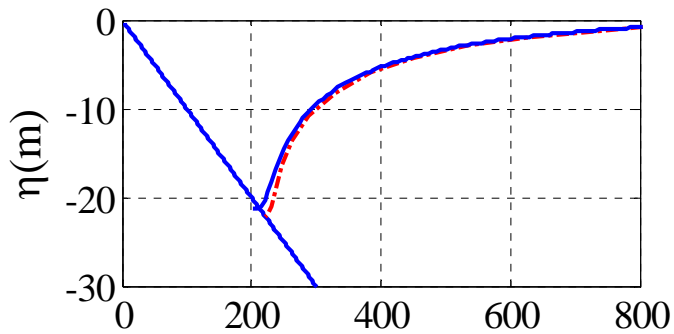
$$\eta(x,0) = 0.006e^{-0.4444(x-4.1209)^2} - 0.018e^{-4.0(x-1.6384)^2}, \quad x \approx \sigma^2/16$$



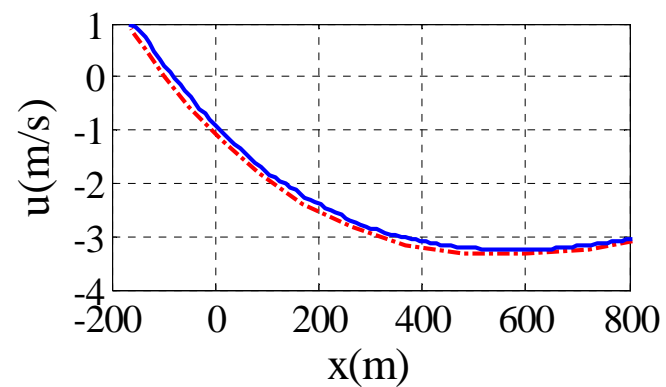
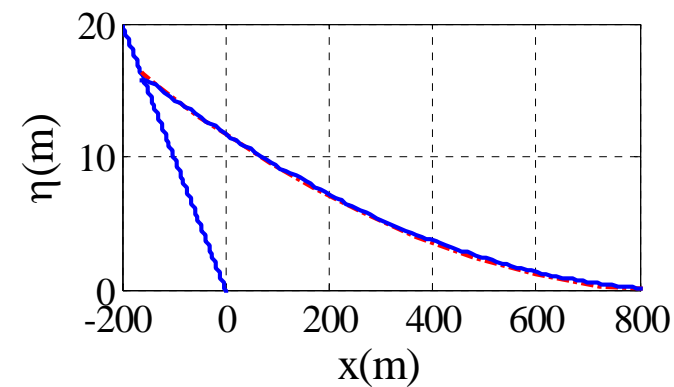
Comparison of the free surface elevation and velocity profiles at given times



$t=160$ s



$t=175$ s



$t=220$ s

Shoreline runup-rundown motion ($\sigma = 0$)

$$\eta_s(\lambda) = \eta(0, \lambda) = -\frac{1}{4} \int_0^\infty \zeta^2 \Phi(\zeta) \left[\int_0^\infty J_1(\omega\zeta) \cos(\omega\lambda) d\omega \right] d\zeta$$

$$-\frac{1}{2} \left\{ \int_0^\infty \zeta^2 \Phi(\zeta) \left[\int_0^\infty \frac{1}{2} \omega J_1(\omega\zeta) \sin(\omega\lambda) d\omega \right] d\zeta \right\}^2$$

$J_0(\omega\sigma) = 1$ (indicated by a red arrow pointing to the \int_0^∞ term in the first equation)

$$\lim_{\sigma \rightarrow 0} J_1(\omega\sigma)/\sigma = \omega/2$$

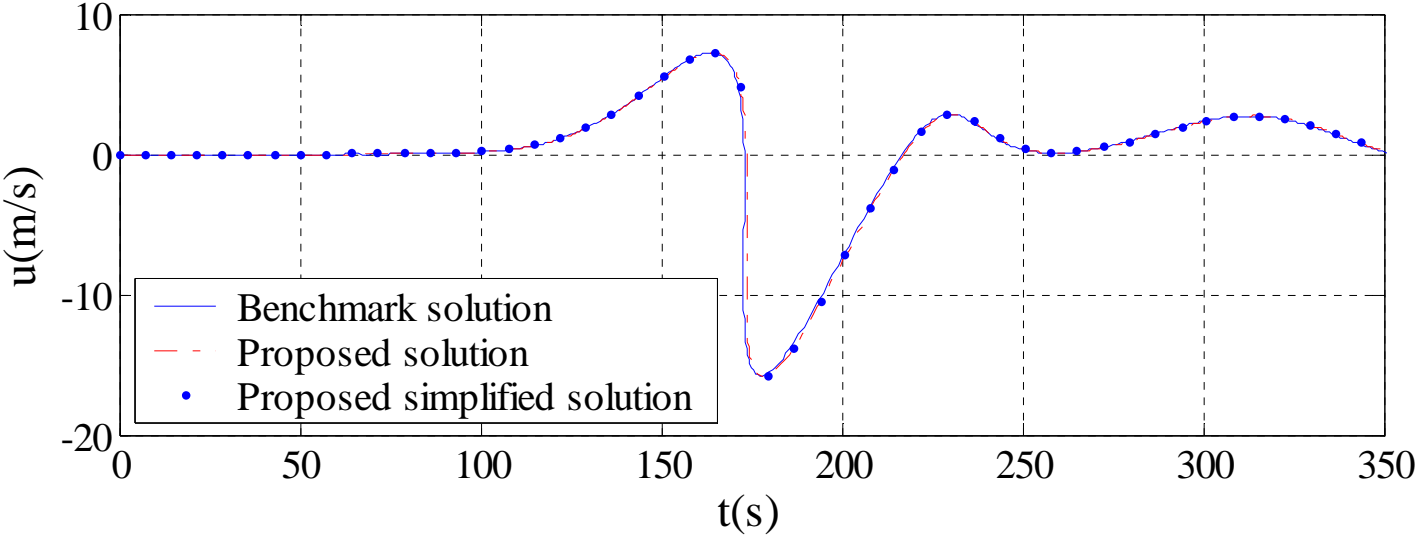
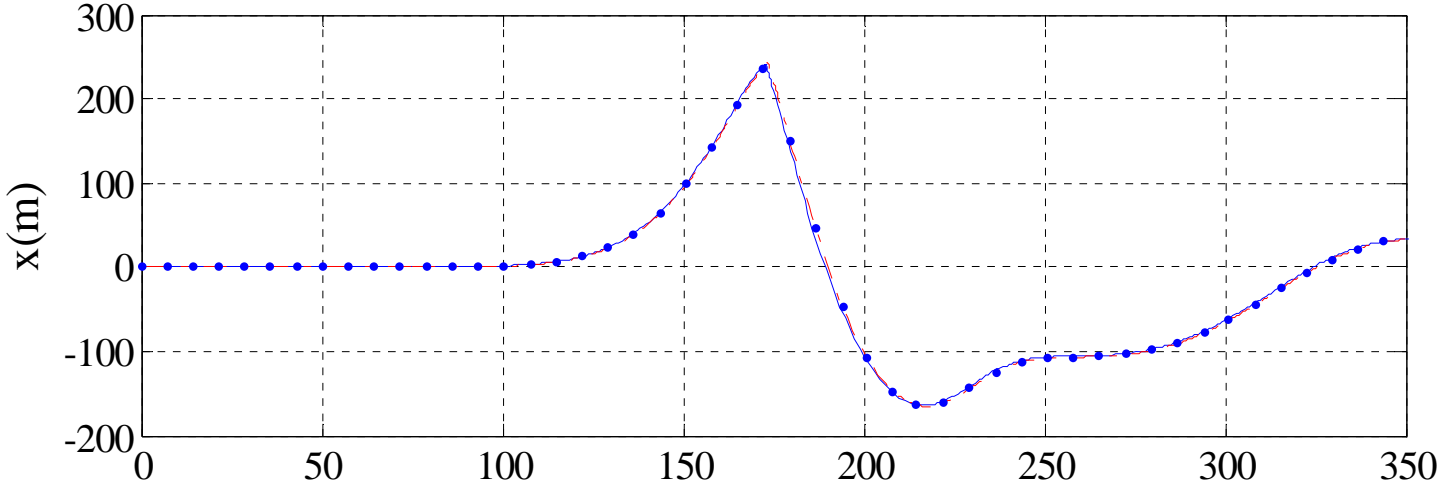
$$\int_0^\infty J_1(\kappa\mu) \cos(\kappa\nu) d\kappa = \begin{cases} \cos(\arcsin(\nu/\mu)) / \sqrt{\mu^2 - \nu^2}, & \nu < \mu \\ 0, & \nu = \mu \\ -\mu / \sqrt{\nu^2 - \mu^2} (\nu + \sqrt{\nu^2 - \mu^2}), & \nu > \mu \end{cases}$$

$$\eta_s(\lambda) = \eta(0, \lambda) = -\frac{1}{4} \left\{ \int_0^\infty \zeta \Phi(\zeta) d\zeta - \lambda^2 \Phi(0) + \int_0^{-\lambda} \lambda \sqrt{\lambda^2 - \zeta^2} \frac{d\Phi(\zeta)}{d\zeta} d\zeta \right\}$$

$$-\frac{1}{2} \left\{ -\lambda^2 \Phi(0) + \frac{1}{2} \int_0^{-\lambda} \frac{2\lambda^2 - \zeta^2}{\sqrt{\lambda^2 - \zeta^2}} \frac{d\Phi(\zeta)}{d\zeta} d\zeta \right\}^2$$

(Note: Several terms in the above equations are crossed out with red X's in the original image.)

Comparison of the shoreline trajectory and velocity



Observations

$$\eta_{elevation}(x,0) = -\eta_{depression}(x,0) \longrightarrow \Phi_{elevation}(\sigma) = -\Phi_{depression}(\sigma)$$

$$\varphi(\sigma, \lambda) = -\int_0^\infty \int_0^\infty (1/\omega) \zeta^2 J_0(\omega\sigma) \sin(\omega\lambda) J_1(\omega\zeta) \Phi(\zeta) d\omega d\zeta \quad \text{where} \quad \Phi(\sigma) = u_\lambda(\sigma,0) = \frac{4}{\sigma} \eta_\sigma(\sigma,0)$$

$$\varphi_{elevation}(\sigma, \lambda) = -\varphi_{depression}(\sigma, \lambda)$$

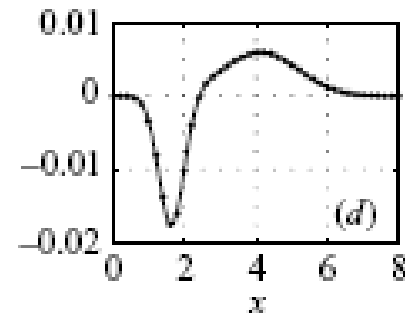
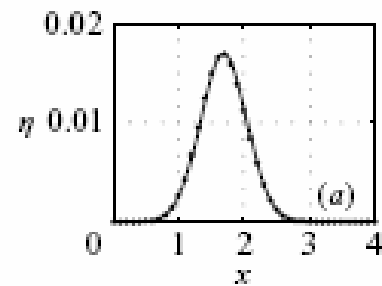
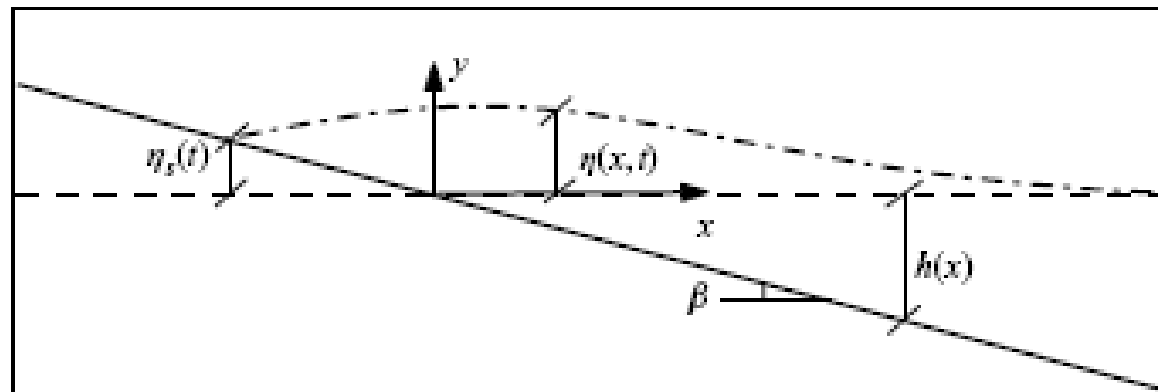
$$u = \frac{\varphi_\sigma}{\sigma}, \quad x = \frac{\sigma^2}{16} - \eta, \quad \eta = \frac{\varphi_\lambda}{4} - \frac{u^2}{2}, \quad t = u - \frac{\lambda}{2}$$

The extreme values of u and η for the leading-elevation and -depression initial waveforms are the inverse of each.

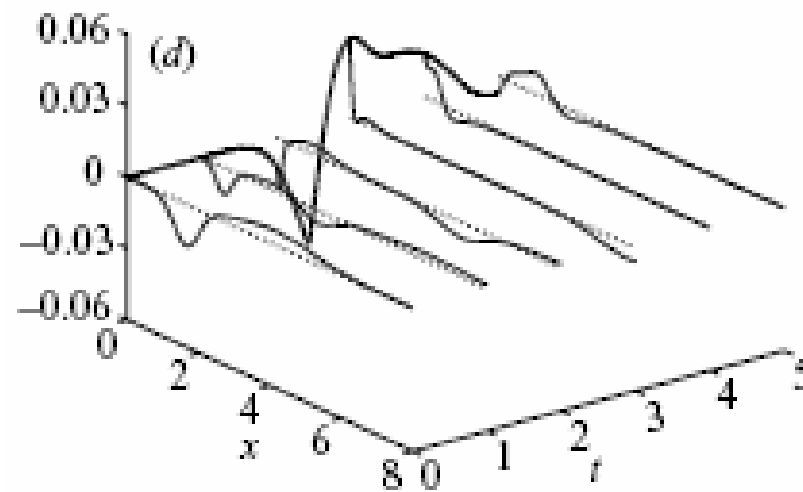
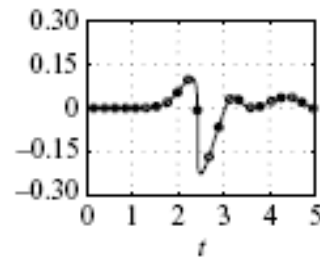
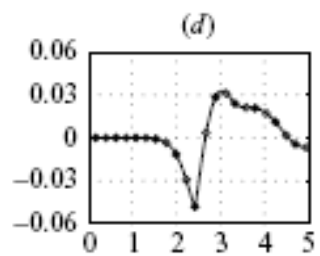
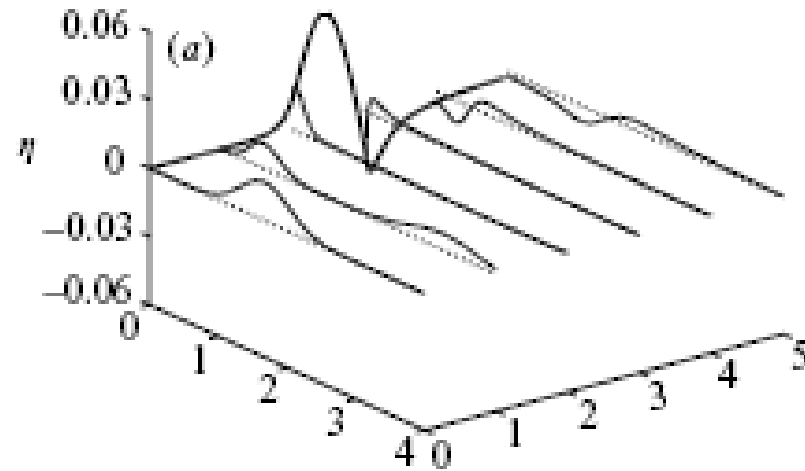
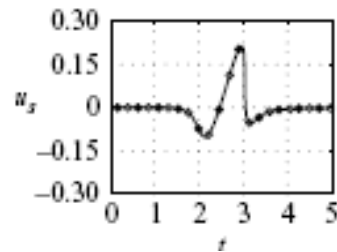
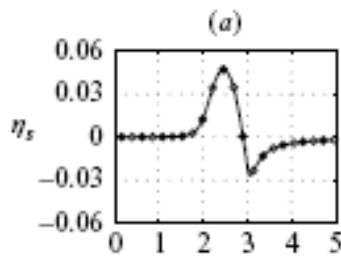
Maximum runup of the elevation wave = Minimum rundown of the depression wave

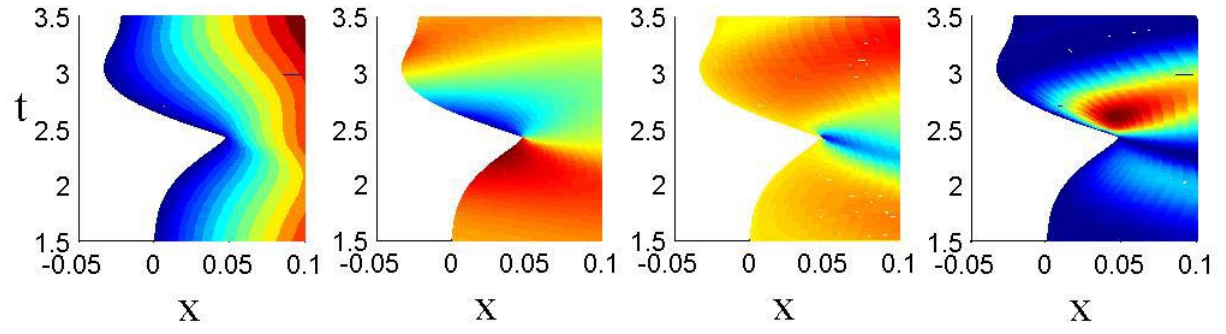
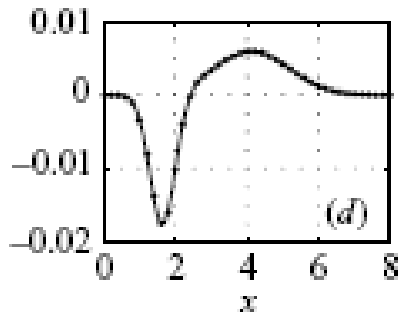
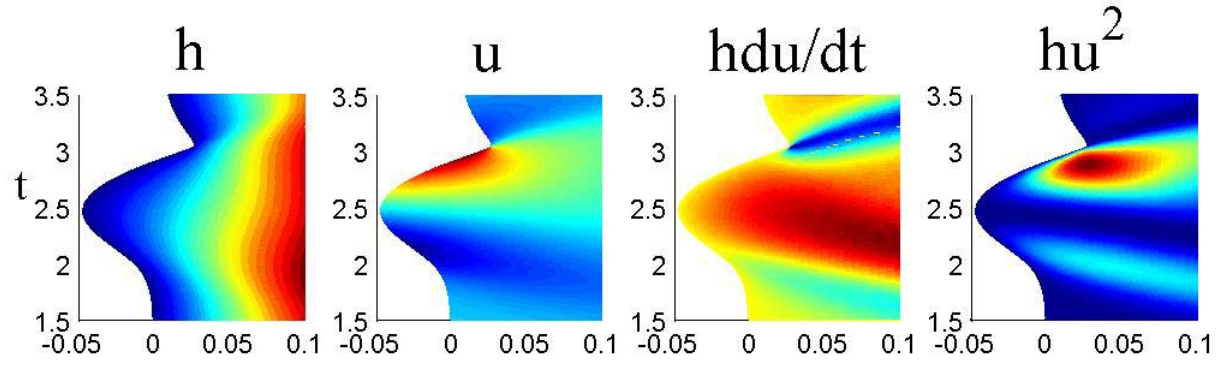
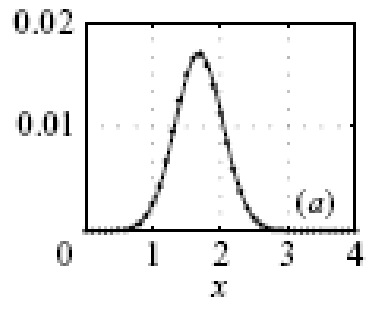
However, spatial and temporal variations of them are different.

1D nonlinear analytical solution



1D nonlinear analytical solution





Which parameter to use?

Both 1D nonlinear analytical study and near/far-field events considered for the Sea Side study suggest:

The momentum flux shows same distribution as current and inertial component.

We therefore recommended the momentum flux as a impact parameter.

However, we presented all these quantities for the Sea Side study.

Conclusion

Not only inundation but also momentum flux is important quantity to consider to have a complete hazard assessment.

Simple 1D analysis shows momentum flux might be an important design criteria for nuclear power plants not only at shore but also offshore.

Therefore impact metrics in addition to inundation needs to be provided to have a complete hazard assessment.

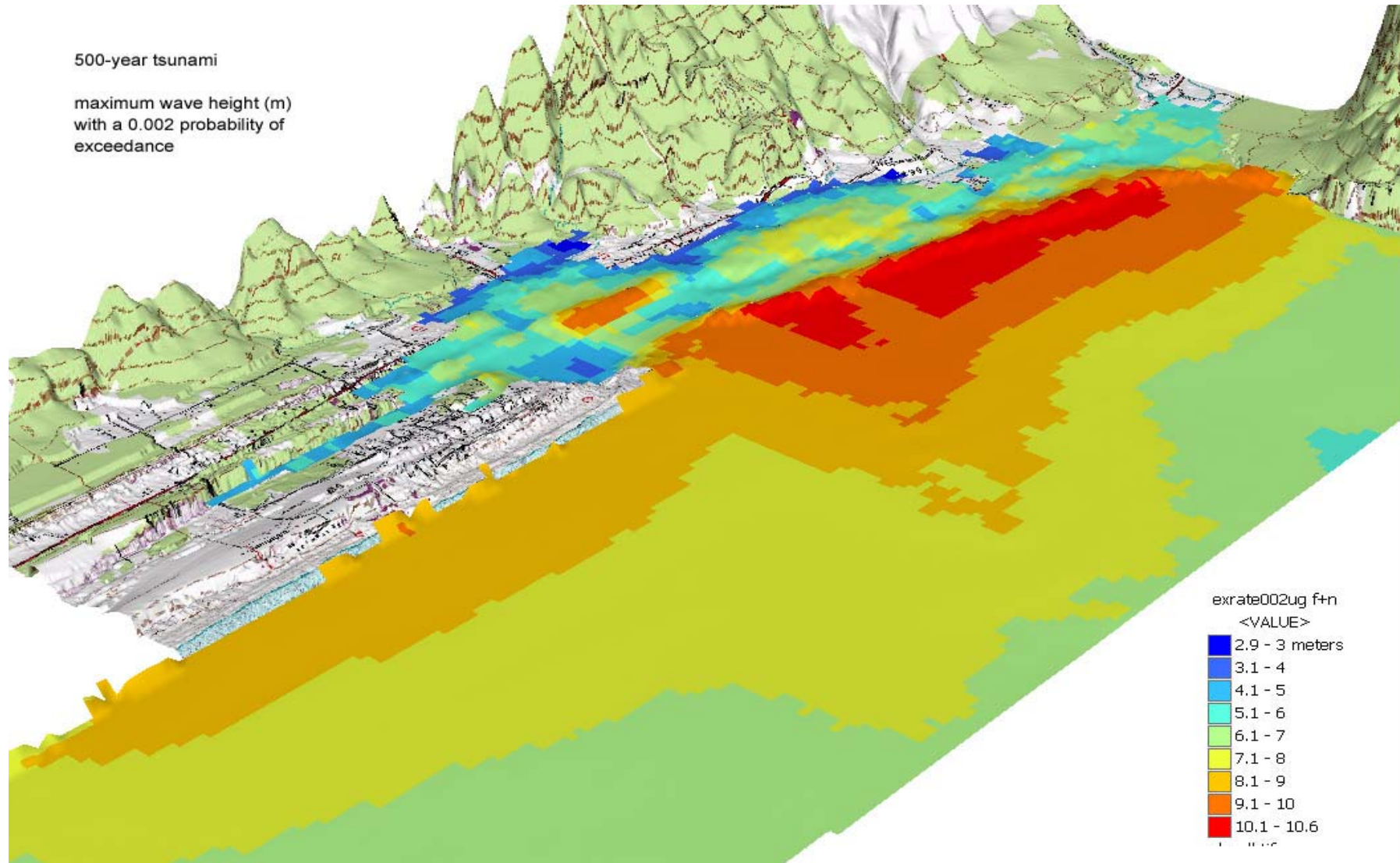
Seaside, Oregon Tsunami Pilot Study

Modernization of FEMA Flood Hazard Maps.



- 1) Combining Tides, Tsunamis, Storm Surges*
- 2) Farfield (Alaska, Peru, Chile) and Nearfield sources*
- 3) Development of comprehensive damage metrics.*
- 4) 100 and 500 year recurrence probability at each coastal location in Seaside.*

Seaside, Oregon Tsunami Pilot Study Modernization of FEMA Flood Hazard Maps



Tsunami in the Maldives

- On the morning of 26 December 2004, at about 6:25 am, tremors were felt for about 5 minutes
- Shortly after 9:00 am, the first wave struck Male and then waves ranging from 4 to 12 feet were reported in all islands.



What we never want to see again.



What do we need beyond DART?

- 1) Realistic inundation maps to complement the warnings.
- 2) Education and training for self-evacuation based on evacuation maps and evacuation drills.
- 3) Training of scientists to update inundation maps and evacuation scenarios based on updated hazard information as it becomes available.
- 4) Design waves for likely events - one can build probabilistic maps with design waves.

Public awareness ...

